A Numerical Model for Two-Phase Shallow Granular Flows over Variable Topography

Marica Pelanti

Département de Mathématiques et Applications, ENS Paris, France

Joint work with:

François Bouchut (DMA-ENS)

Anne Mangeney (IPGP)

GdR CHANT Workshop on Models and Numerical Methods for Granular Materials, ENPC, November 19-21, 2007

Outline

I. Objectives and Motivations

II. Physical and Mathematical Model
- ⋆ Eigenvalues analysis

III. Numerical Solution Method
- ⋆ Solver for the homogeneous system
- ⋆ Topography source terms, inter-phase drag source terms
- ⋆ Numerical experiments

IV. Summary and Future Work

Objectives and Motivations

Goal: Development of a numerical two-phase shallow flow model for mixtures of solid grains and fluid over variable basal surface.

Ultimate objective: Numerical simulation of geophysical flows such as avalanches and debris flows over natural terrain. (Project DMA-ENS & IPGP.)

- Gravitational geophysical flows typically involve both solid granular material and interstitial fluid.
- Inter-phase forces influence flow mechanics: flow deformation, mobility, run-out, deposit.

Source: USGS

Thin Layer Granular Flow Models – State of the Art in brief

Thin layer (shallow flow) models: $H/L \ll 1$. H, L = characteristic flow depth and length.
Continuum flow equations are scaled and depth-averaged.

- First 1D single-phase dry granular flow model: Savage and Hutter, 1989.
  Extensive work on dry granular flows: 2D models, complex topography.

Thin Layer Granular Flow Models – State of the Art in brief

Thin layer (shallow flow) models: $H/L \ll 1$. H, L = characteristic flow depth and length.
Continuum flow equations are scaled and depth-averaged.

- First 1D single-phase dry granular flow model: Savage and Hutter, 1989.

  Extensive work on dry granular flows: 2D models, complex topography.

- Solid-Fluid Mixture Model (Iverson, 1997; Iverson and Denlinger, 2001)

  (Similar mixture theory approach: Pudasaini–Wang–Hutter, 2005).

  Hp: 1) constant fluid volume fraction; 2) fluid velocity = solid velocity.

  System: mass and momentum equations for the mixture.

  No inherent pore fluid motion description $\Rightarrow$ needs supplementary specification of pore fluid pressure evolution

  $\star$ 2D model, treats irregular topography; Numerical simulation of many laboratory experiments and debris-flow-flume tests.

Thin Layer Granular Flow Models – State of the Art in brief

Thin layer (shallow flow) models: $H/L \ll 1$. H, L = characteristic flow depth and length.
Continuum flow equations are scaled and depth-averaged.

- First 1D single-phase dry granular flow model: Savage and Hutter, 1989.

  Extensive work on dry granular flows: 2D models, complex topography.

- Solid-Fluid Mixture Model (Iverson, 1997; Iverson and Denlinger, 2001)

  (Similar mixture theory approach: Pudasaini–Wang–Hutter, 2005).

  Hp: 1) constant fluid volume fraction; 2) fluid velocity = solid velocity.

  System: mass and momentum equations for the mixture.

  No inherent pore fluid motion description $\Rightarrow$ needs supplementary specification of pore fluid pressure evolution

  $\star$ 2D model, treats irregular topography; Numerical simulation of many laboratory experiments and debris-flow-flume tests.

- A Two-Phase Model: Pitman and Le, 2005.

  $\star$ Retains mass and momentum equations for both solid and fluid phases.

  However: non-conservative mixture momentum eq.; no general topography. Numerical method only for reduced model that ignores fluid inertial terms.

Physical and Mathematical Model

Pitman–Le approach (2005)

Consider thin layer of a mixture of solid grains and fluid flowing over a smooth basal surface.

Two-phase flow equations [Anderson and Jackson, 1967]

$$\partial_t(\rho_s\varphi) + \nabla\cdot(\rho_s\varphi\mathcal{V}_s) = 0\,,$$

$$\rho_s\varphi(\partial_t\mathcal{V}_s + (\mathcal{V}_s\cdot\nabla)\mathcal{V}_s) = \nabla\cdot T_s + \varphi\nabla\cdot T_f + \mathcal{I} + \rho_s\varphi\mathfrak{g}\,,$$

$$\partial_t(\rho_f(1-\varphi)) + \nabla\cdot(\rho_f(1-\varphi)\mathcal{V}_f) = 0\,,$$

$$\rho_f(1-\varphi)(\partial_t\mathcal{V}_f + (\mathcal{V}_f\cdot\nabla)\mathcal{V}_f) = (1-\varphi)\nabla\cdot T_f - \mathcal{I} + \rho_f(1-\varphi)\mathfrak{g}\,.$$

ρ_s, ρ_f = solid and fluid specific densities; φ = solid volume fraction;
$\mathcal{V}_s$, $\mathcal{V}_f$ = velocities; T_s, T_f = stress tensors; $\mathfrak{g}$ = gravity vector;
$\mathcal{I}$ = non-buoyancy interaction forces (e.g. drag).

Two-Phase Shallow Granular Flow Model

Material Constitutive Behaviour

- Solid and fluid are incompressible: material densities ρ_s, ρ_f = constant.
- Fluid is inviscid; only fluid stress is a pressure.
- Solid modeled as Coulomb material (as Savage–Hutter).

  Coulomb friction law for solid shear stresses: $T_s^{xz} = -\mathrm{sgn}(V_s)\nu T_s^{zz}$, $\nu \geq 0$, V_s = solid sliding velocity.

  Earth-pressure relation for lateral normal stresses: $T_s^{xx} = K T_s^{zz}$. $(K = 1)$

Boundary Conditions

- Free upper surface stress-free, and material surface for both phases.
- Both solid and fluid motion tangent to the basal surface (no-slip condition).

Moreover: Only non-buoyancy interaction force $\mathcal{I}$ is drag: $\mathcal{I} = \mathcal{D}(\mathcal{V}_f - \mathcal{V}_s)$.

Under the shallow flow hypothesis $H/L \ll 1$:

Scale and depth-average the governing two-phase flow equations.

Model Equations (1D and hp. small topography slopes)

Depth-Averaged Solid and Fluid Mass and Momentum Equations

$$\frac{\partial}{\partial t}(\varphi h) + \frac{\partial}{\partial x}(\varphi h v_s) = 0\,,$$

$$\frac{\partial}{\partial t}(\varphi h v_s) + \frac{\partial}{\partial x}\left(\varphi h v_s^2 + g\frac{1-\gamma}{2}\varphi h^2\right) + \gamma\varphi\frac{g}{2}\frac{\partial h^2}{\partial x} = -g\varphi h\frac{\partial b}{\partial x}$$

$$-\,\mathrm{sgn}(v_s)\nu^{\mathsf{b}}\, g(1-\gamma)\varphi h + \gamma D h(v_f - v_s)\,,$$

$$\frac{\partial}{\partial t}((1-\varphi)h) + \frac{\partial}{\partial x}((1-\varphi)h v_f) = 0\,,$$

$$\frac{\partial}{\partial t}((1-\varphi)h v_f) + \frac{\partial}{\partial x}\left((1-\varphi)h v_f^2\right) + (1-\varphi)\frac{g}{2}\frac{\partial h^2}{\partial x} = -g(1-\varphi)h\frac{\partial b}{\partial x}$$

$$-\,D h(v_f - v_s)\,.$$

h = flow depth; φ = depth-averaged solid volume fraction; v_s, v_f = averaged solid and fluid velocities;
$\gamma = \frac{\rho_f}{\rho_s} < 1$, ρ_s, ρ_f = material specific densities (constant); $b(x)$ = bottom topography;
g = gravity constant; $\nu^{\mathsf{b}} = \tan\delta^{\mathsf{bed}}$, δ^{bed} = basal friction angle; D = average drag function (= $\bar{\mathcal{D}}/\rho_f$).

Presented model vs. original Pitman–Le model

Presented model: variant of the original Pitman–Le model.

Different averaging approximation of fluid motion equation

$\Rightarrow$ Different fluid momentum balance:

Pitman–Le: $\frac{\partial}{\partial t}\left(hv_f\right) + \frac{\partial}{\partial x}\left(hv_f^2\right) + \frac{g}{2}\frac{\partial h^2}{\partial x} = 0.$

Here: $\frac{\partial}{\partial t}\left((1-\varphi)hv_f\right) + \frac{\partial}{\partial x}\left((1-\varphi)hv_f^2\right) + (1-\varphi)\frac{g}{2}\frac{\partial h^2}{\partial x} = 0.$

Difference:

$\tau \equiv hv_f\left(\partial_t(1-\varphi) + v_f\partial_x(1-\varphi)\right) = (1-\varphi)v_f\partial_x(\varphi h(v_s - v_f)).$

$\Rightarrow$ Different mixture momentum balance.

Here: conservative equation for the momentum of the mixture

$$\frac{\partial}{\partial t}\left((\varphi v_s + \gamma(1-\varphi)v_f)h\right) + \frac{\partial}{\partial x}\left((\varphi v_s^2 + \gamma(1-\varphi)v_f^2)h + \frac{g}{2}(\varphi + \gamma(1-\varphi))h^2\right) = 0\,.$$

Consistent with conservative mixture momentum equation of two-phase flow system before averaging and expected physical behaviour.

Two-Phase Shallow Granular Flow Equations. Formulation $(h_s, h_s v_s, h_f, h_f v_f)$.

Set $h_s = \varphi\, h$, $h_f = (1-\varphi)\, h$, φ = solid volume fraction.

(Here no friction.)

$$\frac{\partial h_s}{\partial t} + \frac{\partial}{\partial x}(h_s v_s) = 0\,,$$

$$\frac{\partial}{\partial t}(h_s v_s) + \frac{\partial}{\partial x}\left(h_s v_s^2 + \frac{g}{2} h_s^2 + g\frac{1-\gamma}{2} h_s h_f\right) + \gamma g h_s \frac{\partial h_f}{\partial x} = -g h_s \frac{\partial b}{\partial x} + \gamma F^{\mathsf{D}},$$

$$\frac{\partial h_f}{\partial t} + \frac{\partial}{\partial x}(h_f\, v_f) = 0\,,$$

$$\frac{\partial}{\partial t}(h_f v_f) + \frac{\partial}{\partial x}\left(h_f v_f^2 + \frac{g}{2} h_f^2\right) + g\, h_f \frac{\partial h_s}{\partial x} = -g h_f \frac{\partial b}{\partial x} - F^{\mathsf{D}}.$$

Drag force $F^{\mathsf{D}} = D(h_s + h_f)(v_f - v_s)$; $\quad \gamma = \rho_f / \rho_s$.

Note: Similar to two-layer shallow flow model, except additional cross term $\frac{\partial}{\partial x}\left(g\frac{1-\gamma}{2} h_s h_f\right)$ in the solid momentum balance.

Eigenvalues Analysis

Consider $\quad \partial_t q + A(q)\partial_x q = 0\,, \quad q \in \mathbb{R}^4\,, \quad A \in \mathbb{R}^{4\times 4}\,.$

In general: eigenvalues $\lambda_k\,,\ k = 1,\ldots,4$, cannot be expressed explicitly.

Define: $\qquad a = \sqrt{gh} \qquad$ and $\qquad \beta = \sqrt{\tfrac{1}{2}(1-\varphi)(1-\gamma)} < 1\,.$

If $v_f = v_s \equiv v$ then A has real distinct eigenvalues ($\varphi \neq 1$)

$$\lambda_{1,4} = v \mp a \qquad \text{and} \qquad \lambda_{2,3} = v \mp a\beta\,.$$

We can show that:
There are always two real external eigenvalues $\lambda_{1,4}$, and, moreover

$$\min(v_f, v_s) - a \leq \lambda_1 < \Re\mathfrak{e}(\lambda_2) \leq \Re\mathfrak{e}(\lambda_3) < \lambda_4 \leq \max(v_f, v_s) + a\,.$$

Furthermore:

- If $|v_s - v_f| < 2a\beta$ or $|v_s - v_f| > 2a$ then all the eigenvalues are real and distinct ($\varphi \neq 1$) $\Rightarrow$ the system is strictly hyperbolic.
- If $2a\beta < |v_s - v_f| < 2a$ then the internal eigenvalues may be complex.

Hyperbolicity at least when the velocity difference $|v_s - v_f|$ is sufficiently small.

Eigenvectors

Right Eigenvectors

$q = (h_s, h_s v_s, h_f, h_f v_f)^\mathsf{T}$. Assume $h_s, h_f \neq 0$. For $k = 1, \ldots, 4$:

$$r_k = \begin{pmatrix} 1 \\ \lambda_k \\ \xi_k \\ \xi_k \lambda_k \end{pmatrix}, \quad \xi_k = \frac{(\lambda_k - v_s)^2 - g\left(h_s + \frac{1-\gamma}{2} h_f\right)}{g \frac{1+\gamma}{2} h_s} = \frac{g h_f}{(\lambda_k - v_f)^2 - g h_f}\,.$$

Note: Can show that 1st and 4th fields are genuinely nonlinear: $\nabla \lambda_k \cdot r_k \neq 0, \forall q$.

Left Eigenvectors, $L = R^{-1}$

$$l_k = \frac{n_k}{P'(\lambda_k)}\,, \quad n_k = (\,\vartheta_{s,k}(\lambda_k - 2v_s),\, \vartheta_{s,k},\, \vartheta_f(\lambda_k - 2v_f),\, \vartheta_f\,)\,,$$

$P(\lambda) =$ characteristic polynomial,

$$\vartheta_{s,k} = (\lambda_k - v_f)^2 - g h_f = g\,\frac{h_f}{\xi_k} \qquad \text{and} \qquad \vartheta_f = g\,\frac{1+\gamma}{2} h_s\,.$$

Numerical Solution

• Assume $|v_s - v_f|$ small enough so that the system is strictly hyperbolic.

Class of methods used: Godunov-type Finite Volume Schemes
(Schemes based on Riemann Solvers)

Difficulties:

• Non-conservative system. Many well-established efficient finite volume schemes: only for conservation laws.
(New difficulty with respect to dry granular flow models and mixture models.)

• Topography source terms need to be discretized so that the method is
well-balanced = it preserves steady states and captures accurately perturbations.
Well-known difficulty for systems with sources.

• Positivity preservation: computed values of flow depth and phase volume fractions must be positive.
Important to handle interfaces between flow fronts and dry bed zones ($h = 0$).
$\longrightarrow$ still to be addressed. Here we will consider regimes without dry bed areas.

Godunov-Type Schemes

Riemann problem: $\partial_t q + A(q)\partial_x q = 0$ with I.C. $q(x,0) = \begin{cases} q_\ell & \text{if } x \le \bar{x}\,, \\ q_r & \text{if } x > \bar{x}\,. \end{cases}$

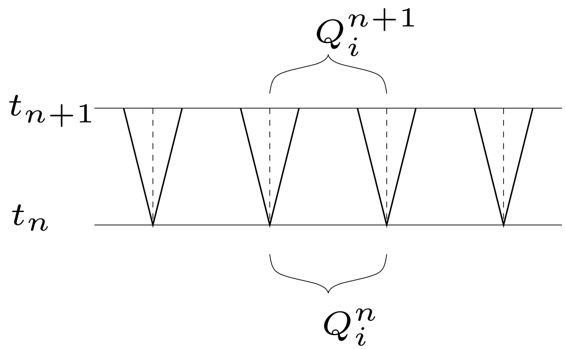

$Q_i^n \longrightarrow$ approximate solution on cell $(x_{i-1/2}, x_{i+1/2})$.
Discontinuities at cell interfaces $\Rightarrow$ Riemann problems.

1) At each cell interface $x_{i+1/2}$ between Q_i^n and Q_{i+1}^n $\longrightarrow$ solve Riemann problem with data Q_i^n and Q_{i+1}^n.

2) Use solution of local Riemann problems to update solution $Q_i^n \longrightarrow Q_i^{n+1}$.

Riemann Solver: $\longrightarrow$ Set of waves $\mathcal{W}^k$ and speeds s^k representing the (approximate) Riemann solution structure.

- $\Delta q \equiv Q_{i+1} - Q_i = \sum_k \mathcal{W}^k$
- For conservative systems $\partial_t q + \partial_x \mathcal{F}(q) = 0$: $\mathcal{F}(Q_{i+1}) - \mathcal{F}(Q_i) = \sum_k s^k \mathcal{W}^k$

Wave-Propagation Algorithm: $Q_i^{n+1} = Q_i^n - \frac{\Delta t}{\Delta x}(\mathcal{A}^+ \Delta Q_{i-1/2} + \mathcal{A}^- \Delta Q_{i+1/2})$,

fluctuations: $\mathcal{A}^\pm \Delta Q_{i+1/2} = \sum_k (s_{i+1/2}^k)^\pm \mathcal{W}_{i+1/2}^k$, $\quad s^+ = \max(s,0)$, $s^- = \min(s,0)$.

Numerical Solution

Homogeneous System $(b(x)=0,\, D=0)$

$$\partial_t q + \partial_x f(q) + w(q, \partial_x q) = 0\,, \qquad q = (h_s, h_s v_s, h_f, h_f v_f)^{\mathsf{T}}\,,$$

$$f(q) = \left(h_s v_s,\; h_s\, v_s^2 + \tfrac{g}{2}\, h_s^2 + g\tfrac{1-\gamma}{2} h_s\, h_f,\; h_f\, v_f,\; h_f\, v_f^2 + \tfrac{g}{2}\, h_f^2\right)^{\mathsf{T}}\,,$$

$$w(q, \partial_x q) = (0,\; \gamma g h_s\, \partial_x h_f,\; 0,\; g h_f\, \partial_x h_s)^{\mathsf{T}}\;.$$

- ⋆ Solid and fluid mass equations are conservative.
- ⋆ Mixture momentum equation is conservative: $\partial_t m + \partial_x f_{\mathsf{m}}(q) = 0\,,$

$$m = h_s v_s + \gamma\, h_f v_f\,, \quad f_{\mathsf{m}}(q) = f^{(2)}(q) + \gamma\, f^{(4)}(q) + \gamma\, g\, h_s h_f\;.$$

- ⋆ Non-conservative products $\gamma g h_s \frac{\partial h_f}{\partial x}$, $g h_f \frac{\partial h_s}{\partial x}$ in the momentum balances couple sets of equations of the two phases $\Rightarrow$ avoid uncoupled schemes that may generate instabilities.

We employ a Roe-type Riemann Solver.

Roe-type Riemann Solver

Consider the quasi-linear form of the system $\partial_t q + A(q)\partial_x q = 0\,.$

At each local cell interface $x_{i+1/2}$ between solution values Q_i and Q_{i+1} solve a Riemann problem for a linearized system

$$\partial_t q + \hat{A}(Q_i, Q_{i+1})\partial_x q = 0$$

with initial data Q_i and Q_{i+1}.

The Roe matrix $\hat{A}(Q_i, Q_{i+1})$ is defined so as to guarantee conservation for the mass of each phase and for the momentum of the mixture:

$$f^{(p)}(Q_{i+1}) - f^{(p)}(Q_i) = \hat{A}^{(p,:)}\,(Q_{i+1} - Q_i)\,, \quad p = 1, 3\,,$$

$$f_{\mathsf{m}}(Q_{i+1}) - f_{\mathsf{m}}(Q_i) = (\hat{A}^{(2,:)} + \gamma \hat{A}^{(4,:)})(Q_{i+1} - Q_i)\,.$$

We take $\hat{A} = A(\hat{h}_s, \hat{h}_f, \hat{v}_s, \hat{v}_f)$, with the choice

$$\hat{h}_\theta = \frac{h_{\theta,i} + h_{\theta,i+1}}{2} \qquad \text{and} \qquad \hat{v}_\theta = \frac{\sqrt{h_{\theta,i}}\, v_{\theta,i} + \sqrt{h_{\theta,i+1}}\, v_{\theta,i+1}}{\sqrt{h_{\theta,i}} + \sqrt{h_{\theta,i+1}}}\,, \quad \theta = s, f\,.$$

Then: waves $\mathcal{W}^k = \alpha_k\, \hat{r}_k$, $\Delta q = \sum_{k=1}^{4} \alpha_k\, \hat{r}_k$, and speeds $s^k = \hat{\lambda}_k$, $k = 1, \ldots, 4$.

$\{\hat{r}_k\,, \hat{\lambda}_k\}$ = eigenpairs of $\hat{A}$.

Wave Propagation Algorithms (LeVeque, 1997) – F-Wave Formulation

Basic software: CLAWPACK.

1) Classical Riemann solver: $\Delta q = \sum_k \mathcal{W}^k$; Roe: $\mathcal{W}^k = \alpha_k \hat{r}_k$, $s^k = \hat{\lambda}_k$

2) F-wave Approach: For a conservative system $\partial_t q + \partial_x \mathcal{F}(q) = 0$,

decompose flux jump $\Delta\mathcal{F} \equiv \mathcal{F}(Q_{i+1}) - \mathcal{F}(Q_i) = \sum_k \mathcal{Z}^k$.

Local Riemann solution approximated by f-waves $\mathcal{Z}^k$ and associated speeds s^k.

Roe: $\mathcal{Z}^k = \zeta_k \hat{r}_k$, $s^k = \hat{\lambda}_k$, $\{\hat{r}_k, \hat{\lambda}_k\}$ = eigenpairs of Roe matrix for $\mathcal{F}'(q)$.

Fluctuations

$$\mathcal{A}^-\Delta Q_{i+1/2} = \sum_{k:s^k_{i+1/2}<0} \mathcal{Z}^k_{i+1/2}\,, \quad \mathcal{A}^+\Delta Q_{i+1/2} = \sum_{k:s^k_{i+1/2}>0} \mathcal{Z}^k_{i+1/2}\,.$$

Algorithm

$$Q_i^{n+1} = Q_i^n - \frac{\Delta t}{\Delta x}\left(\mathcal{A}^+\Delta Q_{i-1/2} + \mathcal{A}^-\Delta Q_{i+1/2}\right)$$

(2) can be equivalent to (1), but useful framework to include source terms.

Wave Propagation Algorithms (LeVeque, 1997) – F-Wave Formulation

Basic software: CLAWPACK.

1) Classical Riemann solver: $\Delta q = \sum_k \mathcal{W}^k$; Roe: $\mathcal{W}^k = \alpha_k \hat{r}_k$, $s^k = \hat{\lambda}_k$

2) F-wave Approach: For a conservative system $\partial_t q + \partial_x \mathcal{F}(q) = 0$,

decompose flux jump $\Delta\mathcal{F} \equiv \mathcal{F}(Q_{i+1}) - \mathcal{F}(Q_i) = \sum_k \mathcal{Z}^k$.

Local Riemann solution approximated by f-waves $\mathcal{Z}^k$ and associated speeds s^k.

Roe: $\mathcal{Z}^k = \zeta_k \hat{r}_k$, $s^k = \hat{\lambda}_k$, $\{\hat{r}_k , \hat{\lambda}_k\}$ = eigenpairs of Roe matrix for $\mathcal{F}'(q)$.

Fluctuations

$$\mathcal{A}^-\Delta Q_{i+1/2} = \sum_{k:s^k_{i+1/2}<0} \mathcal{Z}^k_{i+1/2}\,, \quad \mathcal{A}^+\Delta Q_{i+1/2} = \sum_{k:s^k_{i+1/2}>0} \mathcal{Z}^k_{i+1/2}\,.$$

Algorithm (high-resolution)

$$Q_i^{n+1} = Q_i^n - \frac{\Delta t}{\Delta x}(\mathcal{A}^+\Delta Q_{i-1/2} + \mathcal{A}^-\Delta Q_{i+1/2}) - \frac{\Delta t}{\Delta x}(F^{\mathsf{c}}_{i+1/2} - F^{\mathsf{c}}_{i-1/2})$$

$F^{\mathsf{c}}_{i+1/2}$ = correction fluxes for second order accuracy

(2) can be equivalent to (1), but useful framework to include source terms.

The Roe-Type Solver in the F-Wave Framework

Difficulty: Here non-conservative system $\partial_t q + \partial_x f(q) + w(q, \partial_x q) = 0\,,$

$$w(q, \partial_x q) = (0,\, \gamma g h_s\, \partial_x h_f,\, 0,\, g h_f\, \partial_x h_s)^{\mathsf{T}}\ .$$

We lack a flux function $\mathcal{F}$ to be used for f-wave decomposition.

The Roe-Type Solver in the F-Wave Framework

Difficulty: Here non-conservative system $\partial_t q + \partial_x f(q) + w(q, \partial_x q) = 0\,,$

$$w(q, \partial_x q) = (0,\ \gamma g h_s\, \partial_x h_f,\ 0,\ g h_f\, \partial_x h_s)^{\mathsf{T}}\ .$$

We lack a flux function $\mathcal{F}$ to be used for f-wave decomposition.

Nonetheless can still formulate our Roe-type method into the f-wave framework:

Take local linearization of $w(q, \partial_x q)$ consistent with Roe linearization and define approximate flux difference

$$\Delta\tilde{\mathcal{F}} = \Delta f + (0,\ \gamma\, g\, \hat{h}_s\, \Delta h_f,\ 0,\ g\, \hat{h}_f\, \Delta h_s)^{\mathsf{T}}\,.$$

Then decompose

$$\Delta\tilde{\mathcal{F}} = \sum_{k=1}^{4} \zeta_k\, \hat{r}_k\ ,$$

and set $\quad \mathcal{Z}^k = \zeta_k\, \hat{r}_k\ , \quad s^k = \hat{\lambda}_k\ , \qquad k = 1, \ldots, 4\,.$

$\{\hat{r}_k\,,\, \hat{\lambda}_k\}$ = eigenpairs of $\hat{A}$.

Note: $\quad \Delta\tilde{\mathcal{F}} = \hat{A}\, \Delta q \quad$ (classical Roe property).

Topography Source Terms

Consider system with topography terms:

$$\partial_t q + A(q)\partial_x q = \psi^{\mathsf{b}}(q)\,, \qquad q = (h_s, h_s v_s, h_f, h_f v_f)^{\mathsf{T}}\,,$$

$$\psi^{\mathsf{b}}(q) = -\left(0,\, g h_s \partial_x b,\, 0,\, g h_f\, \partial_x b\right)^{\mathsf{T}}\,, \quad b = b(x)\,.$$

Need well-balancing: efficient modeling of equilibrium and quasi-equilibrium states $\longrightarrow\ A(q)\partial_x q \approx \psi^{\mathsf{b}}(q)\,.$

Steady states at rest ($v_s = v_f = 0$):

$$h_s + h_f + b = \text{const.} \qquad \text{and} \qquad \frac{h_f}{h_s} = \text{const.}$$

That is

$$h + b = \text{const.} \qquad \text{and} \qquad \varphi = \text{const.}$$

Well-Balancing Topography Terms - F-Wave Method

(Bale–LeVeque–Mitran–Rossmanith, 2002)

Idea: Concentrate source term at interfaces $\rightarrow \Psi^{\mathsf{b}}_{i+1/2}$ and incorporate topography contribution $\Psi^{\mathsf{b}}_{i+1/2}\,\Delta x$ into the Riemann solution. Now we decompose:

$$\Delta\tilde{\mathcal{F}} - \Psi^{\mathsf{b}}_{i+1/2}\,\Delta x = \sum_{k=1}^{4} \zeta_k\,\hat{r}_k\,.$$

Then, same algorithm with f-waves $\mathcal{Z}^k = \zeta_k\,\hat{r}_k$ and speeds $s^k = \hat{\lambda}_k$.

The interface source term $\Psi^{\mathsf{b}}_{i+1/2}$ must satisfy the discrete steady state condition

$$\Delta\tilde{\mathcal{F}}/\Delta x = \Psi^{\mathsf{b}}_{i+1/2}\,,$$

whenever initial data correspond to equilibrium at rest.

We take $\quad \Psi^{\mathsf{b}}_{i+1/2}\,\Delta x = -(0,\, g\,\hat{h}_s\,\Delta b,\, 0,\, g\,\hat{h}_f\,\Delta b)^{\mathsf{T}}\,, \quad \Delta b = b_{i+1} - b_i\,.$

Then, if initially steady state $\Rightarrow \mathcal{Z}^k \equiv 0 \Rightarrow$ updating formula gives $Q_i^{n+1} = Q_i^n$ $\Rightarrow$ equilibrium is maintained.

If solution close to a steady state, it is the deviation from equilibrium that is decomposed $\Rightarrow$ perturbations are well modeled.

Interphase Drag Terms

Consider system with drag source terms:

$$\partial_t q + A(q)\partial_x q = \psi^{\mathsf{b}}(q) + \psi^{\mathsf{D}}(q)\,,$$

$$\psi^{\mathsf{D}}(q) = (0, \gamma\, F^{\mathsf{D}},\, 0,\, -F^{\mathsf{D}})^{\mathsf{T}}\,, \qquad F^{\mathsf{D}} = D(h_s + h_f)(v_f - v_s)\,.$$

Drag function: $D = \mathcal{D}/\rho_f\,, \qquad \mathcal{D} = S_1(\varphi;\sigma) + S_2(\varphi;\sigma)|v_f - v_s|$.

σ = parameters, e.g. ρ_s, ρ_f, d_s (grain diameter).

Note: At rest $\psi^{\mathsf{D}}(q) = 0 \quad \Rightarrow$ no influence on balance conditions at rest.

Fractional Step Method

1. Solve over Δt the system $\partial_t q + A(q)\partial_x q - \psi^{\mathsf{b}}(q) = 0$, as described.
2. Solve exactly over Δt the system of ODEs $\partial_t q = \psi^{\mathsf{D}}(q)$.

$\longrightarrow$ Efficient modeling of both fast and slow velocity relaxation processes.

Eigenvalues Computation

Explicit expression of the eigenvalues not available: need numerical computation.

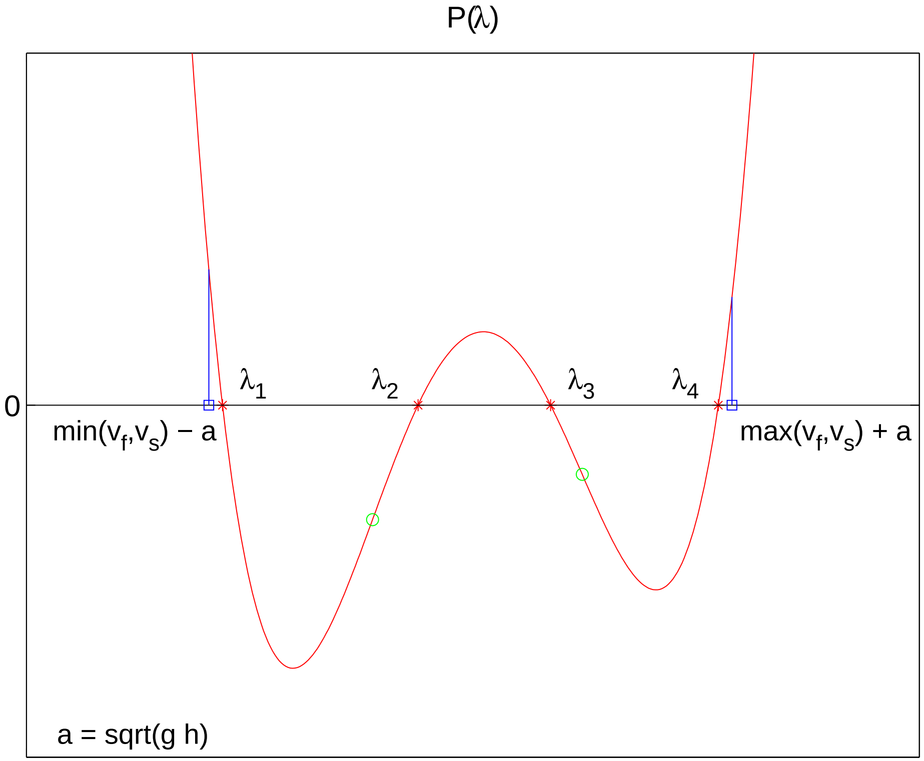

External eigenvalues $\lambda_{1,4}$ computed through Newton iteration with starting guess $\min(v_f, v_s) - a$ for λ_1 and $\max(v_f, v_s) + a$ for λ_4.

For $\lambda \in [\min(v_f, v_s) - a, \lambda_1]$: $P'(\lambda) < 0, P''(\lambda) > 0,$

For $\lambda \in [\lambda_4, \max(v_f, v_s) + a]$: $P'(\lambda) > 0,\ P''(\lambda) > 0.$

- Known $\lambda_{1,4}$: Vieta's formulas to obtain the internal eigenvalues $\lambda_{2,3}$.
- Explicit expressions of right eigenvectors r_k and left eigenvectors l_k in terms of $\lambda_k,\ k = 1, \ldots, 4$.

Initial flow hump with higher fluid content

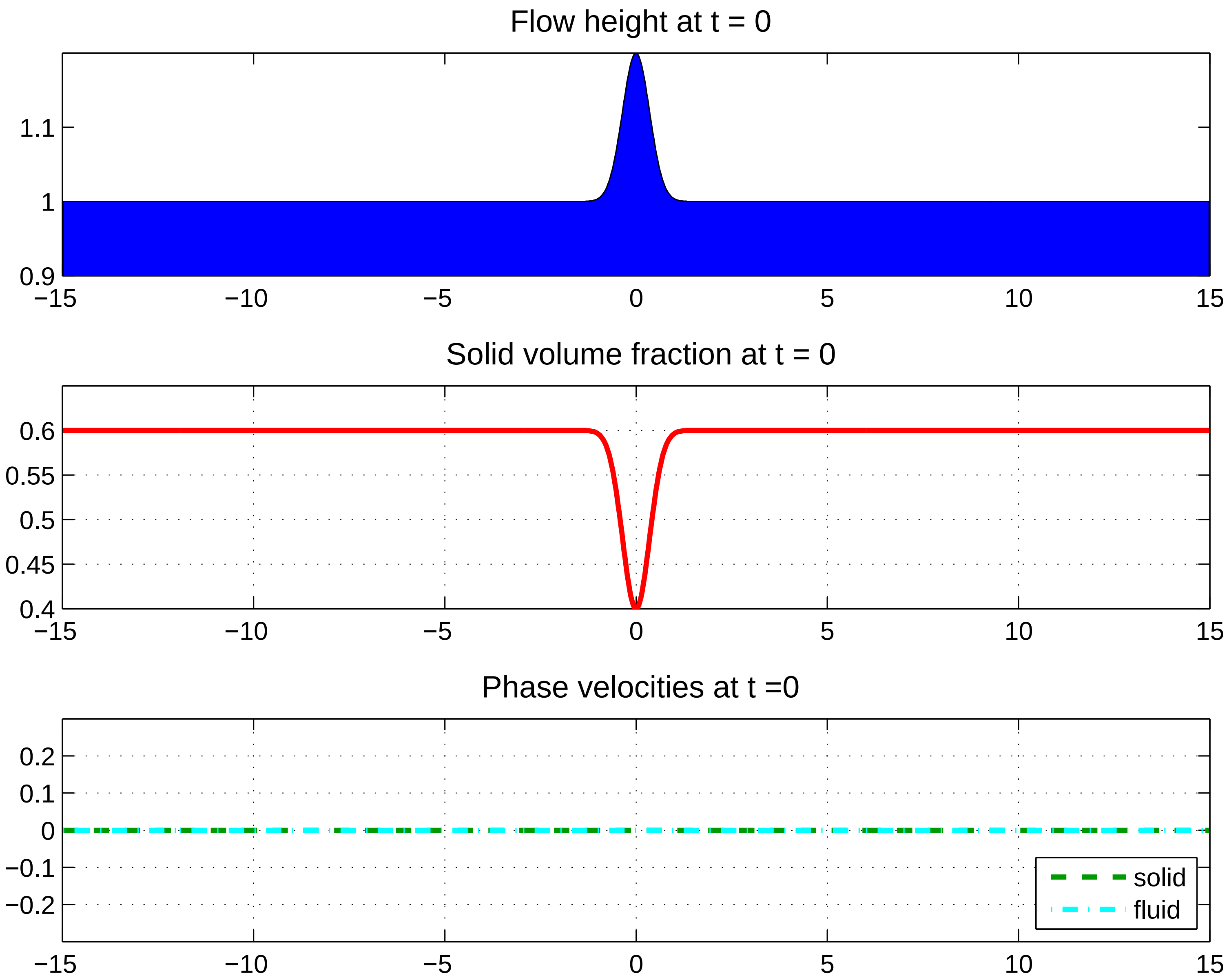

Grid cells = 1000, 2nd order (MC limiter), CFL = 0.9.

Initial flow hump with higher fluid content

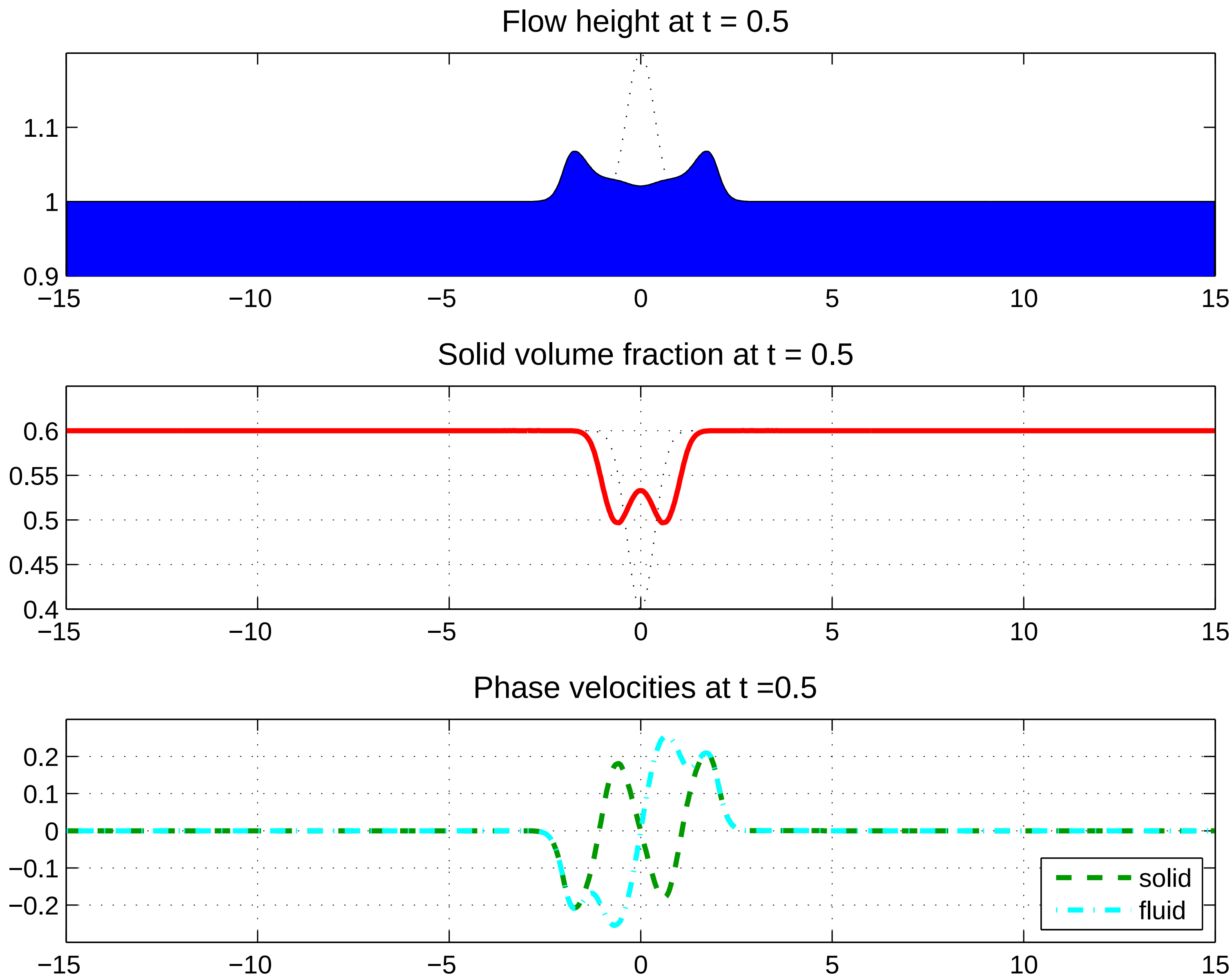

Initial flow hump with higher fluid content

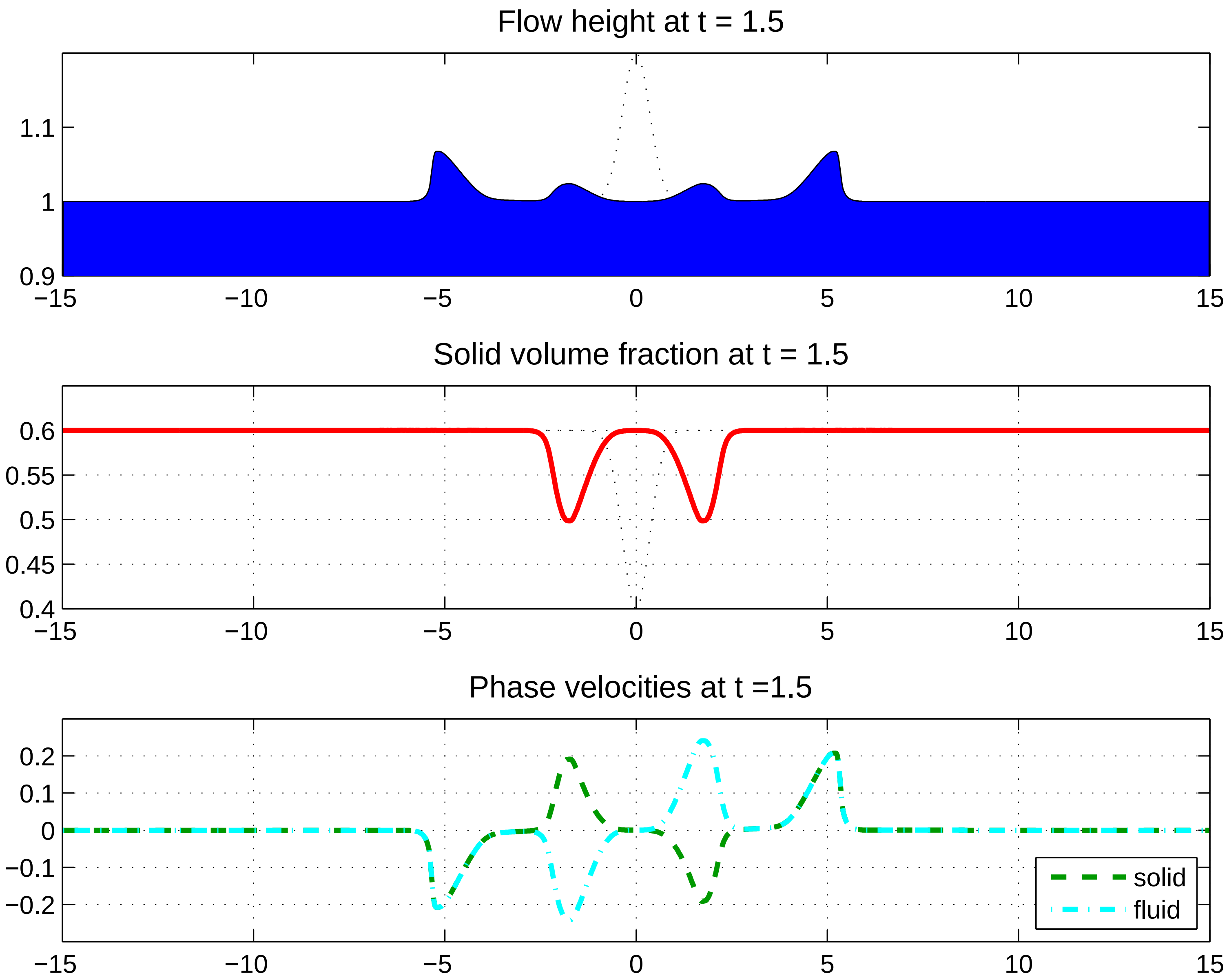

Initial flow hump with higher fluid content

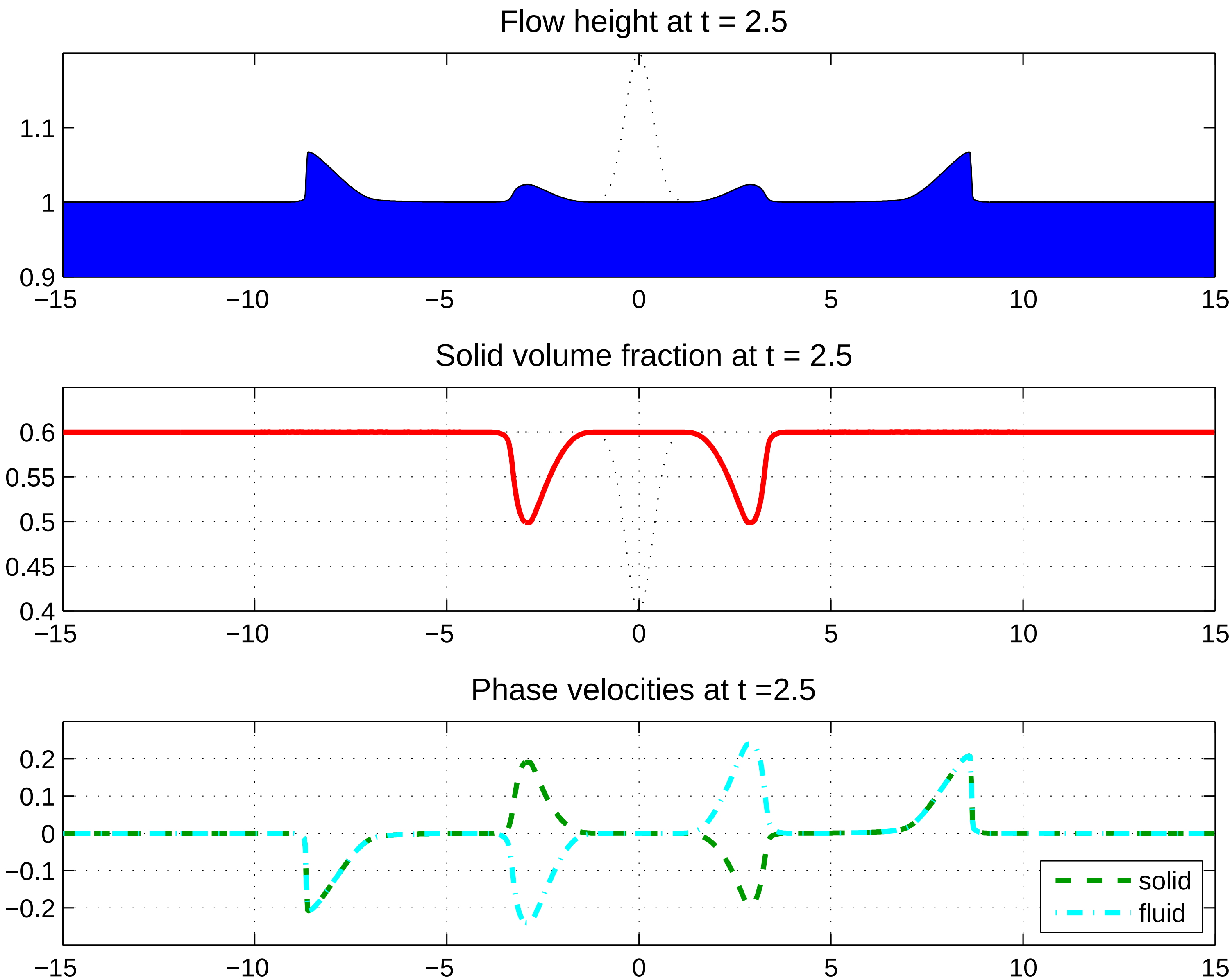

Initial flow hump with higher fluid content

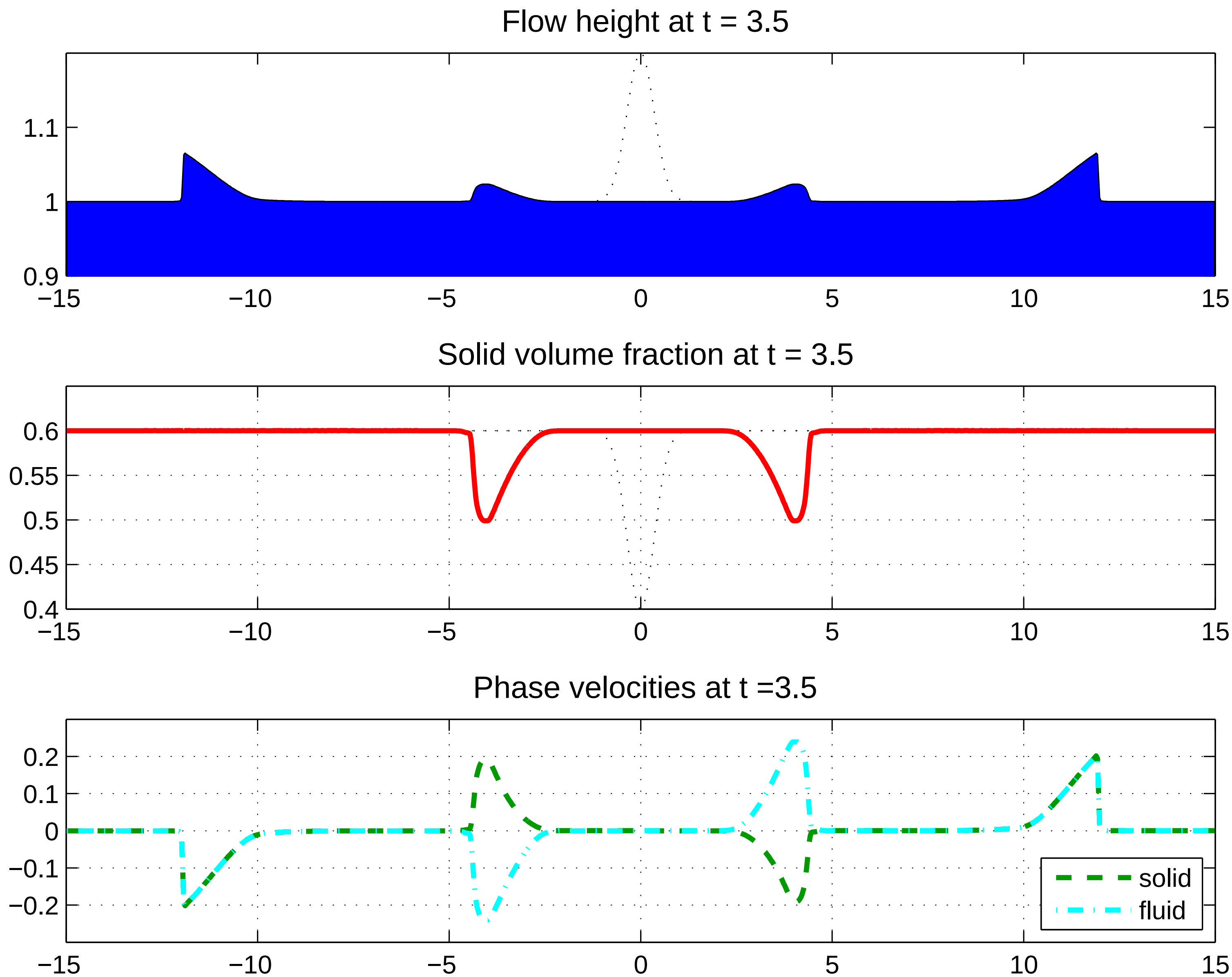

Only initial variation of h

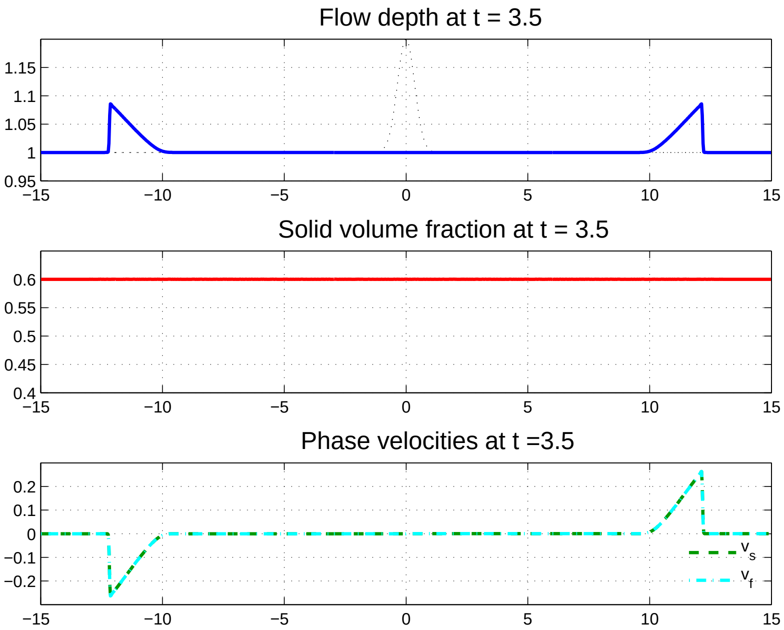

Only initial variation of φ

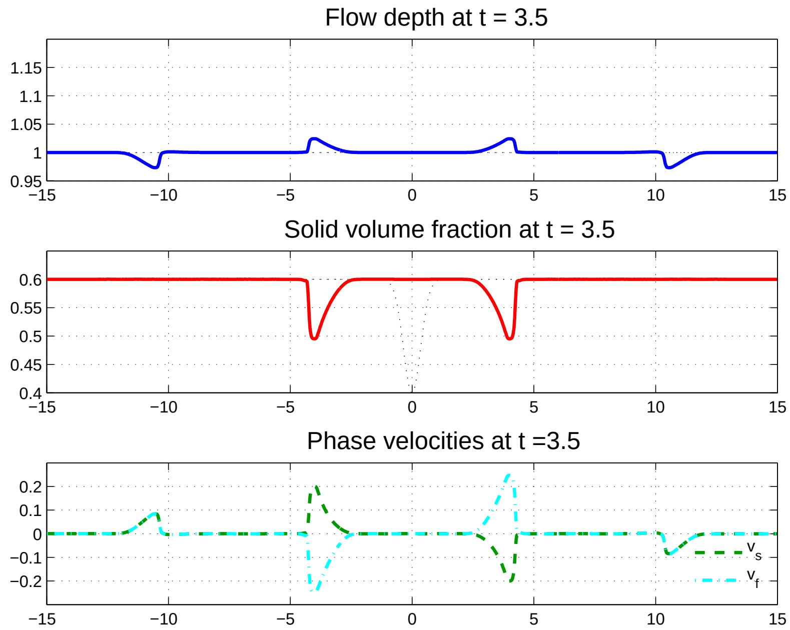

Numerical Test: Perturbation of a steady state at rest

Extension of LeVeque's classical test [JCP, vol. 146, 1998]

$$b(x) = \begin{cases} 0.25(\cos(\pi(x-0.5)/0.1)+1) & \text{if } |x-0.5| < 0.1\,, \\ 0 & \text{otherwise.} \end{cases}$$

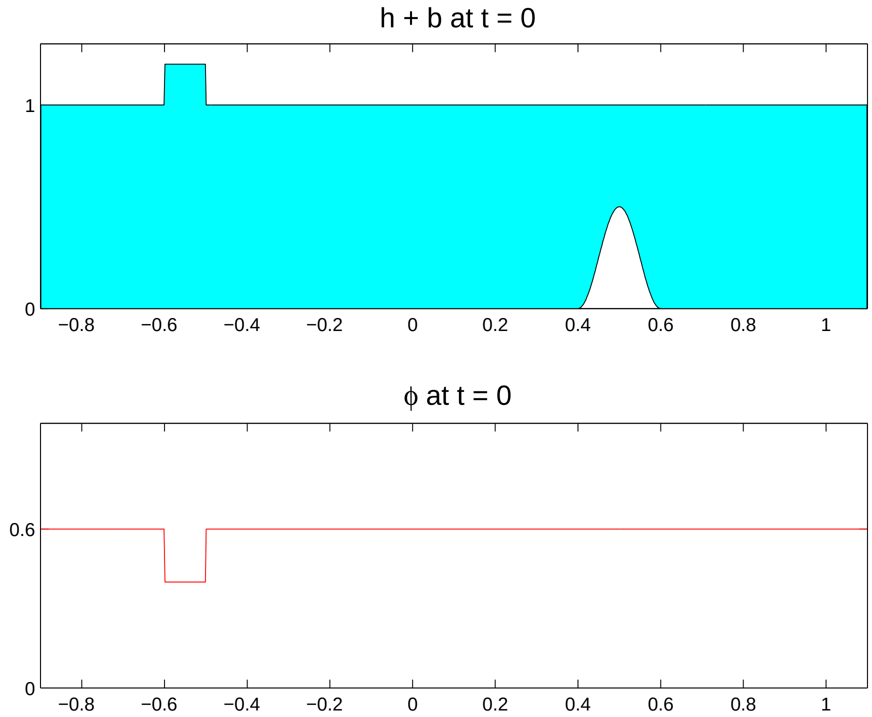

For $-0.6 < x < -0.5$:

$h(x,0) = h_0 + \tilde{h}$ and

$\varphi(x,0) = \varphi_0 - \tilde{\varphi}\,.$

$h_0 = 1\,,\ \varphi_0 = 0.6\,,$

$\tilde{h} = \tilde{\varphi} = 10^{-3}\,.$

Grid cells = 100, 2nd order, CFL = 0.9.

Reference curve: Grid cells = 1000.

Perturbation of a steady state at rest

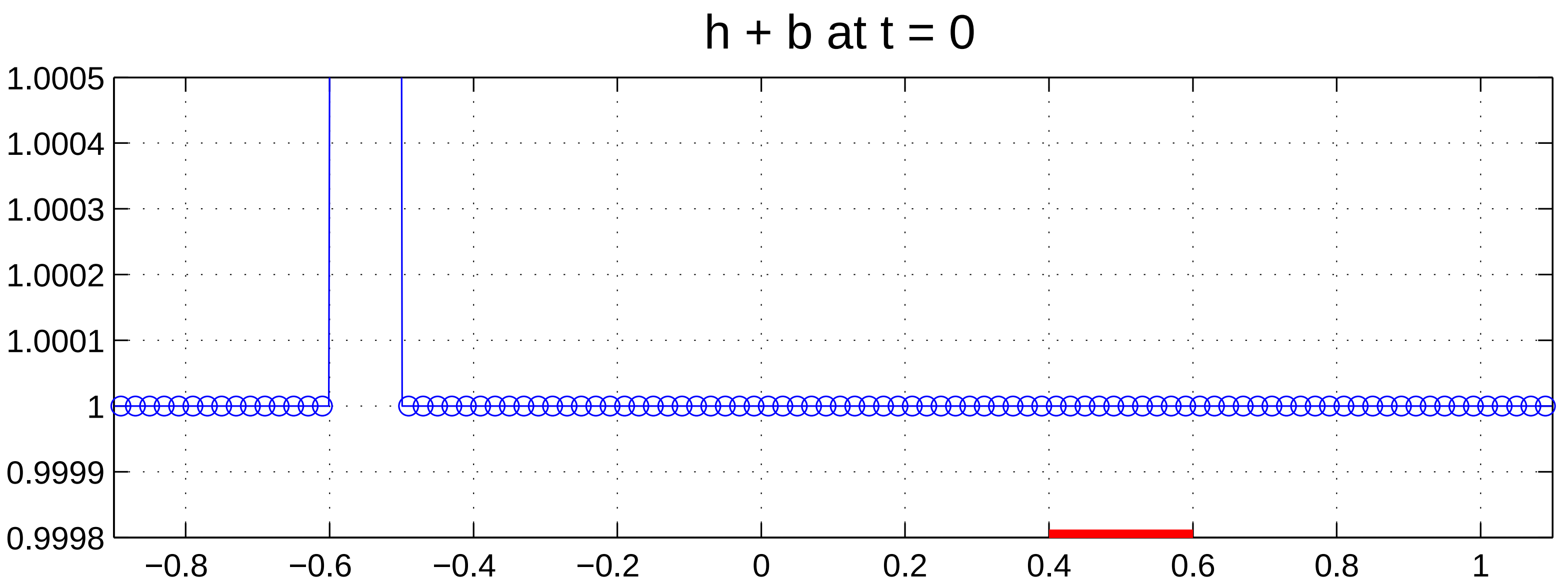

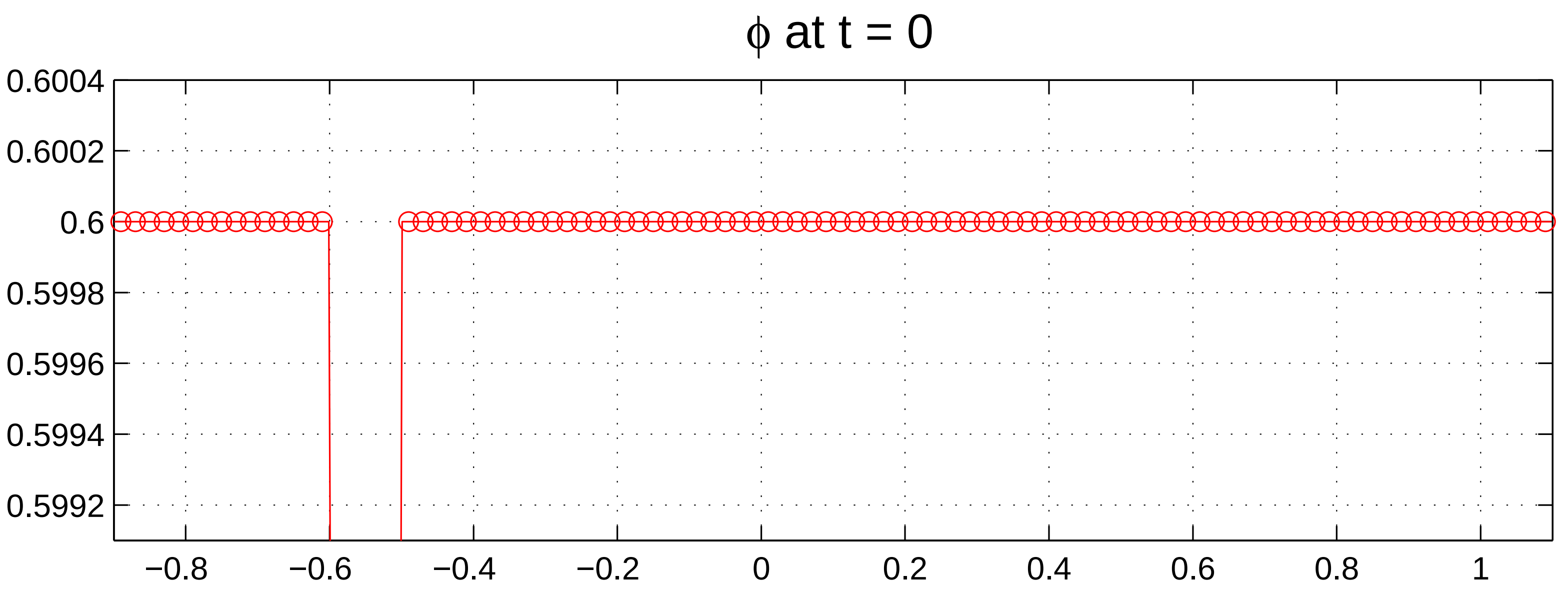

Perturbation of a steady state at rest

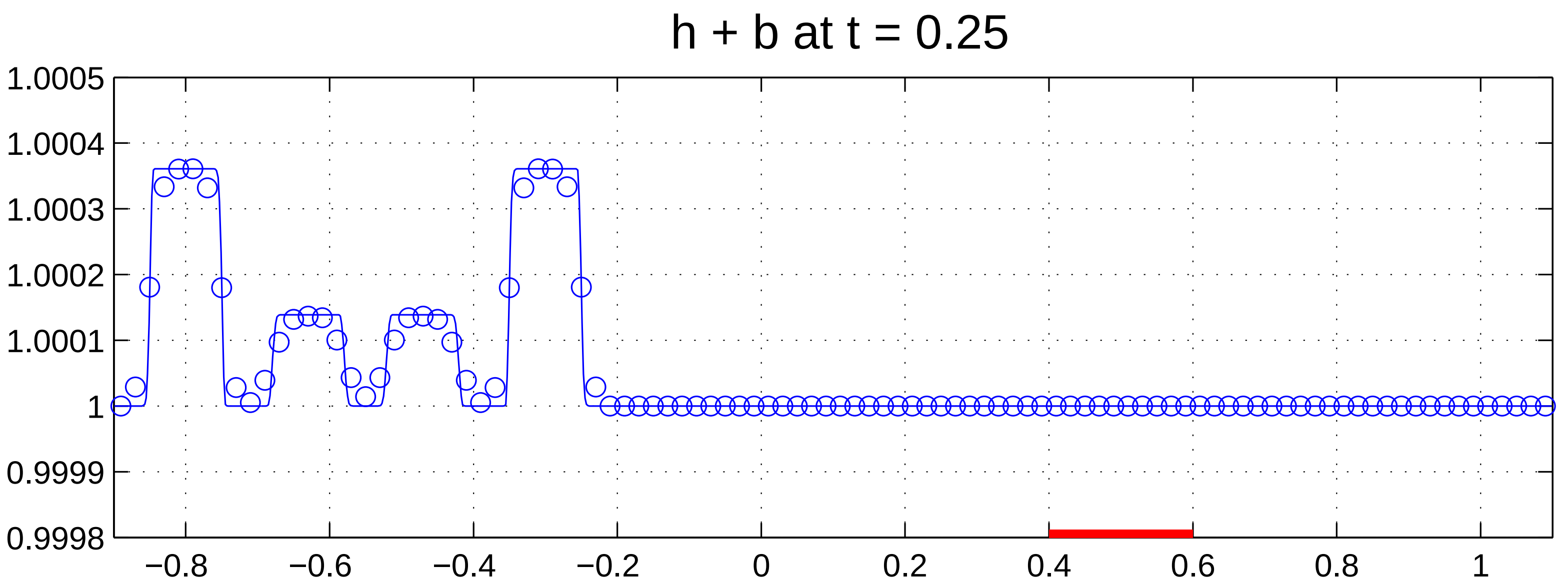

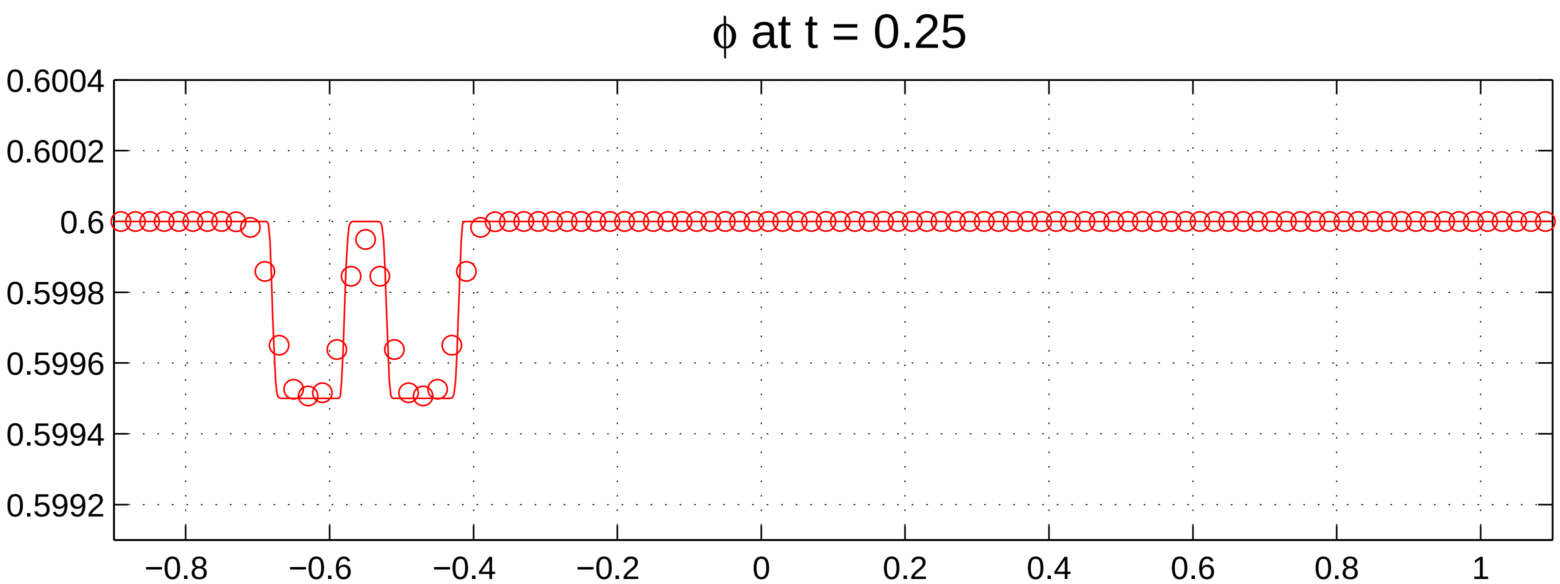

Perturbation of a steady state at rest

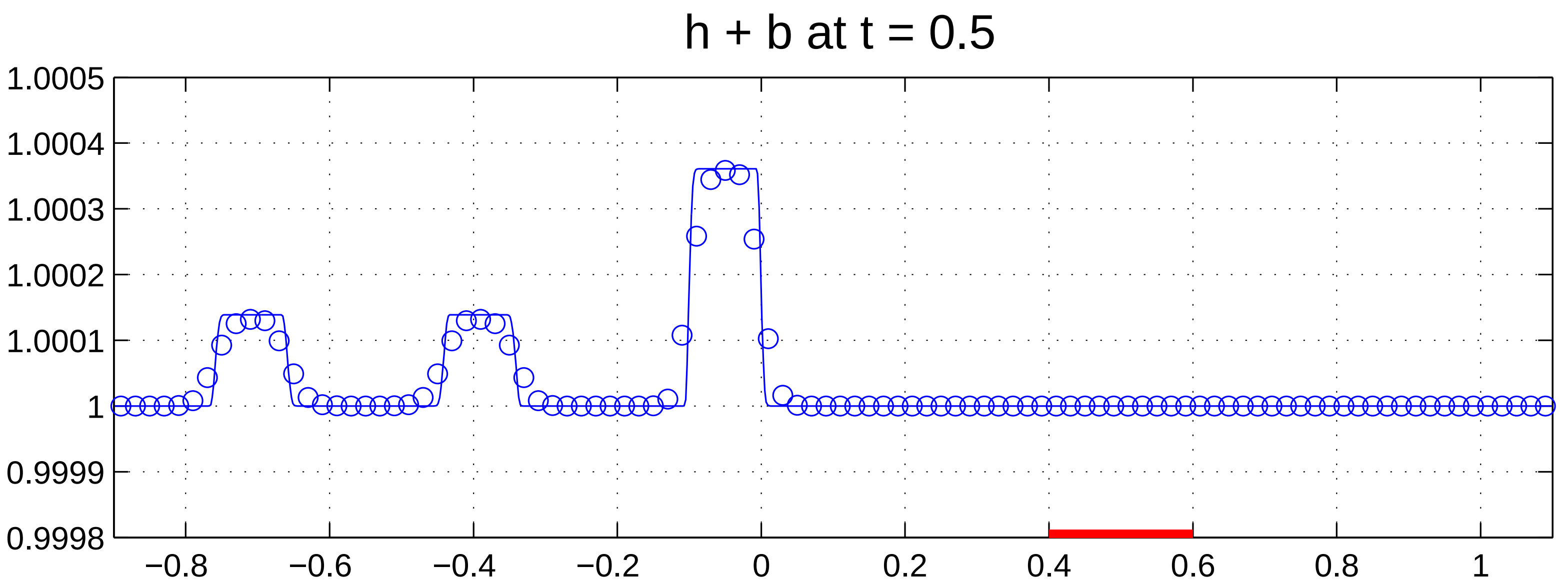

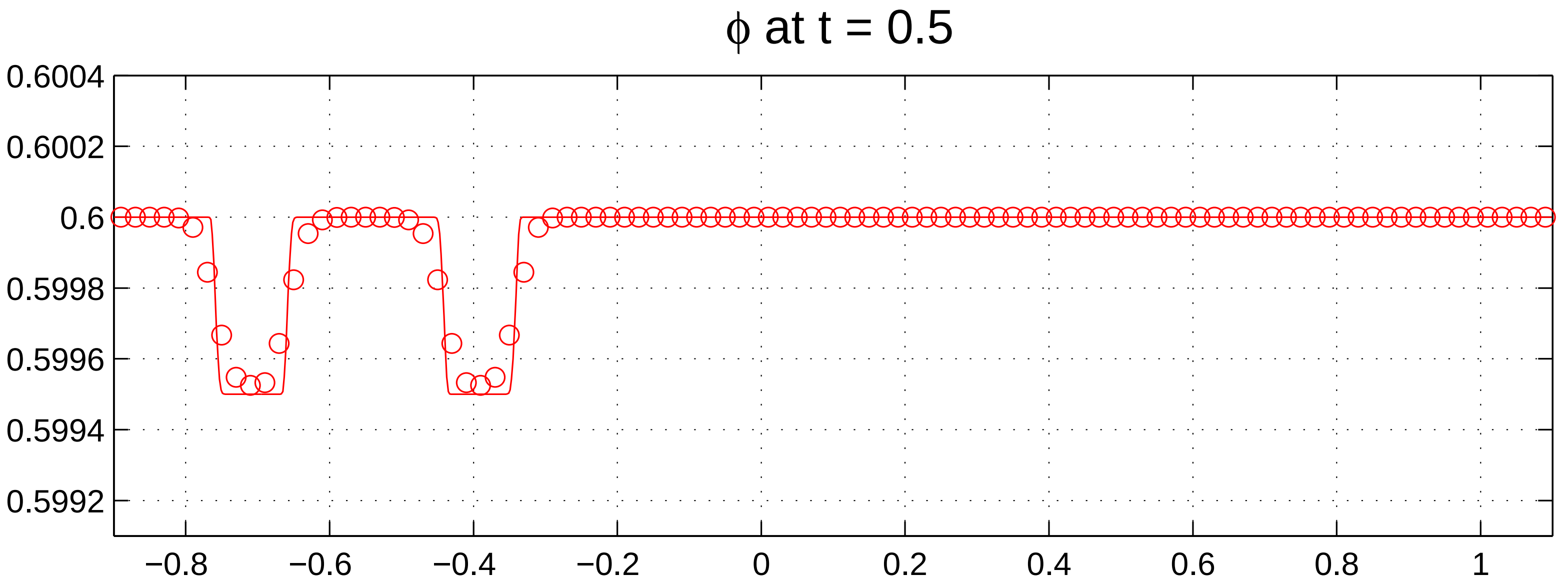

Perturbation of a steady state at rest

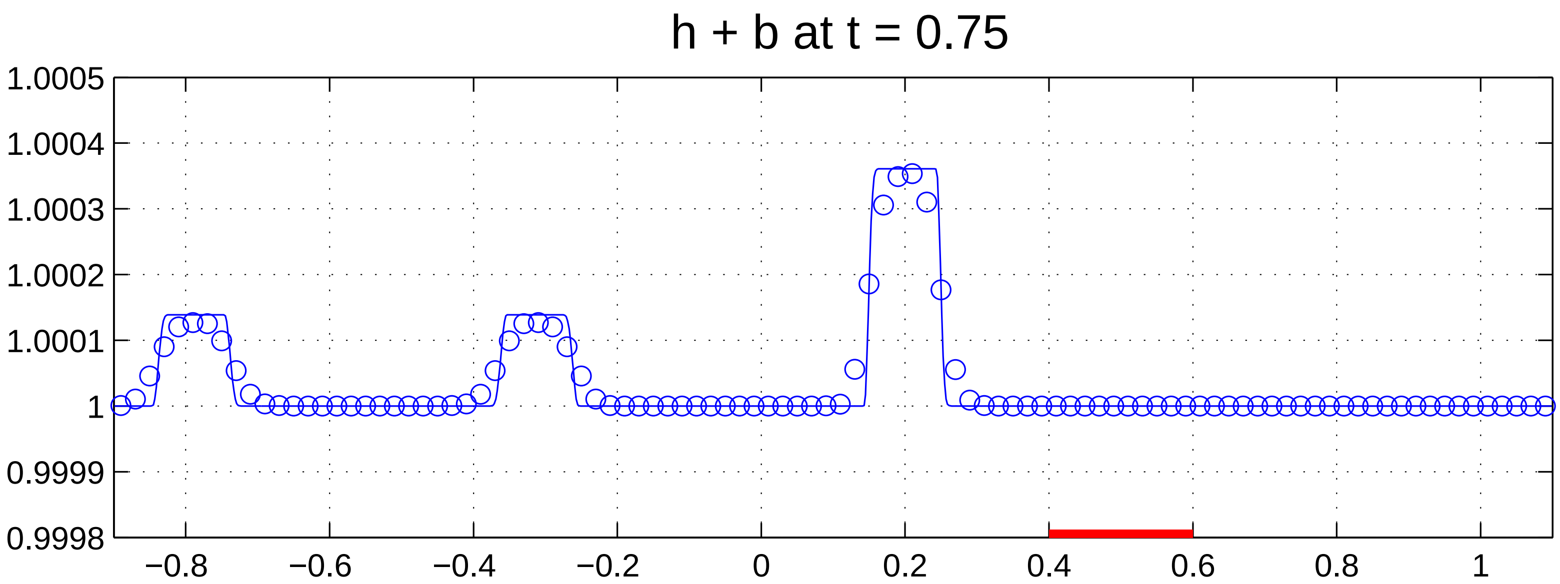

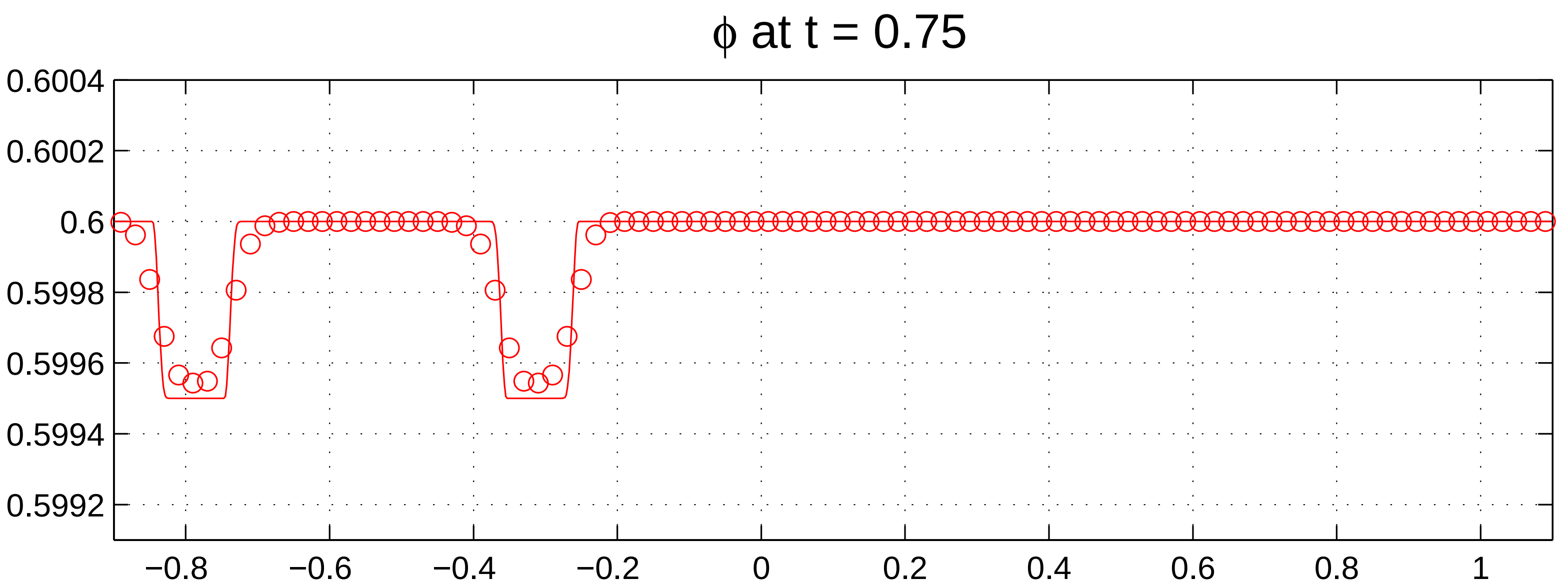

Perturbation of a steady state at rest

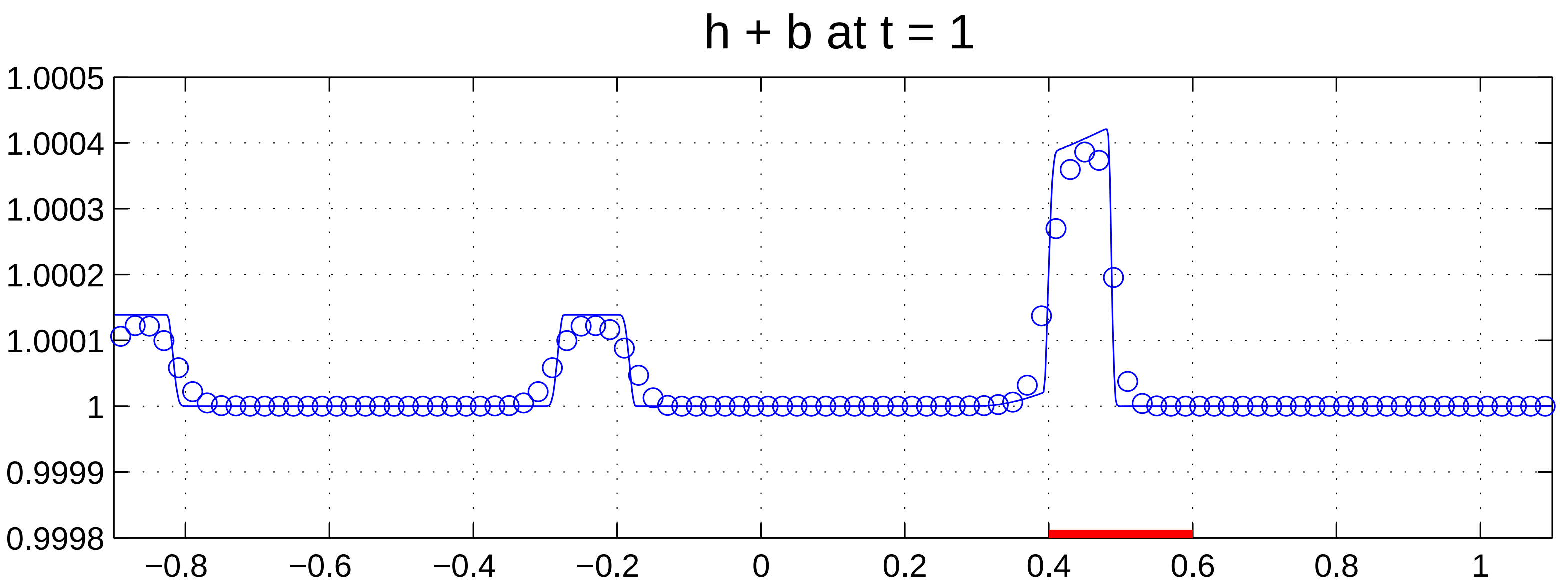

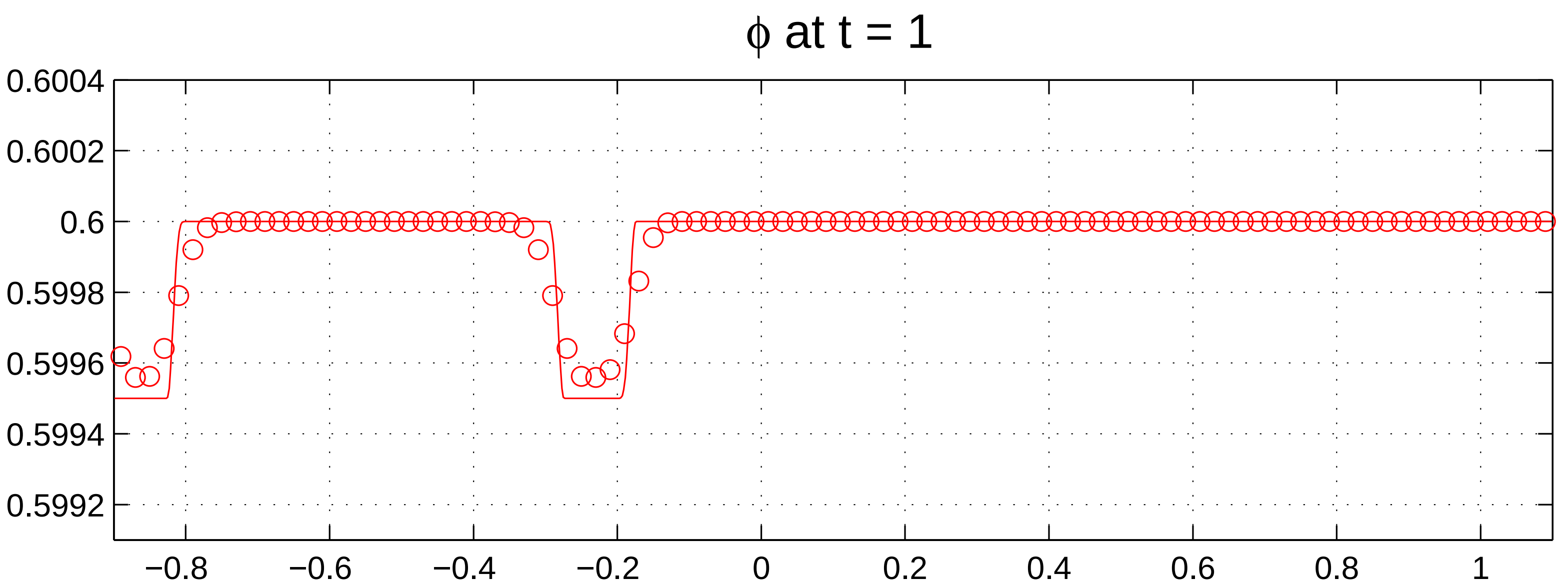

Perturbation of a steady state at rest

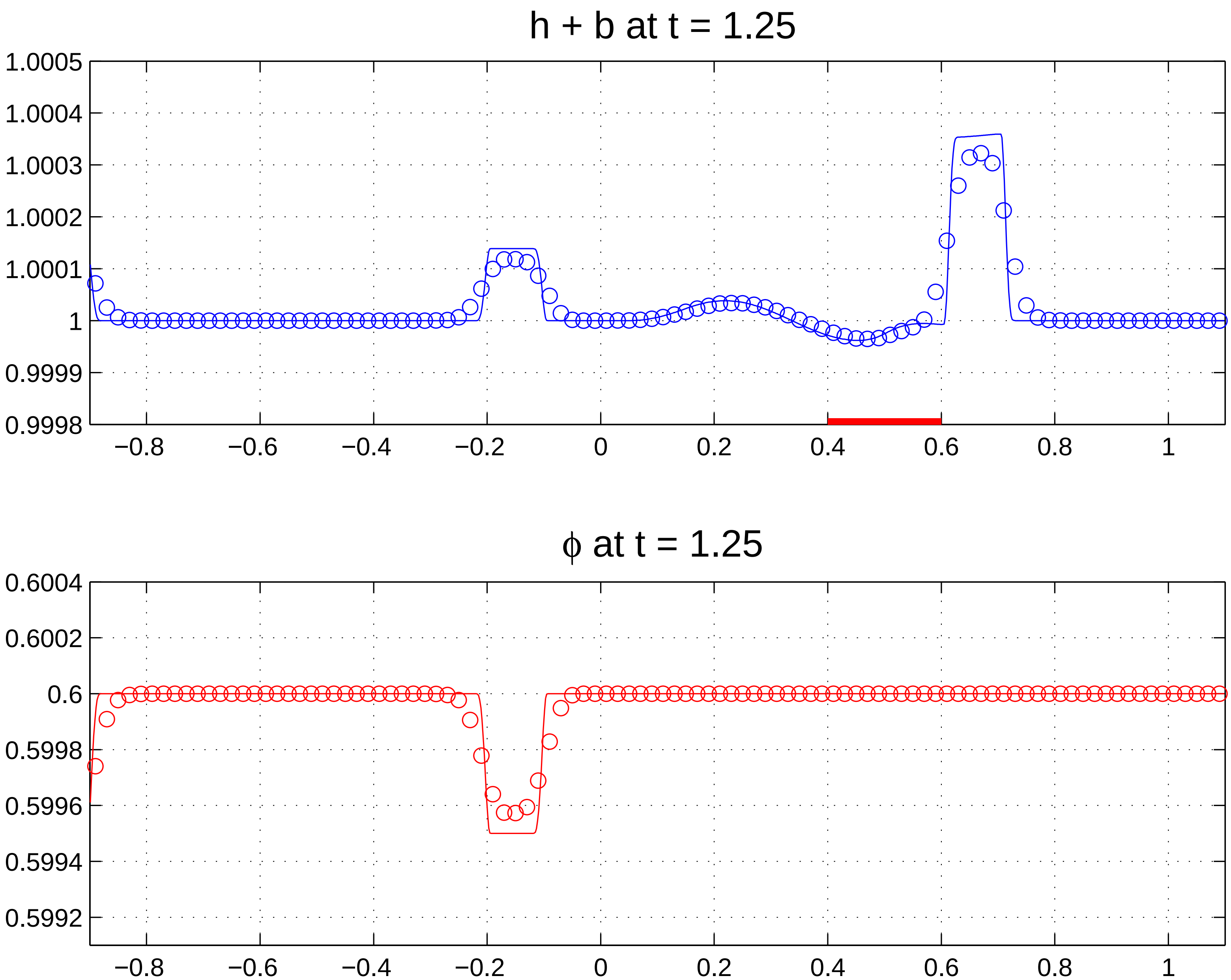

Perturbation of a steady state at rest

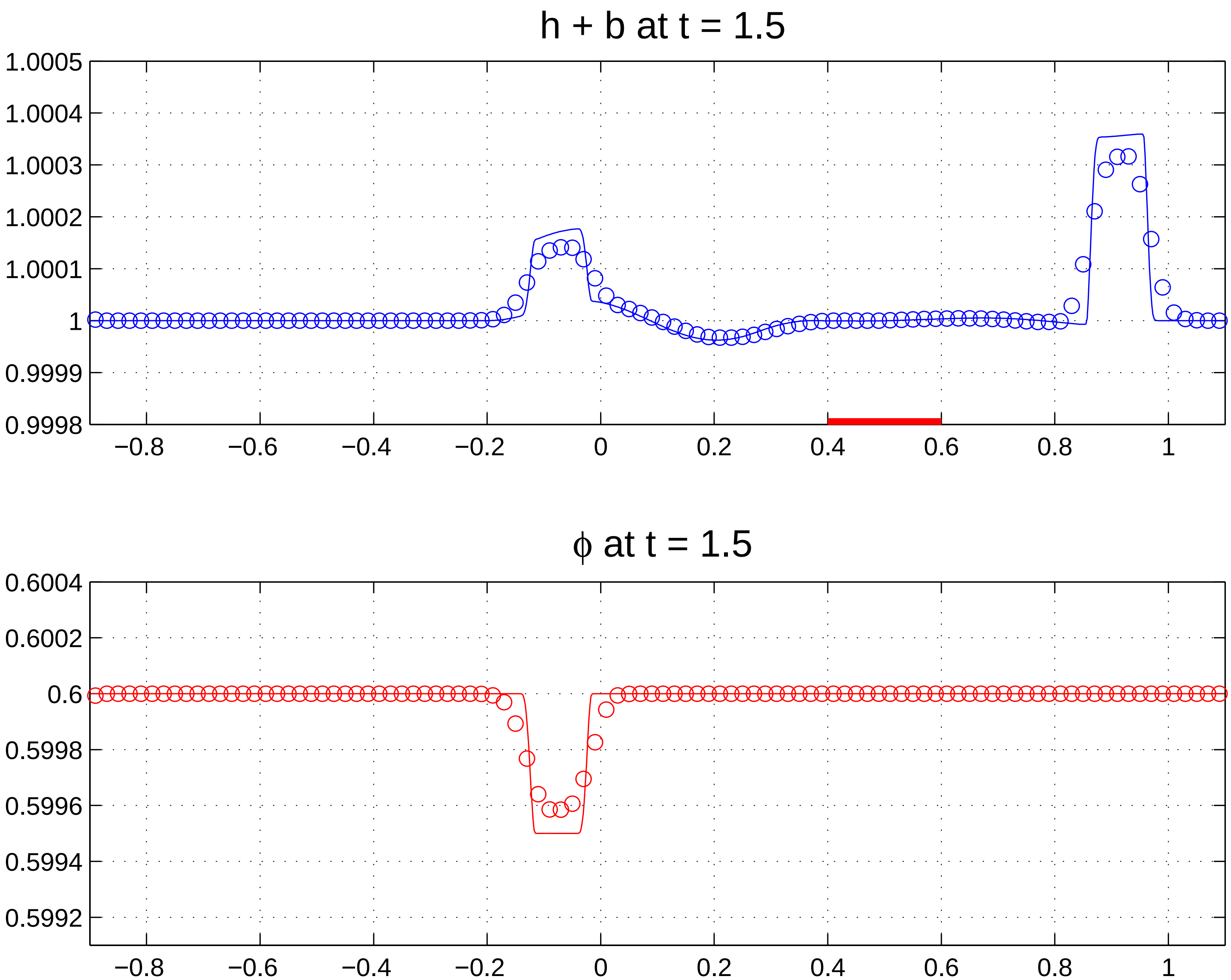

Perturbation of a steady state at rest

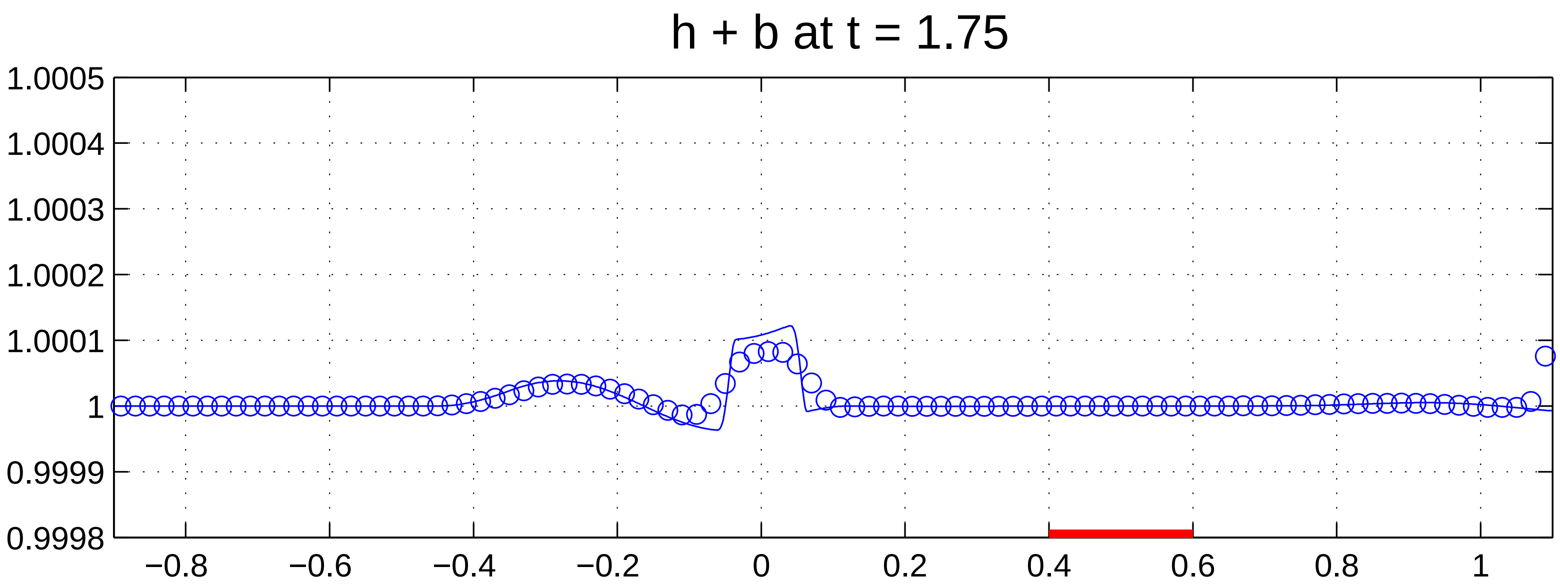

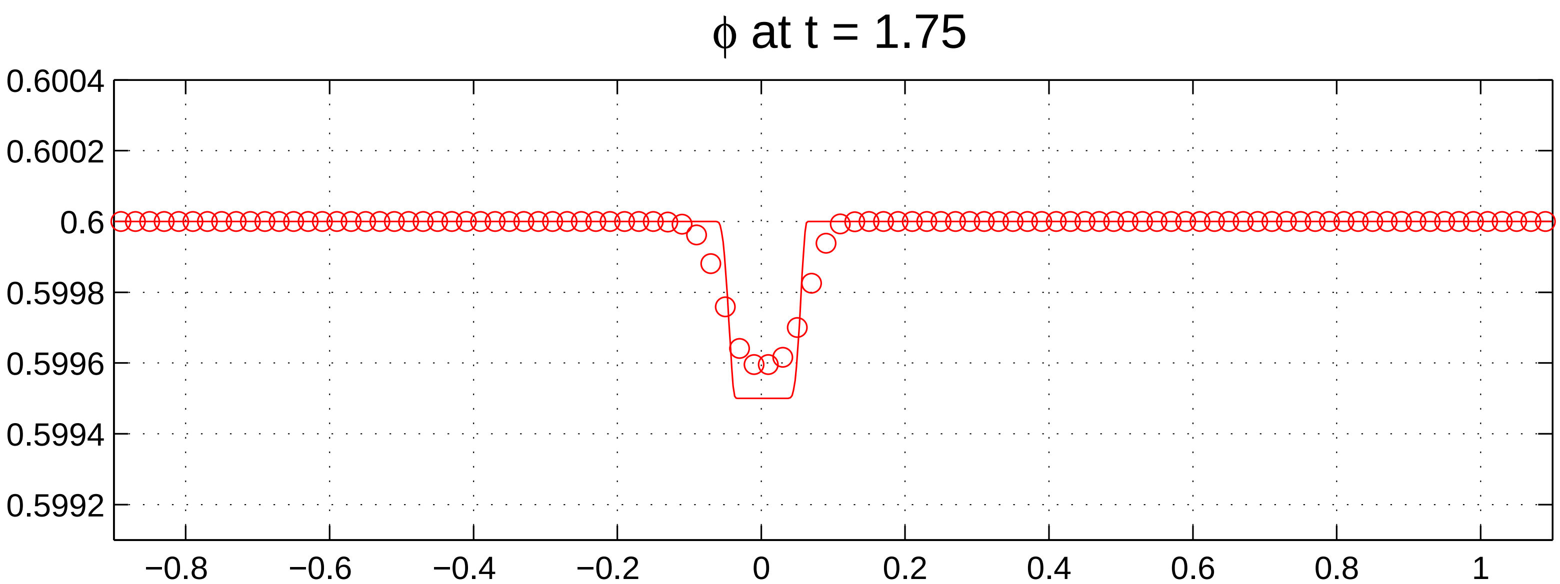

Perturbation of a steady state at rest

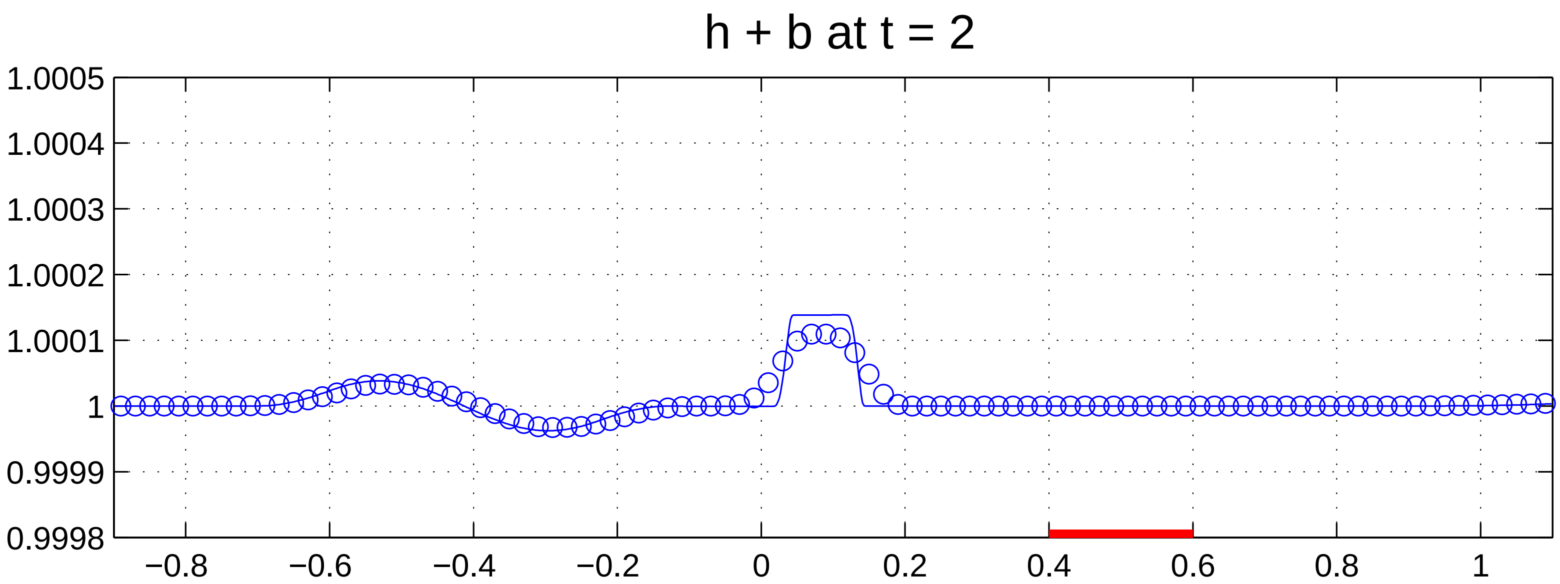

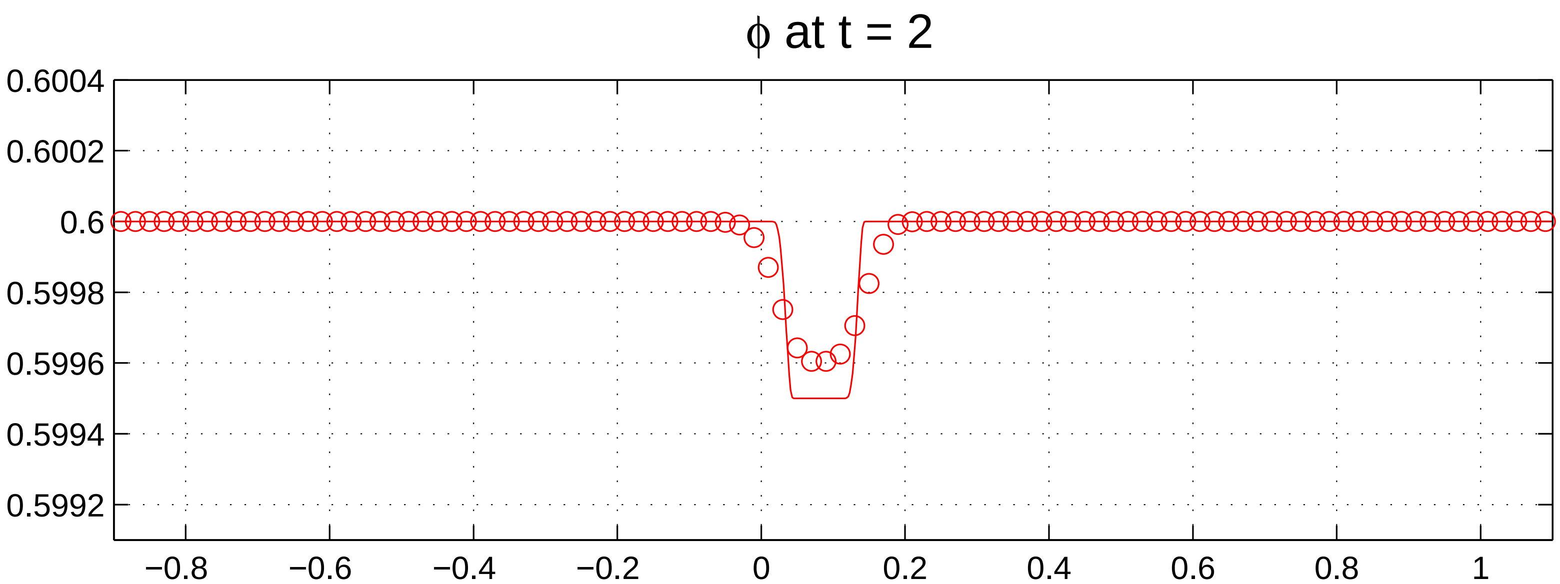

Perturbation of a steady state at rest

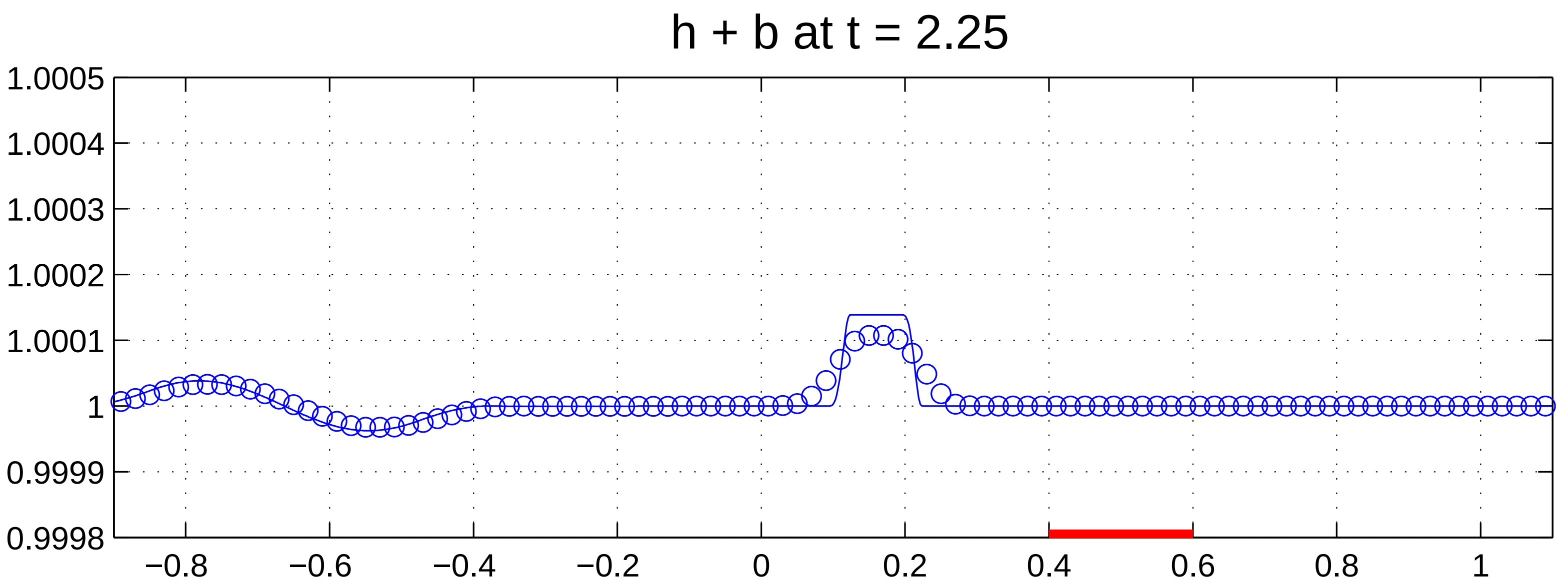

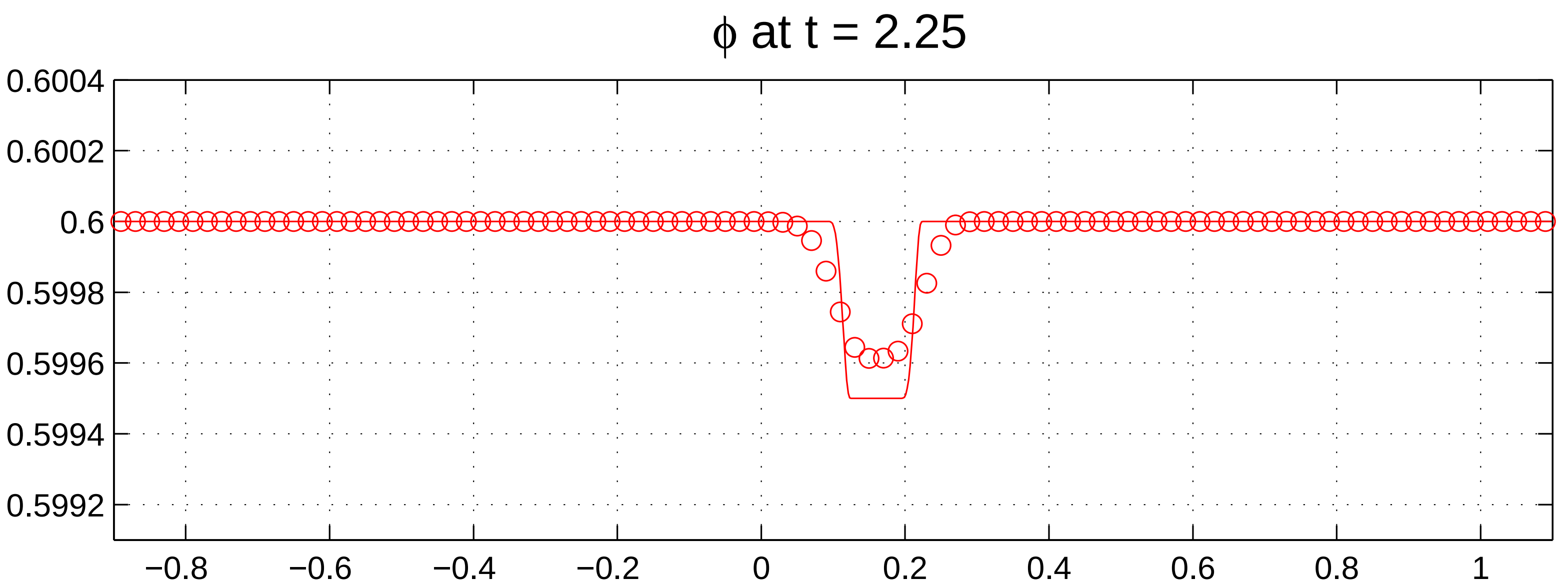

Perturbation of a steady state at rest

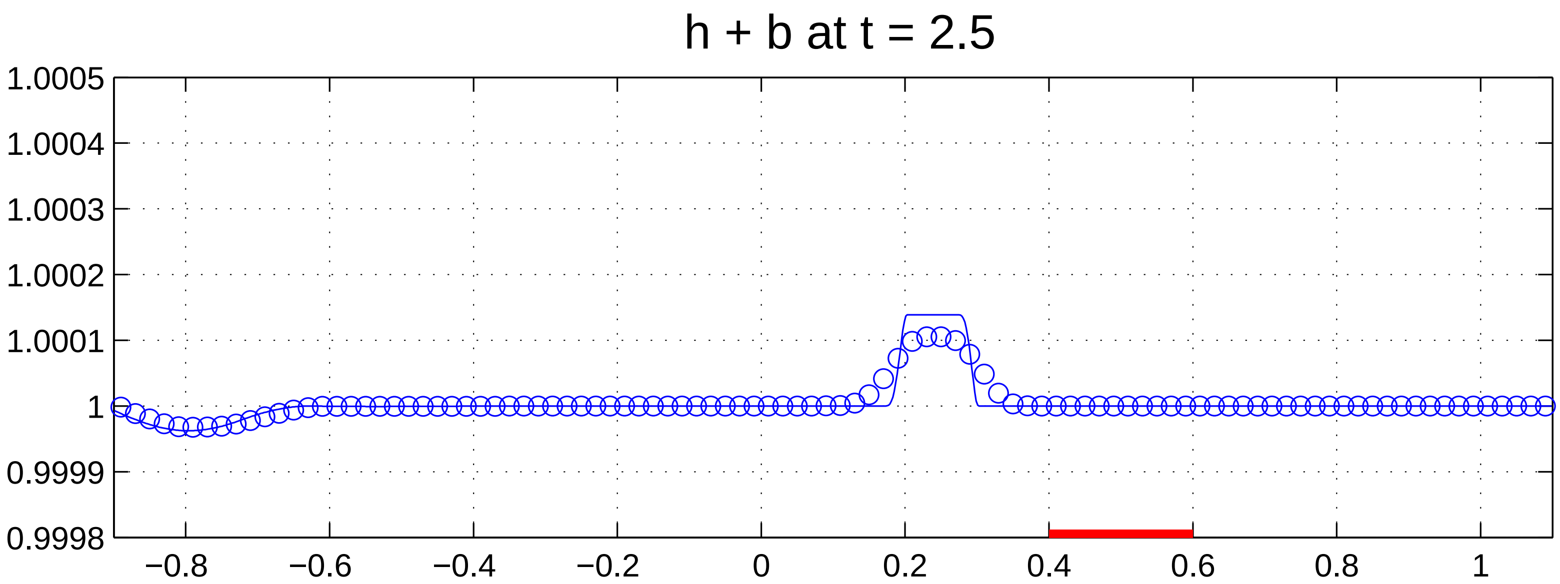

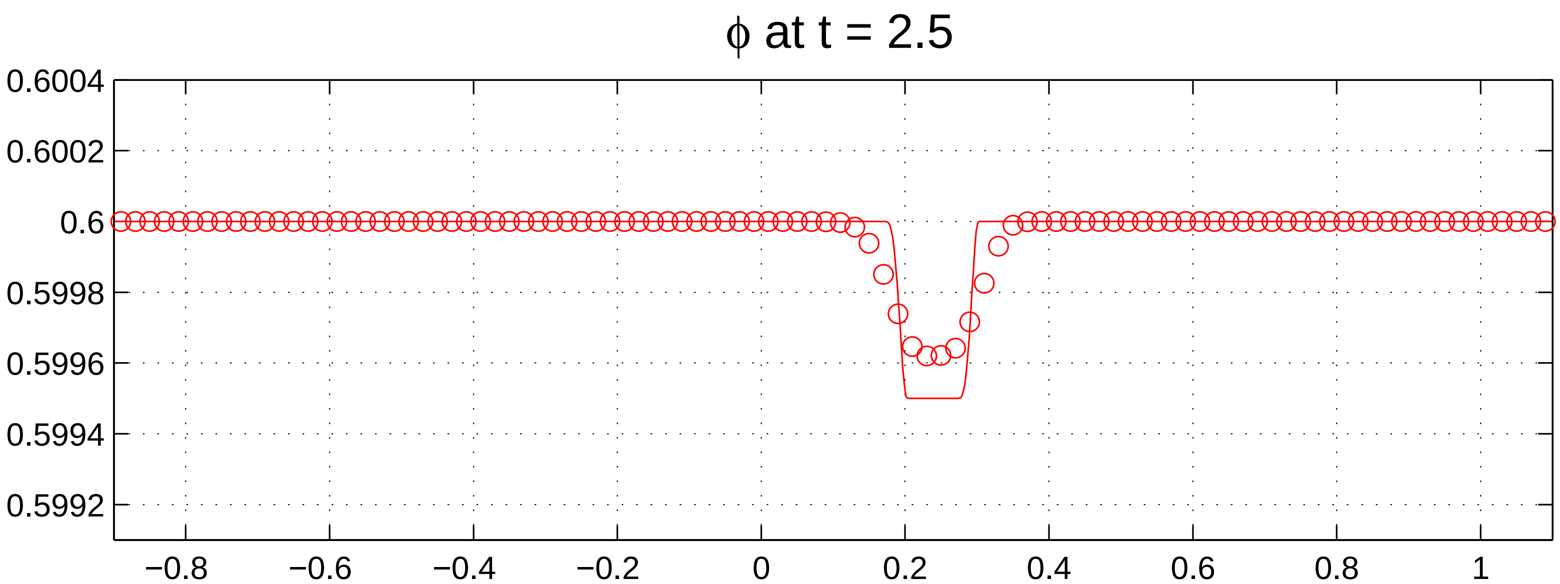

Perturbation of a steady state at rest

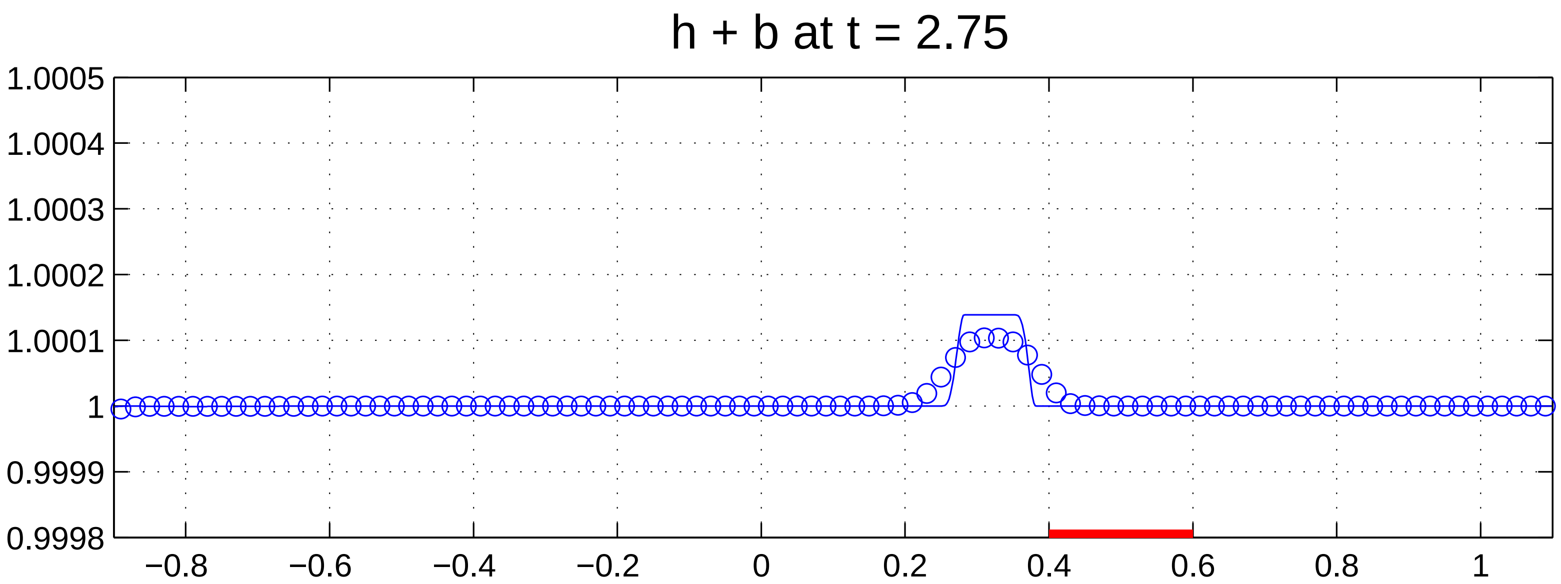

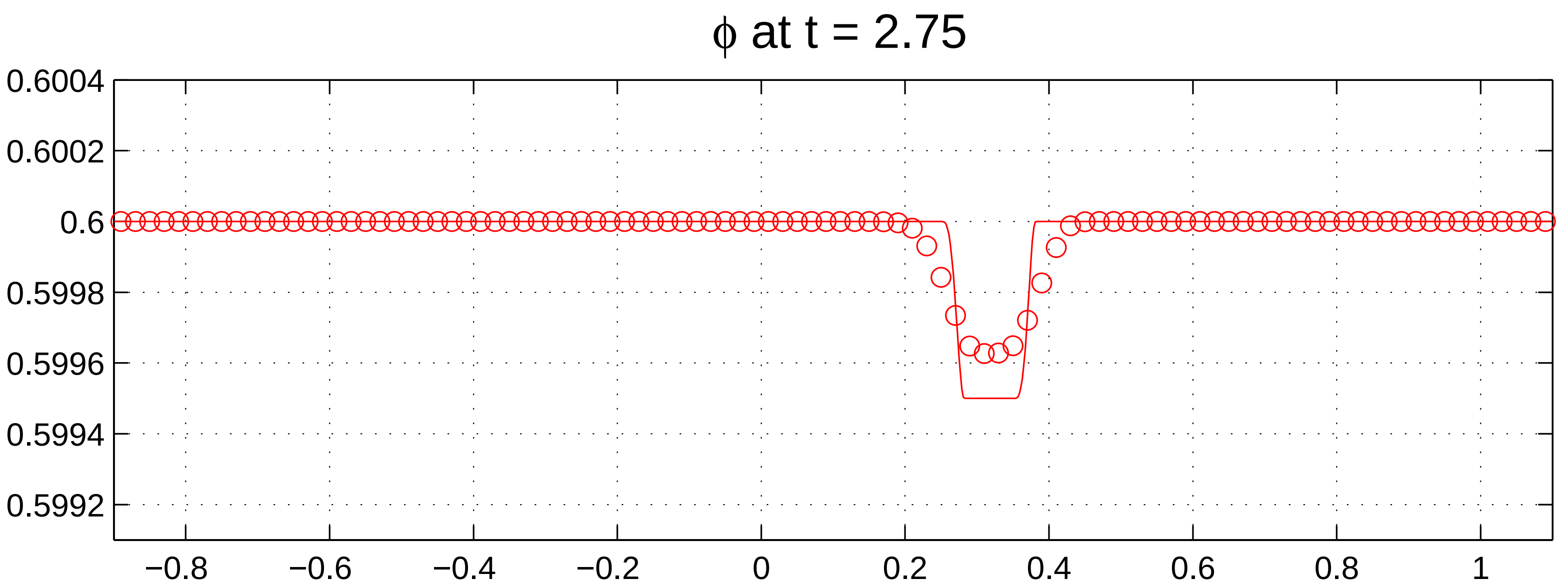

Perturbation of a steady state at rest

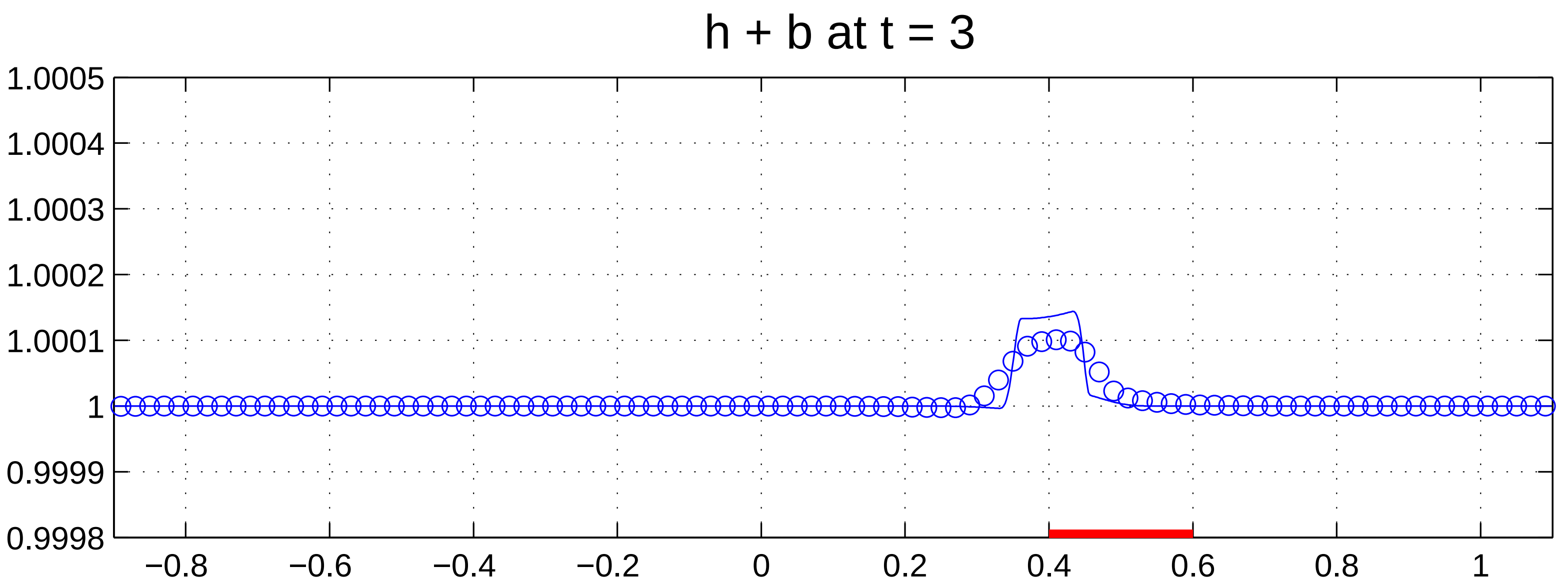

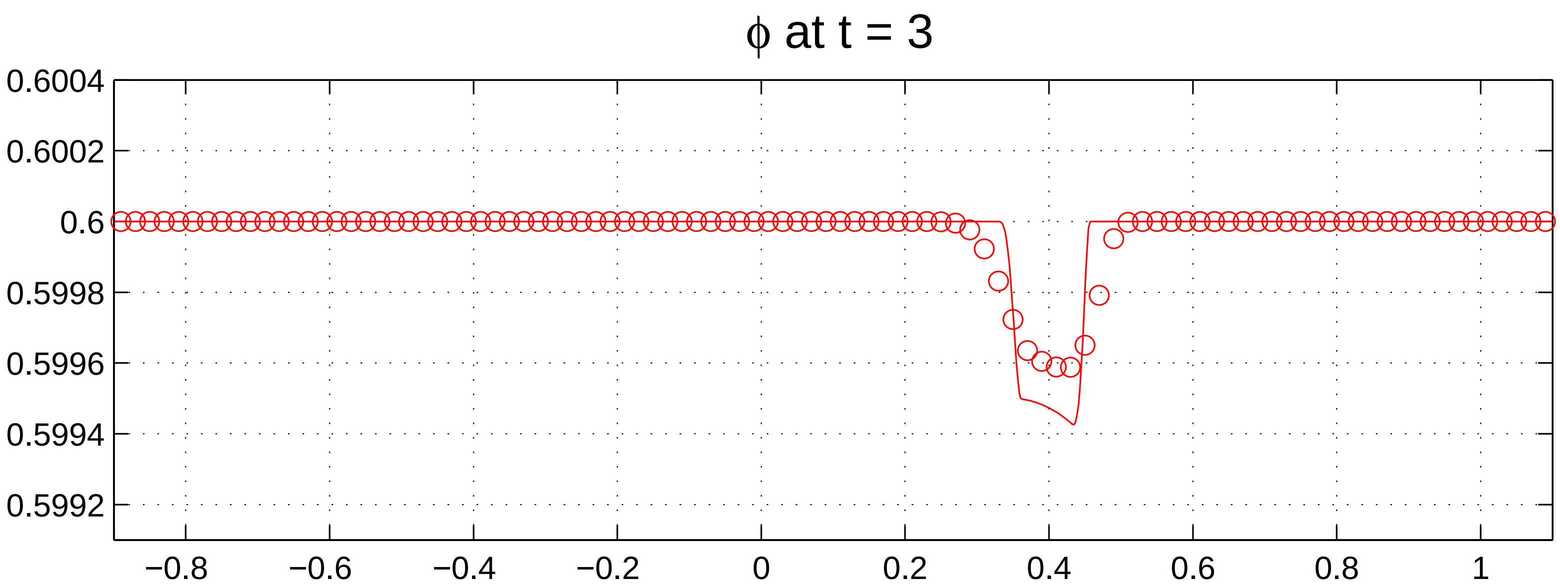

Perturbation of a steady state at rest

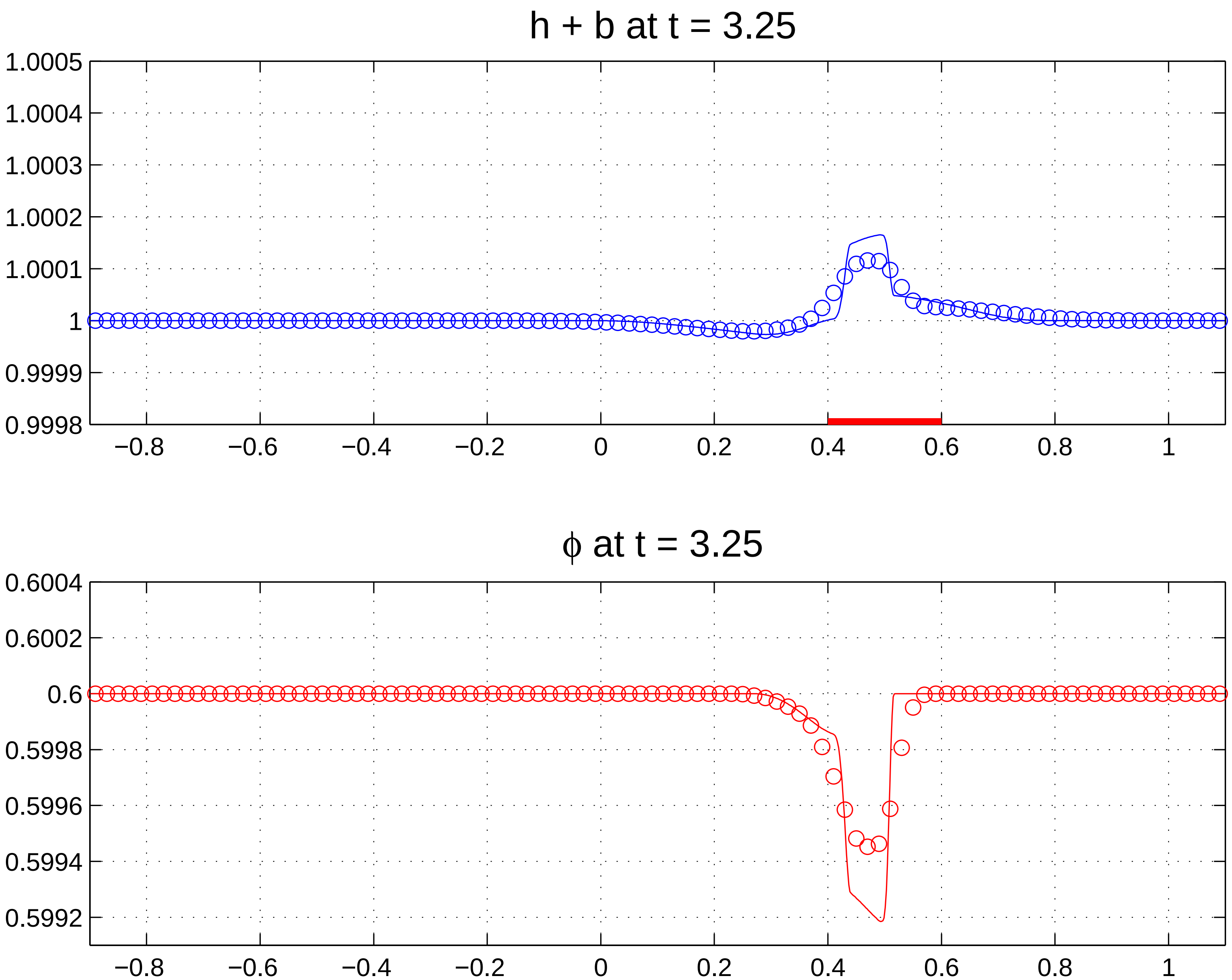

Perturbation of a steady state at rest

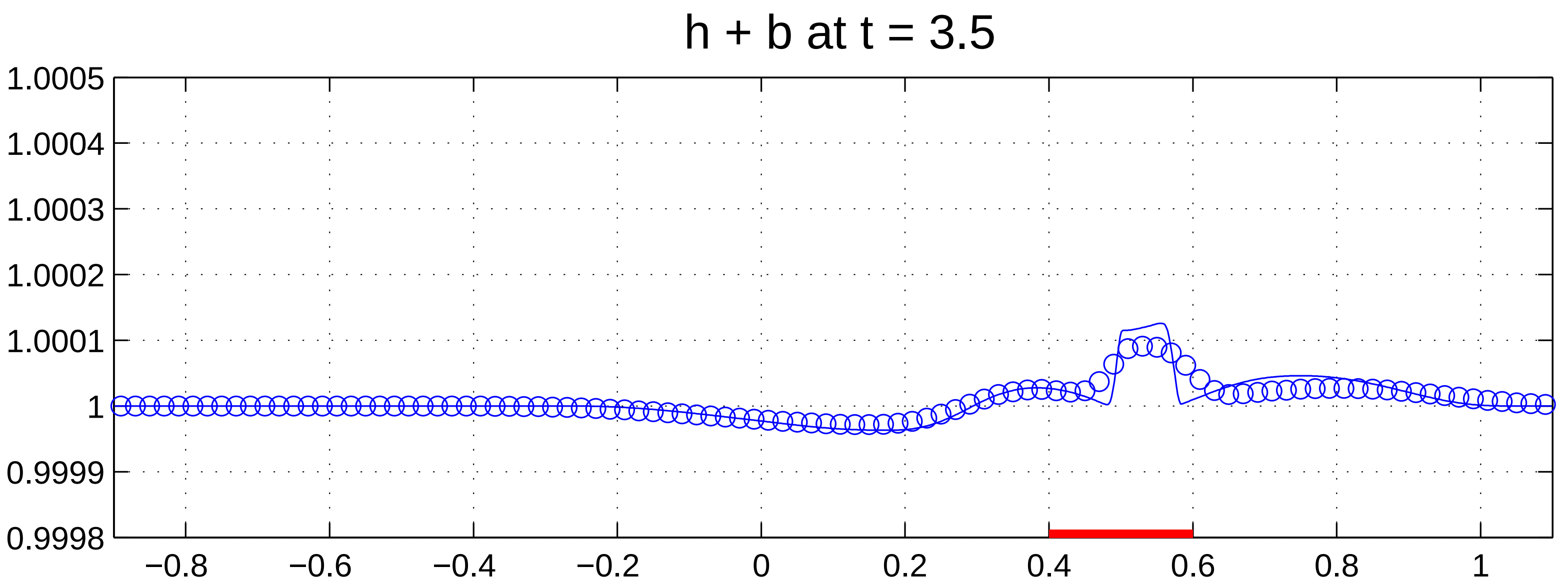

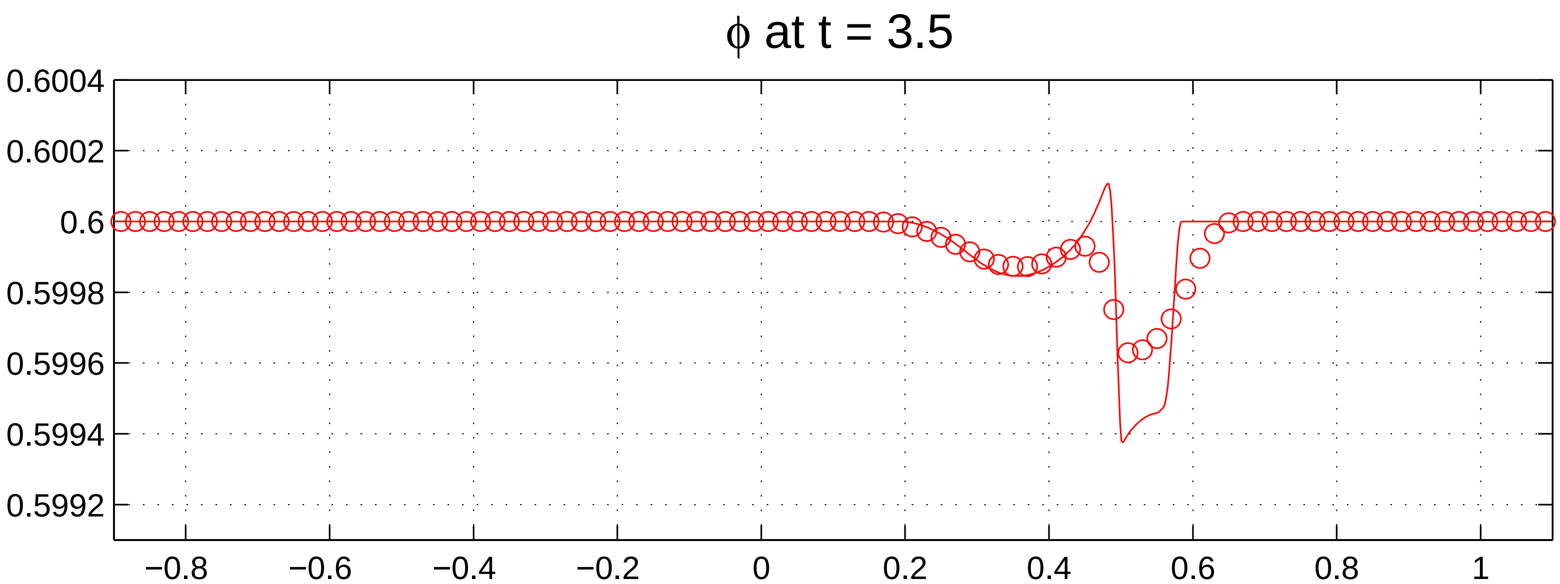

Perturbation of a steady state at rest

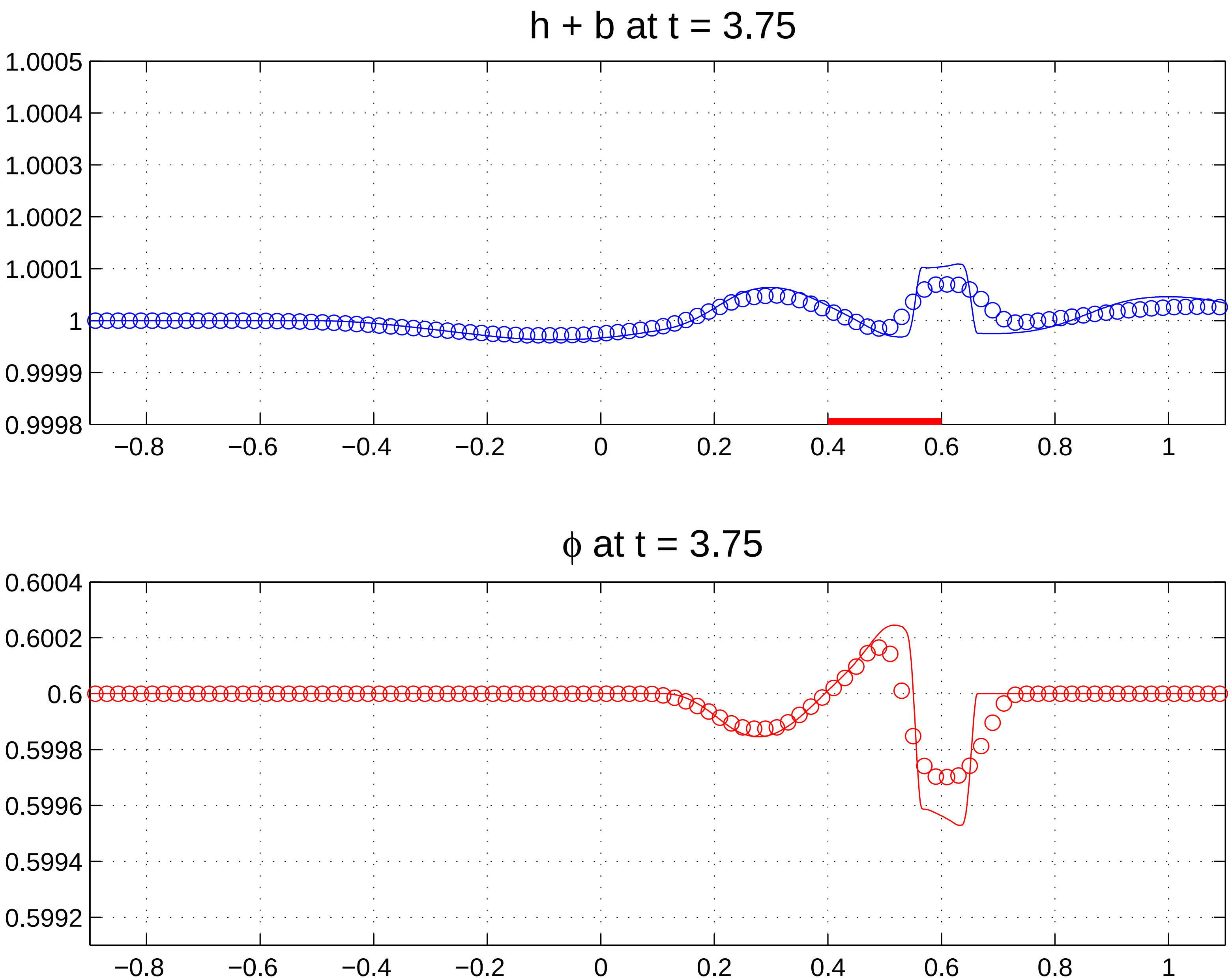

Perturbation of a steady state at rest

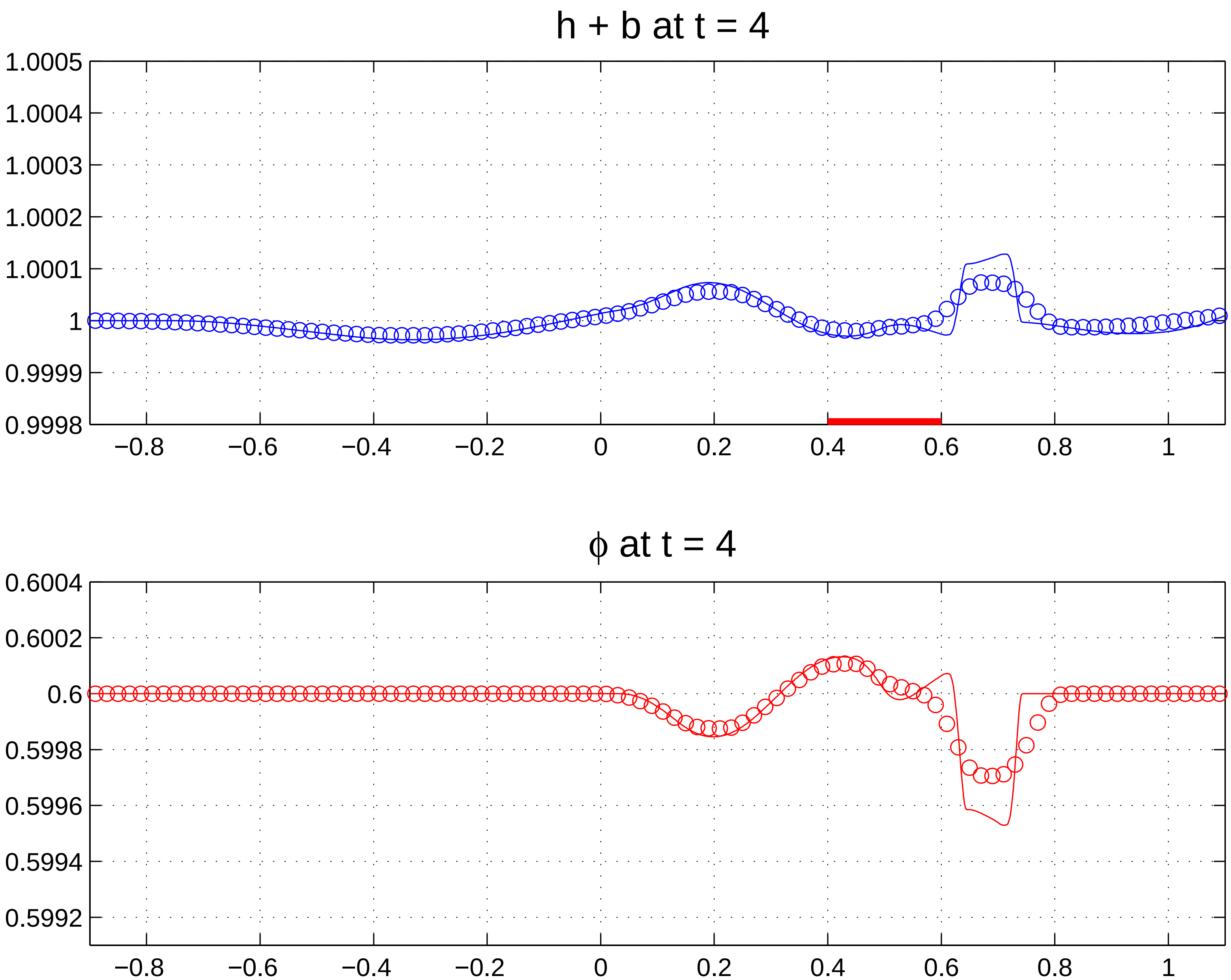

Perturbation of a steady state at rest

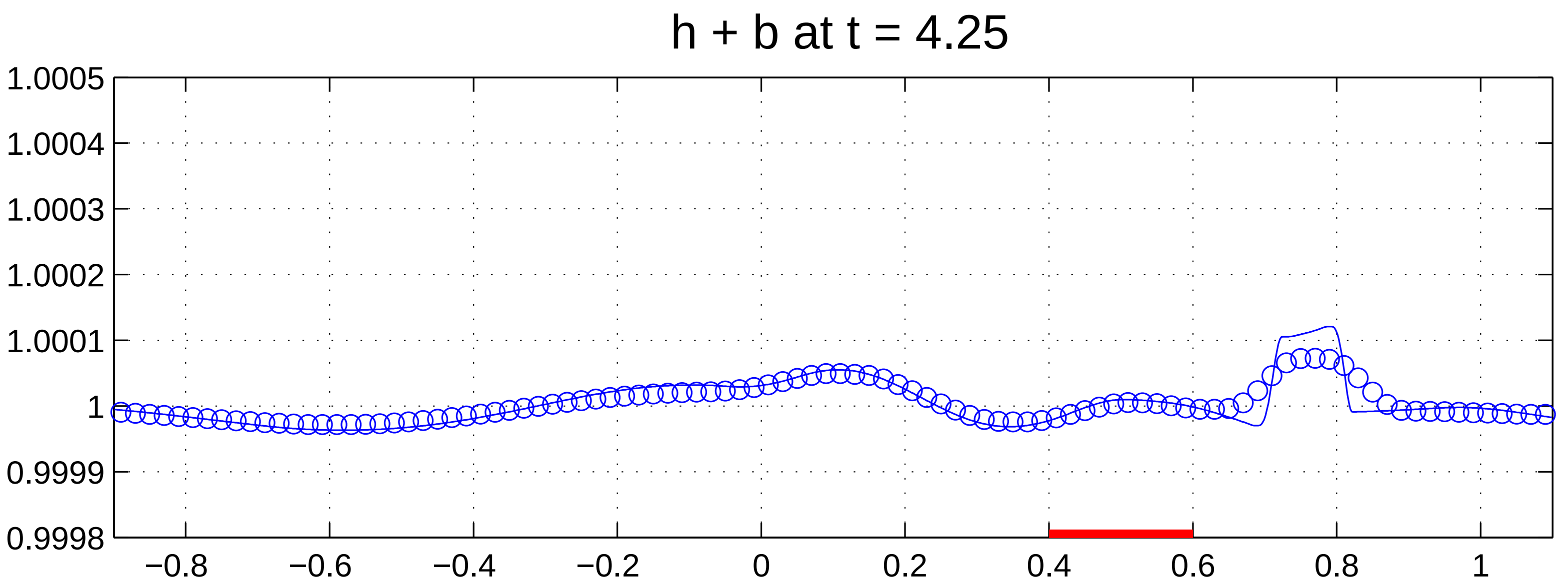

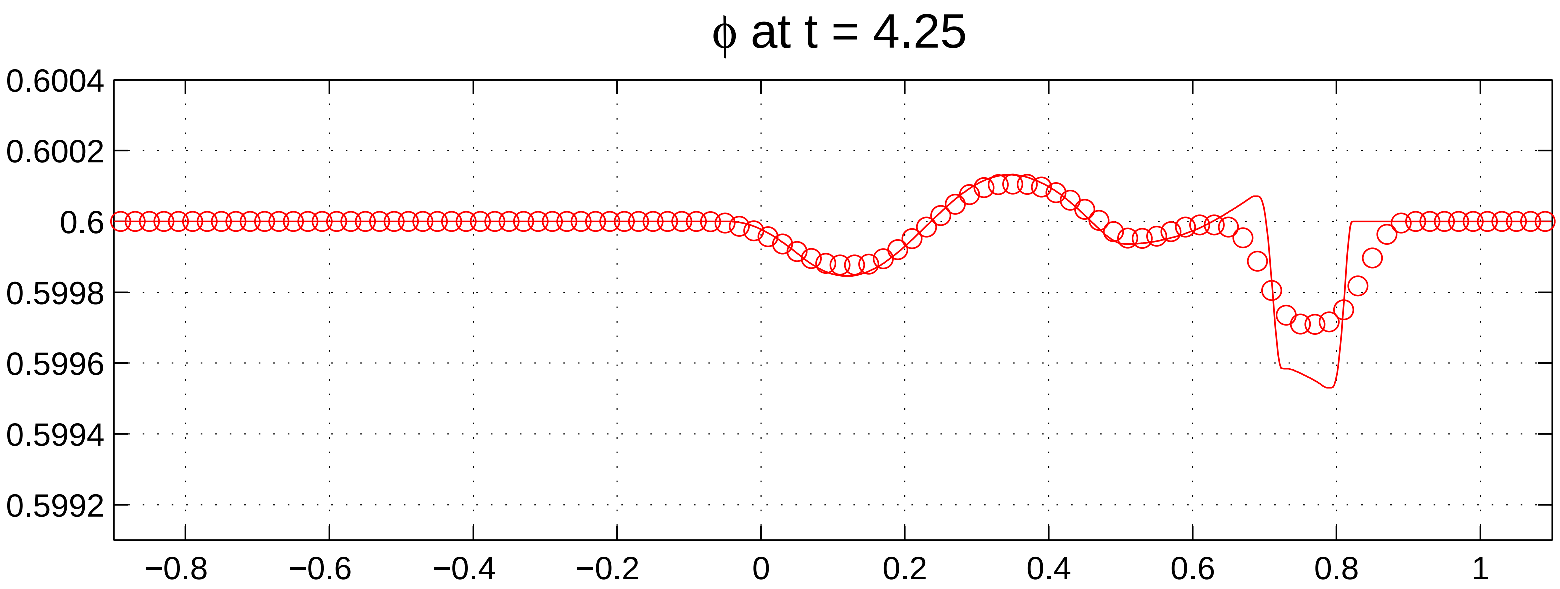

Perturbation of a steady state at rest

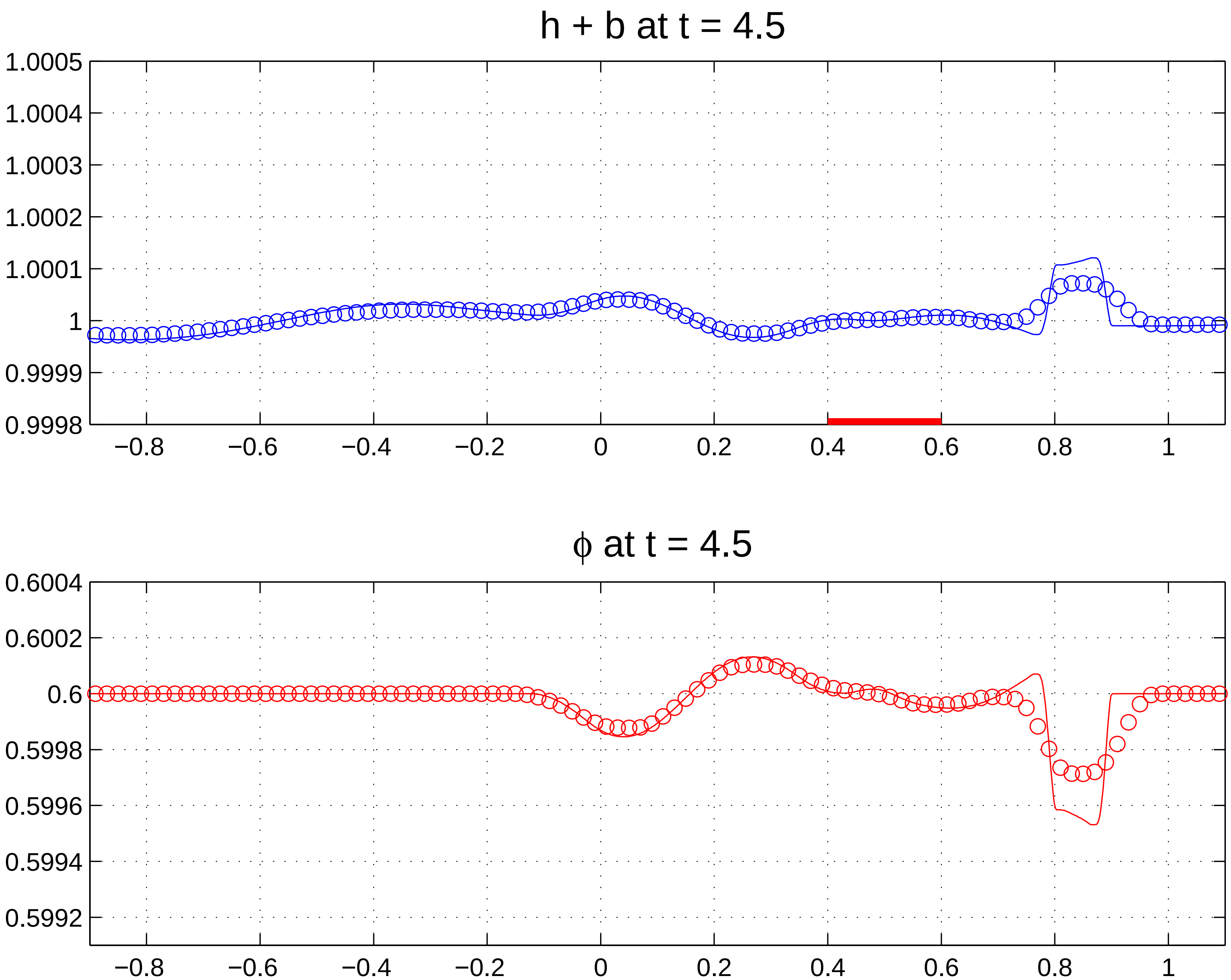

Perturbation of a steady state at rest

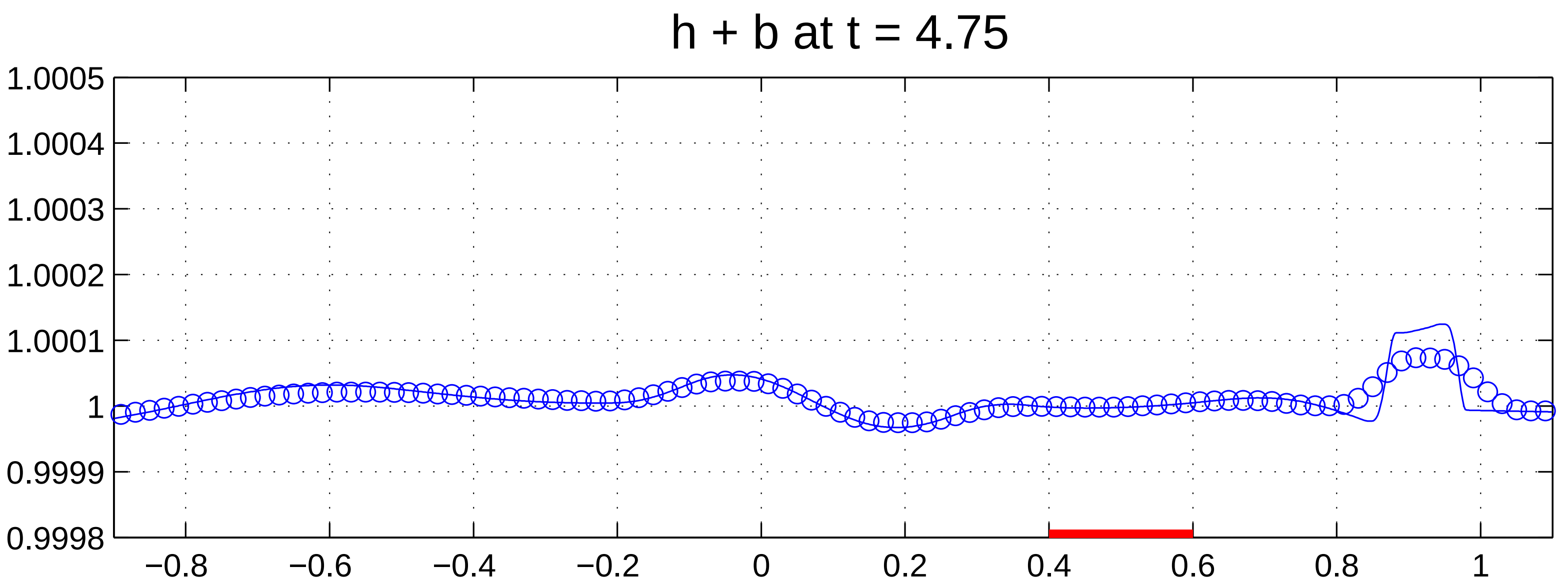

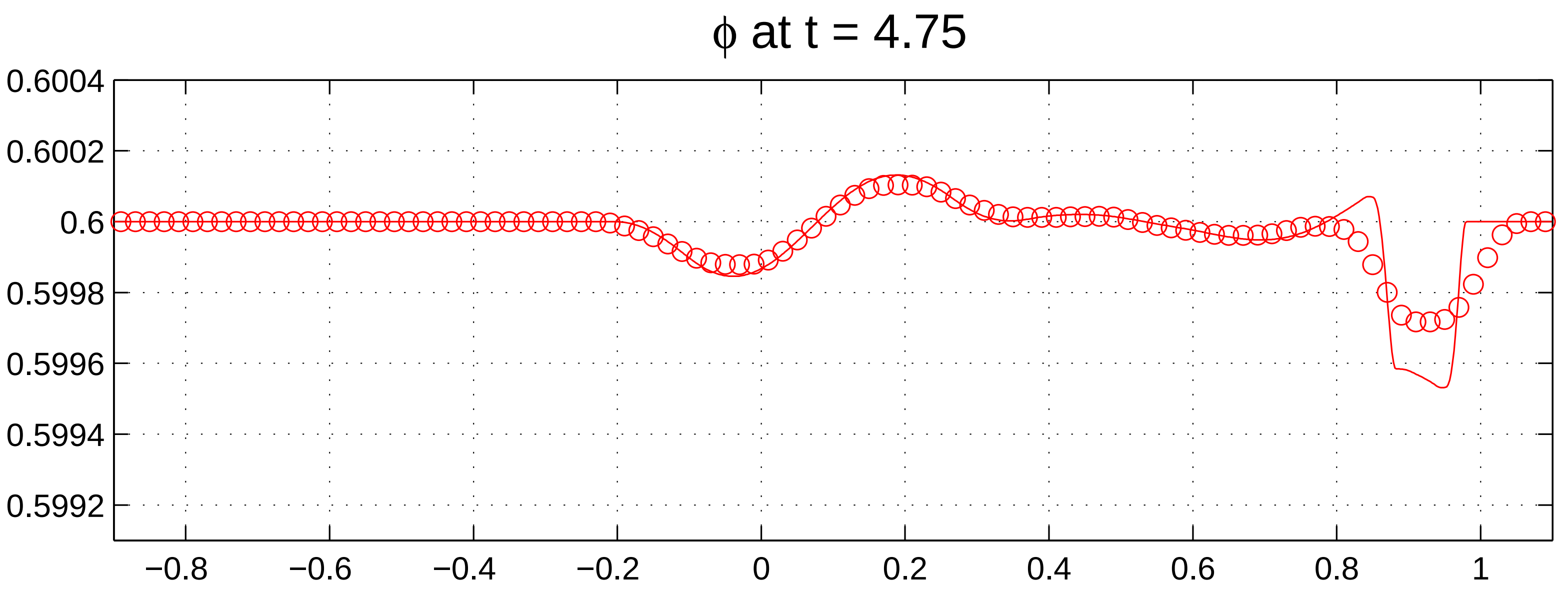

Perturbation of a steady state at rest

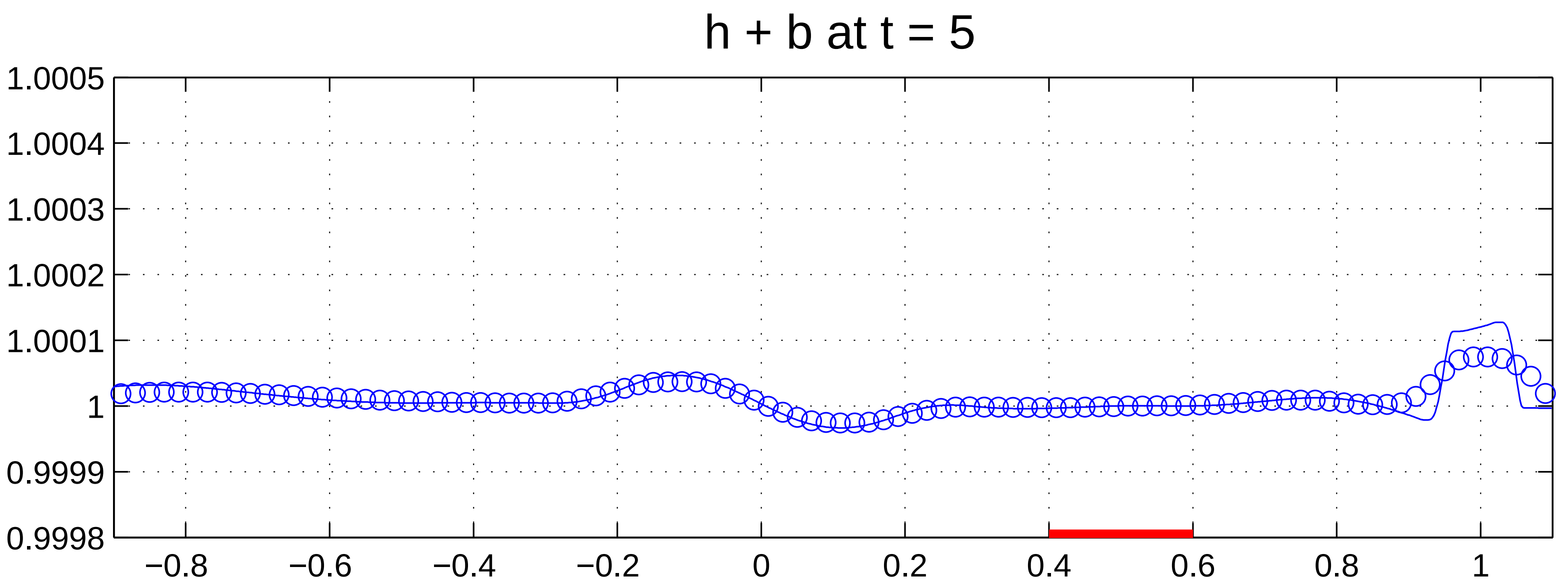

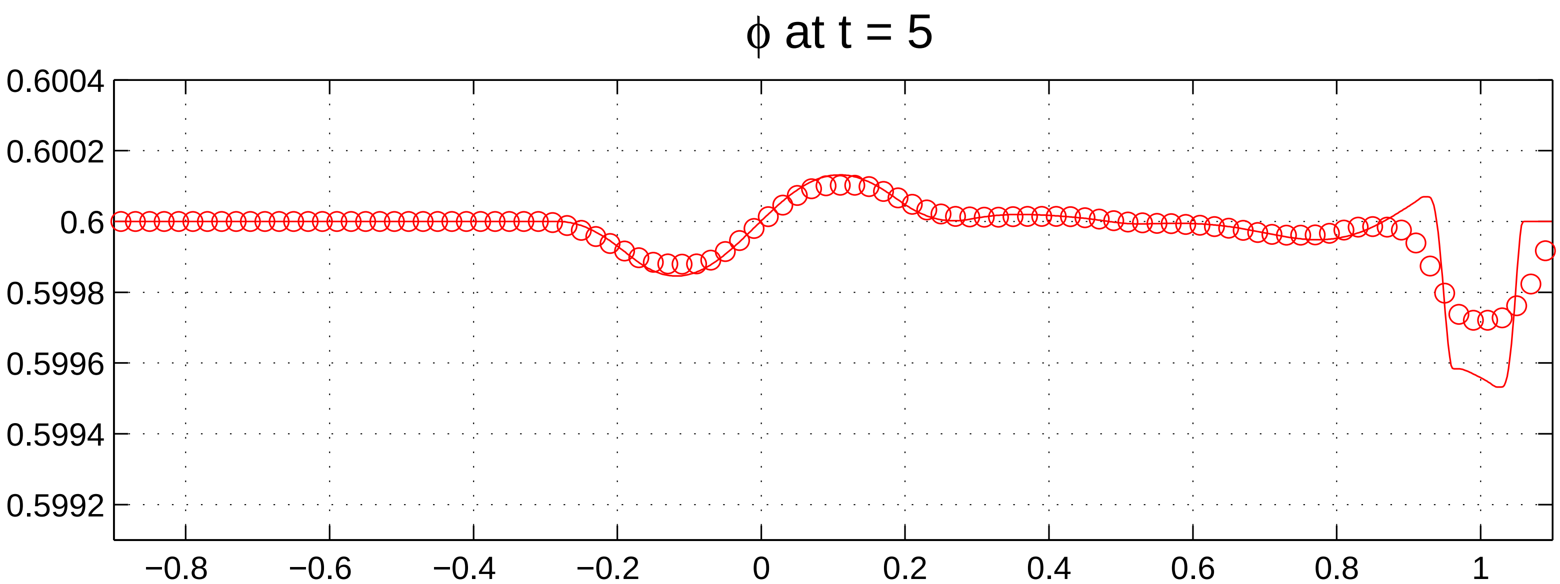

Perturbation of a steady state at rest

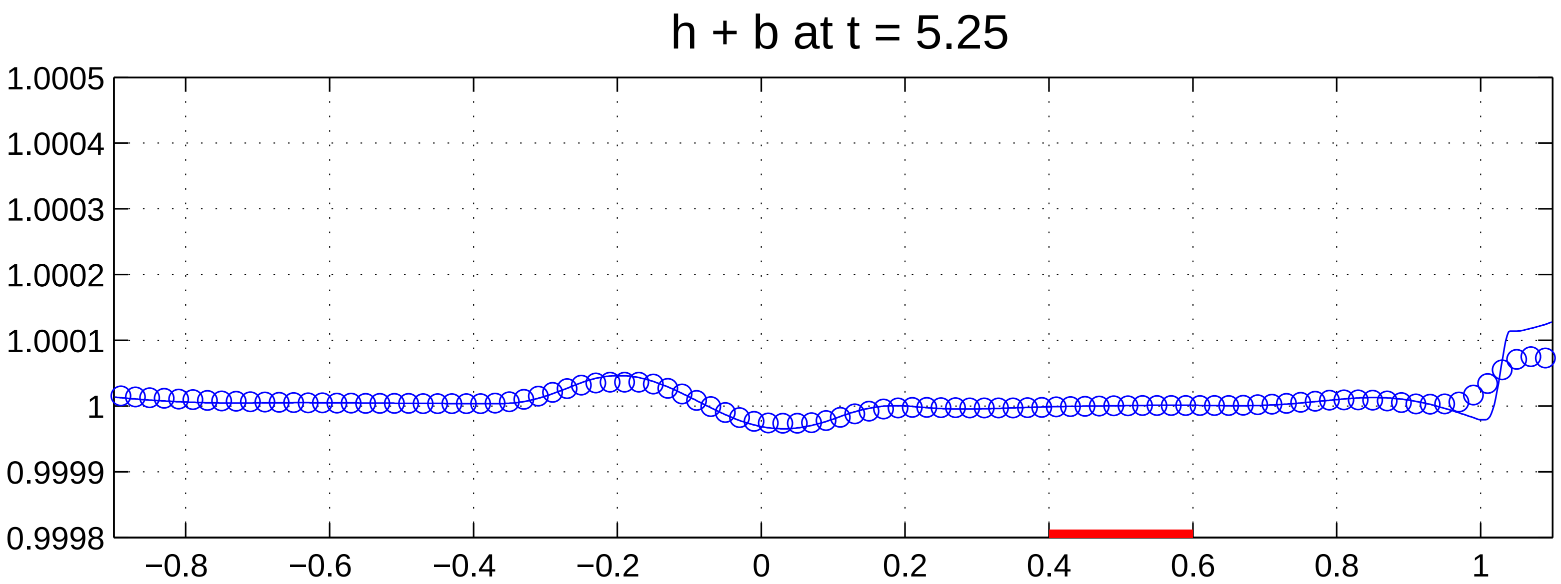

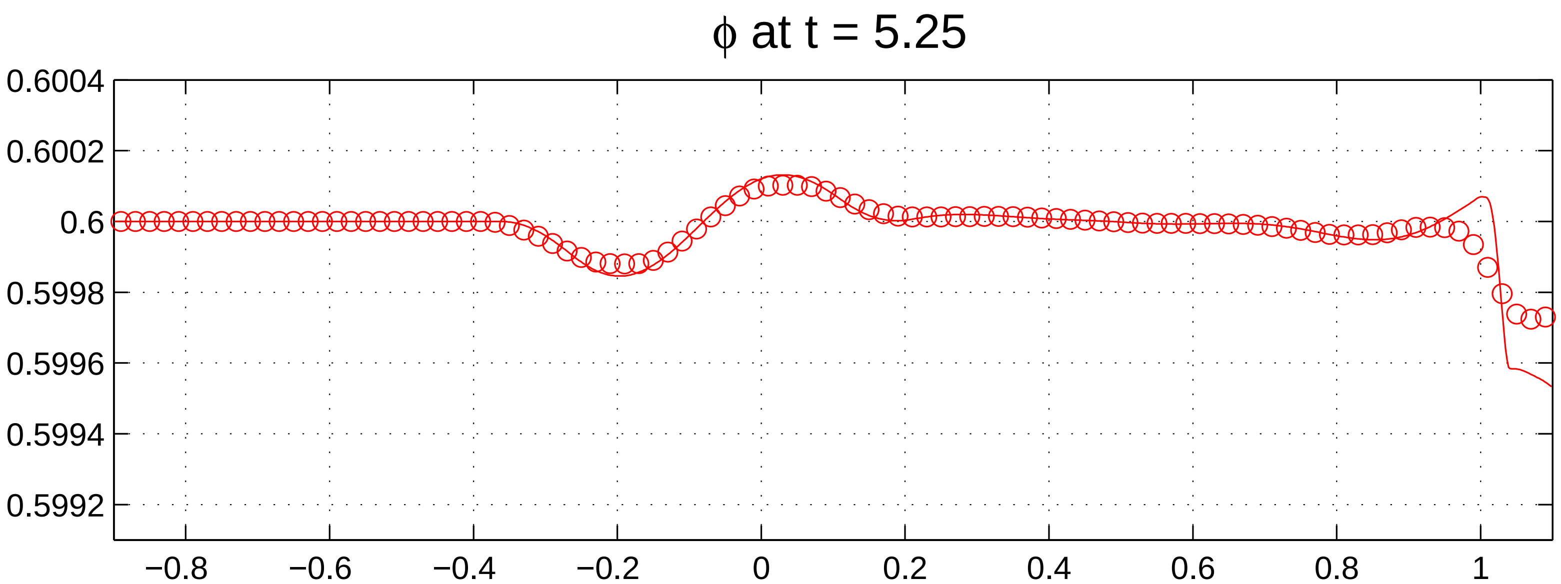

Perturbation of a steady state at rest

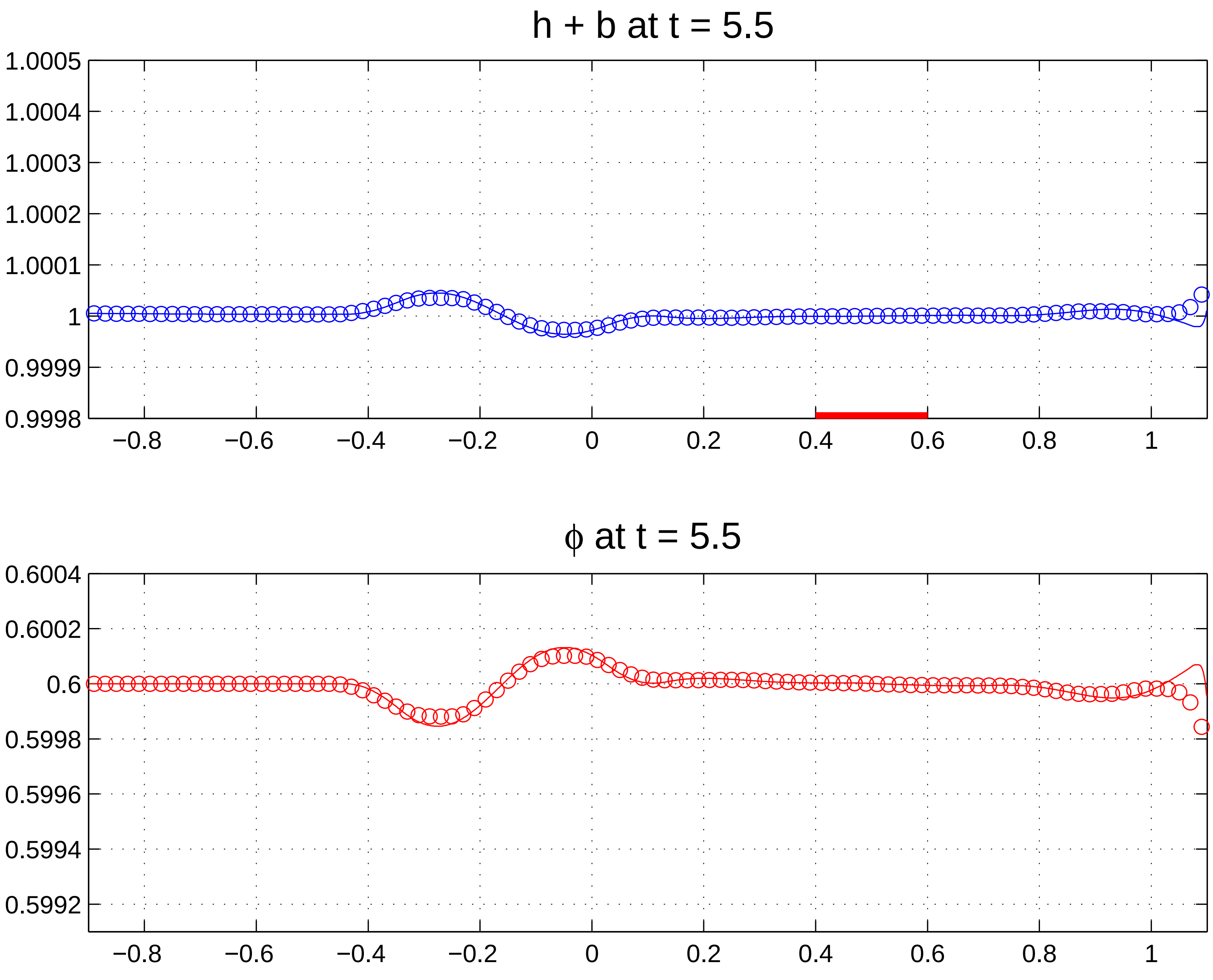

Perturbation of a steady state at rest

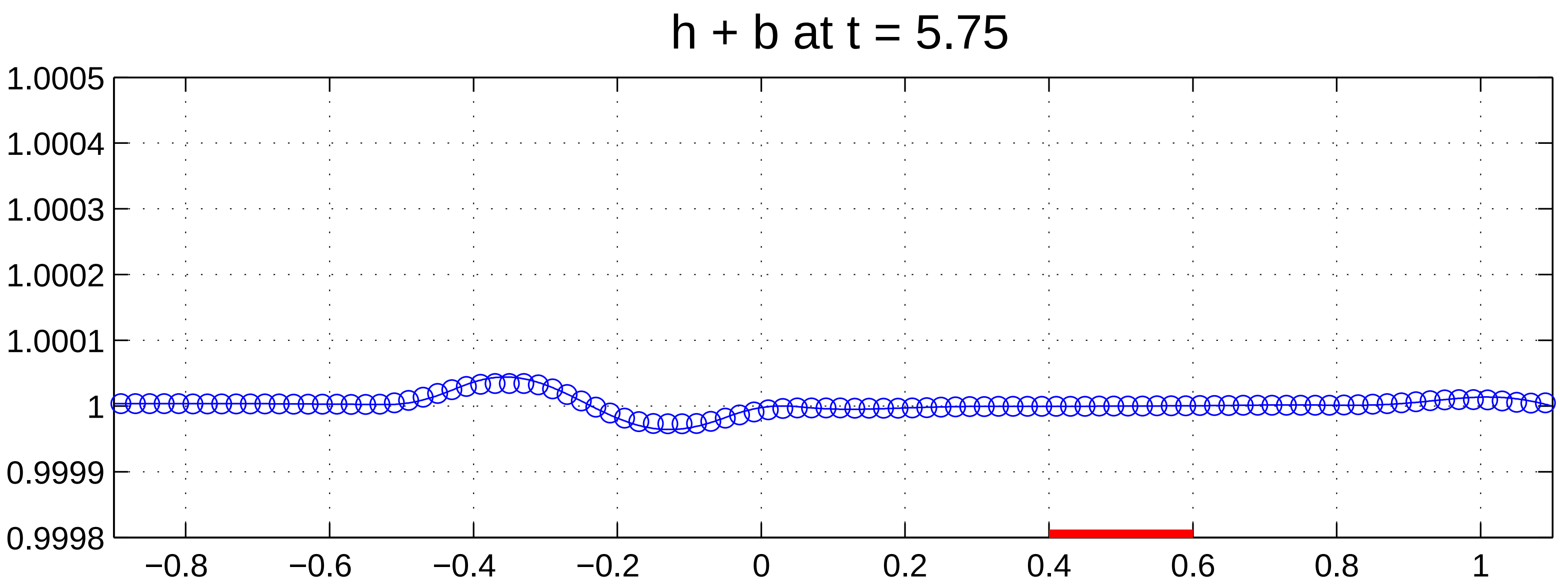

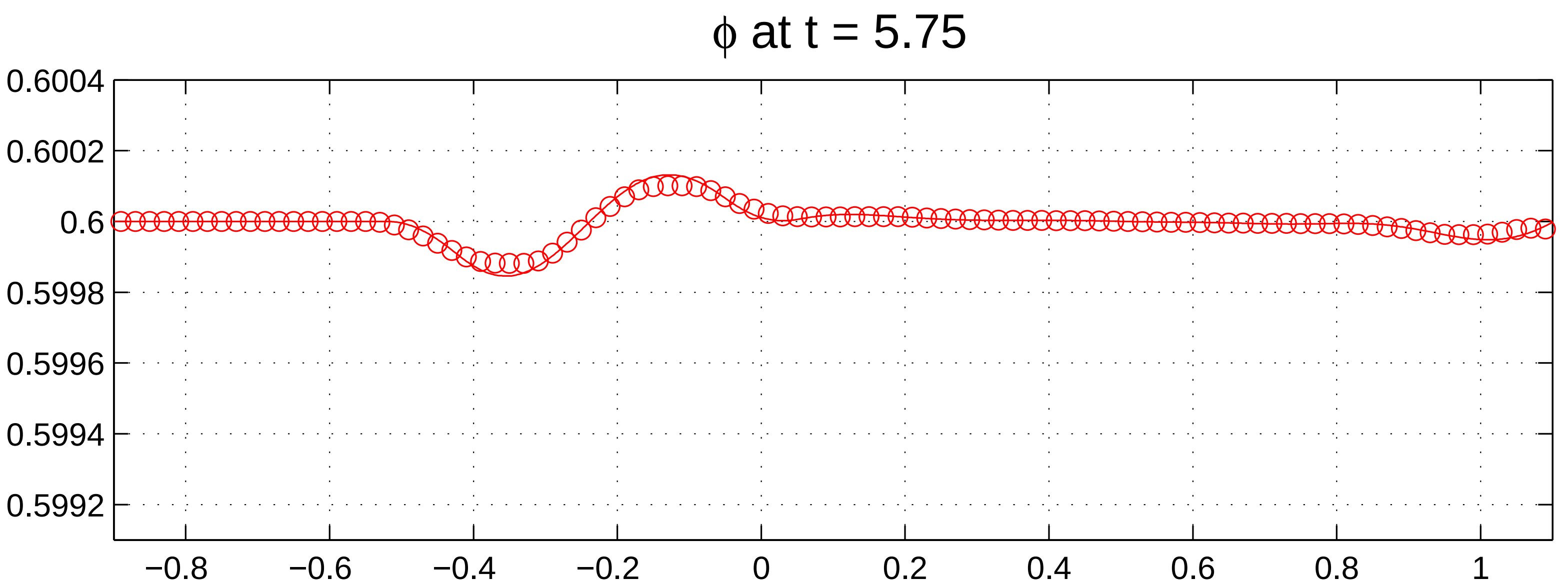

Perturbation of a steady state at rest

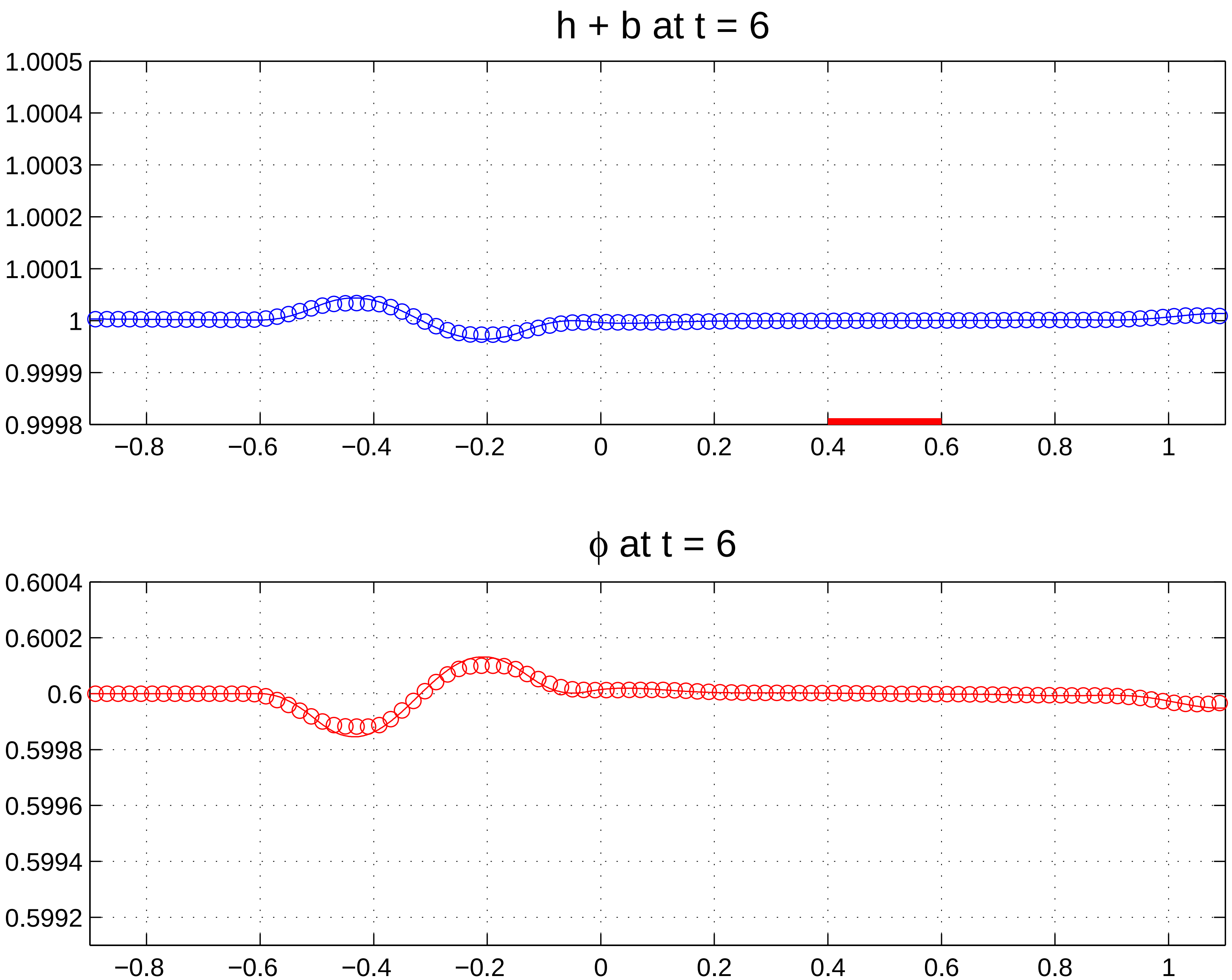

Perturbation of a steady state at rest

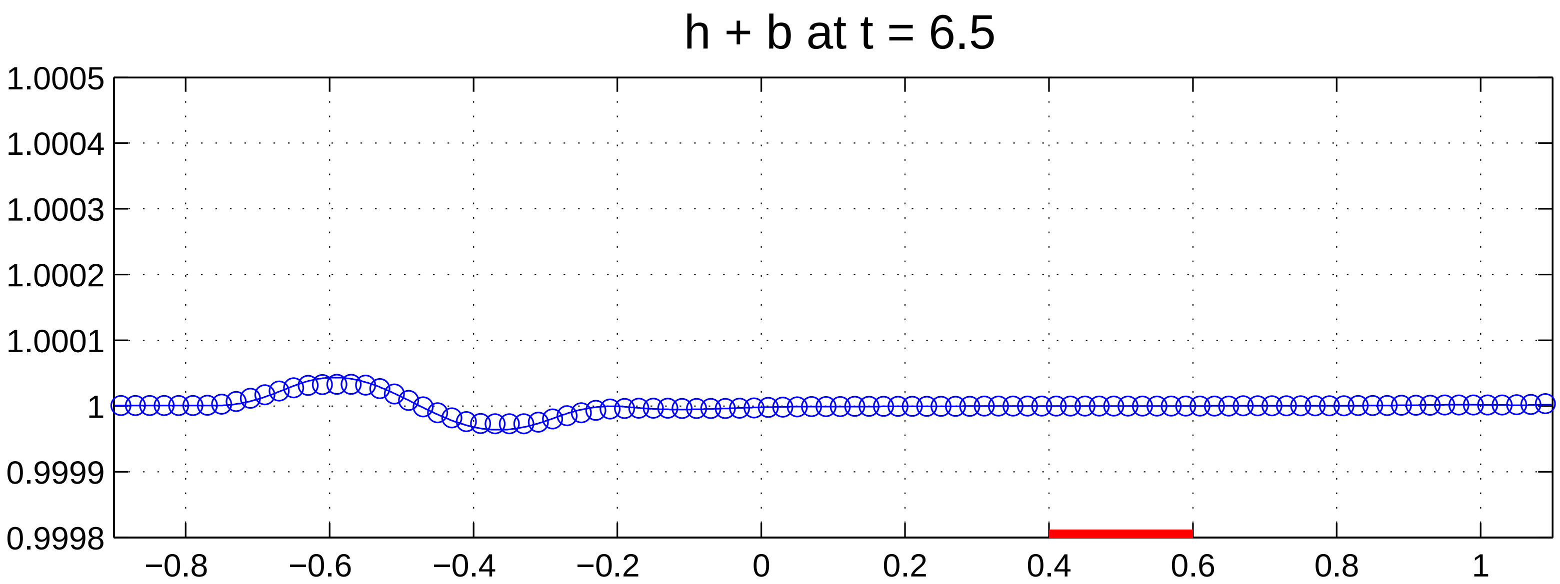

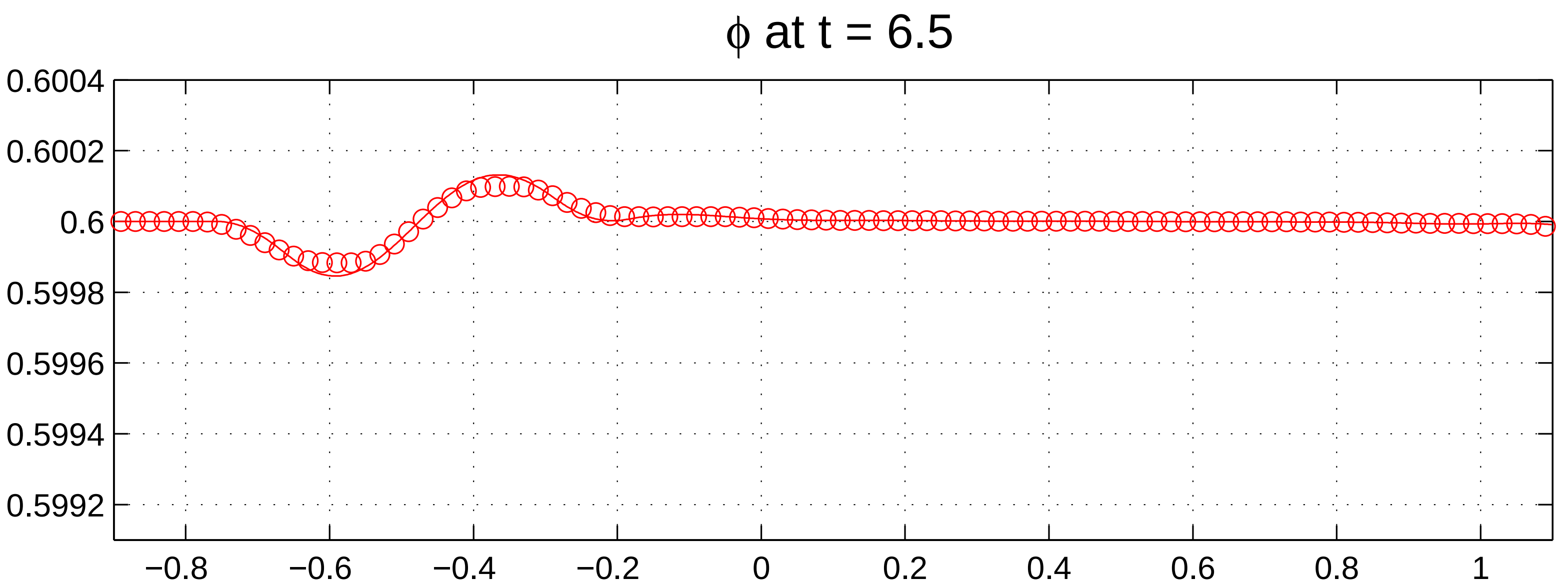

Perturbation of a steady state at rest

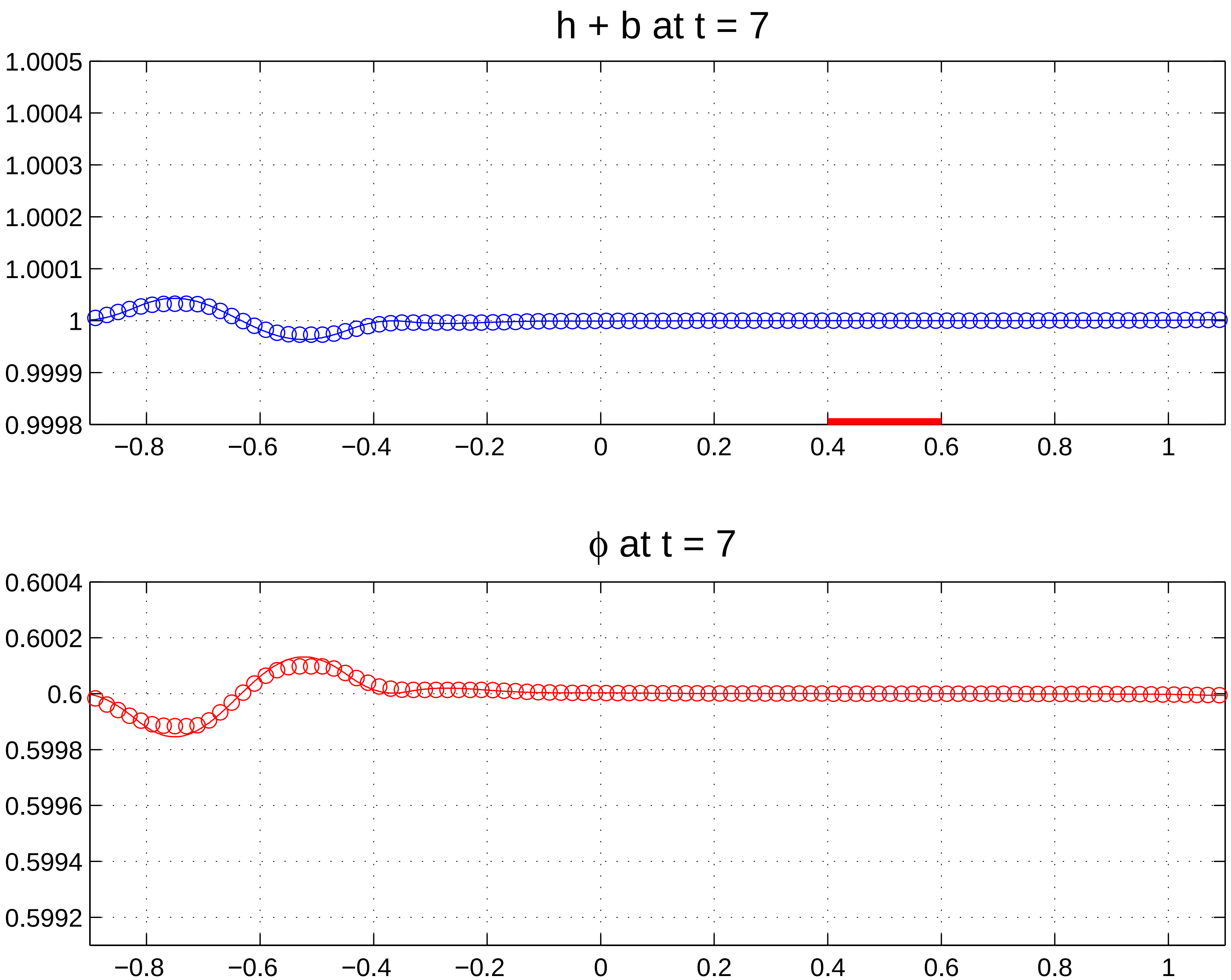

Perturbation of a steady state at rest

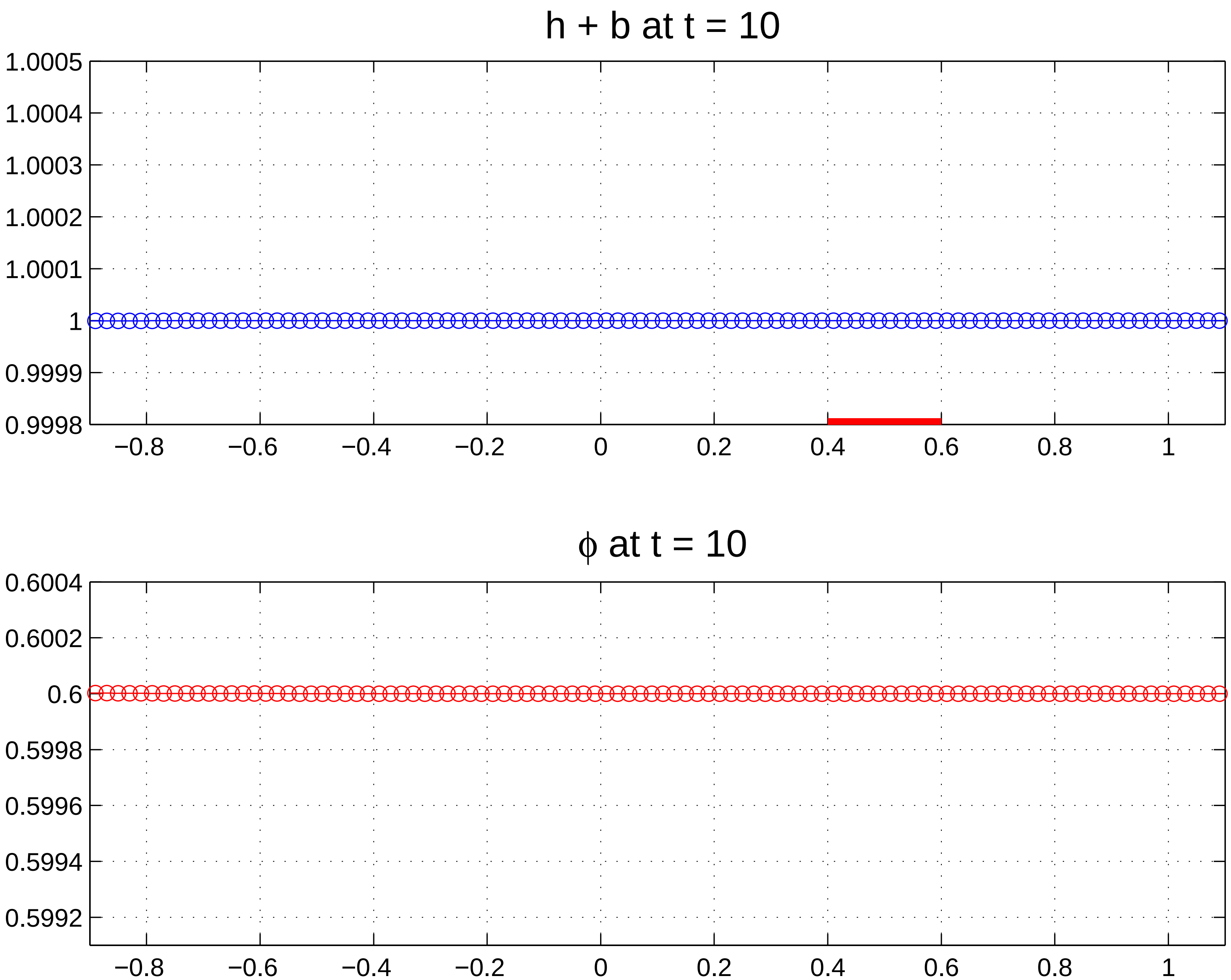

Numerical Test: Perturbation of a steady flow moving over a bump

Steady state conditions for a moving flow with $v_s = v_f \equiv v$:

$$\varphi = \text{const.}\,, \qquad hv = \text{const.}\,, \qquad g(h+b) + \frac{1}{2}v^2 = \text{const.}$$

Test 1: Convergence to a steady subcritical flow over a bump (as single-phase s.w.)

$$b(x) = \begin{cases} 0.2 - 0.05(x-10)^2 & \text{if } 8 < x < 12, \\ 0 & \text{otherwise}. \end{cases}$$

I.C. $\quad h = 2\,, \quad \varphi = \text{const.}, \quad v_s = v_f = 0.$

B.C. $\quad (hv)_{\text{in}} = 4.42, \quad h_{\text{out}} = 2\,.$

100 grid cells; solution at $t = 50$.

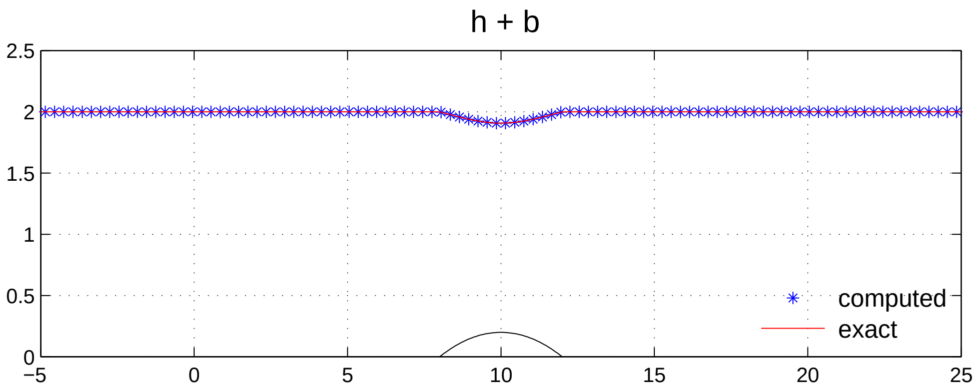

Now: take initial disturbance of φ.

$$\varphi(x,0) = \varphi_0 + \tilde{\varphi}\,, \qquad \varphi_0 = 0.6\,, \quad \tilde{\varphi} = 10^{-3}\,, \qquad \text{for } -3.5 \le x \le -2.5\,.$$

Grid cells = 150, Reference curve: 1500 cells. 2nd order; CFL = 0.9.

Perturbation of a steady flow in motion

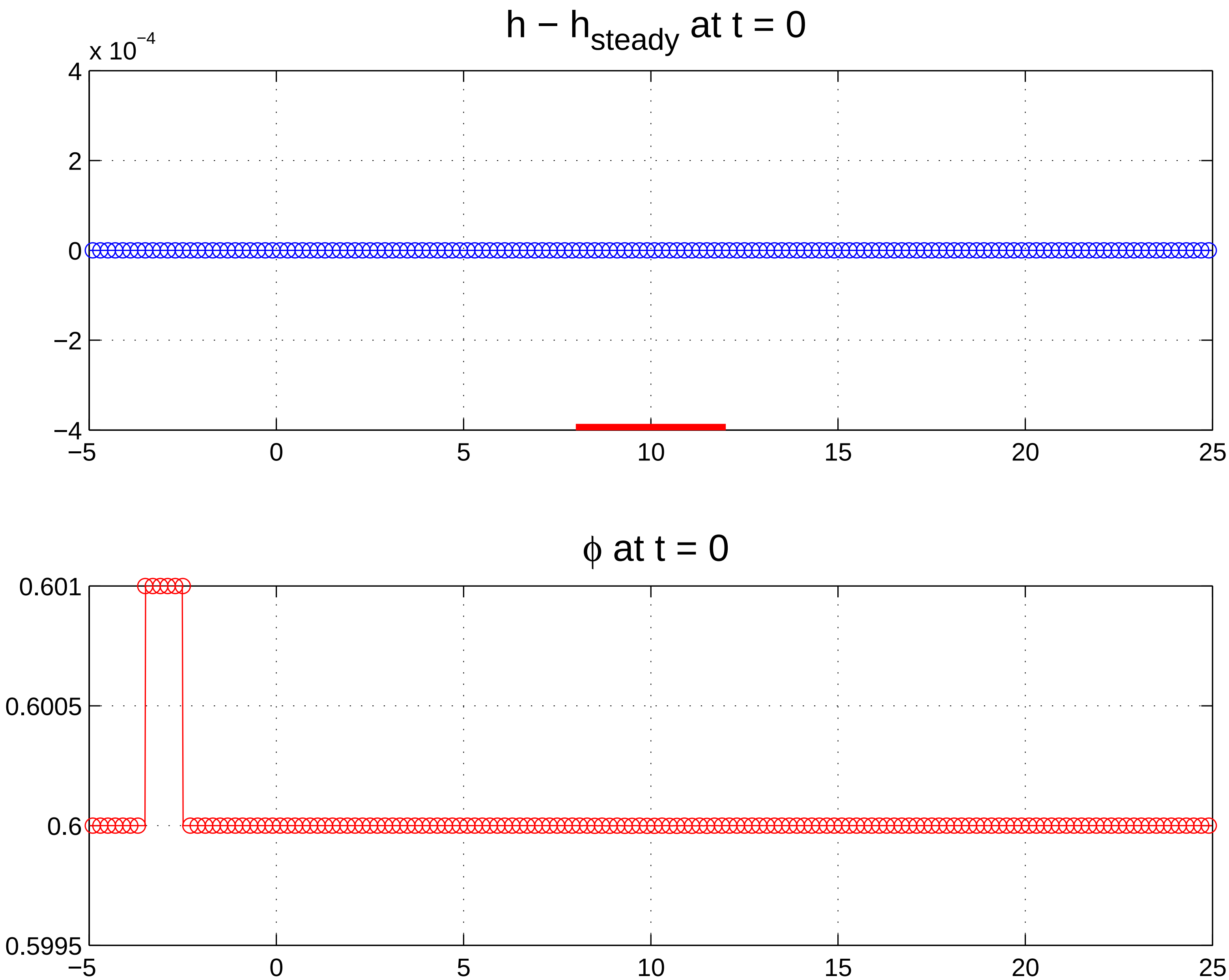

Perturbation of a steady flow in motion

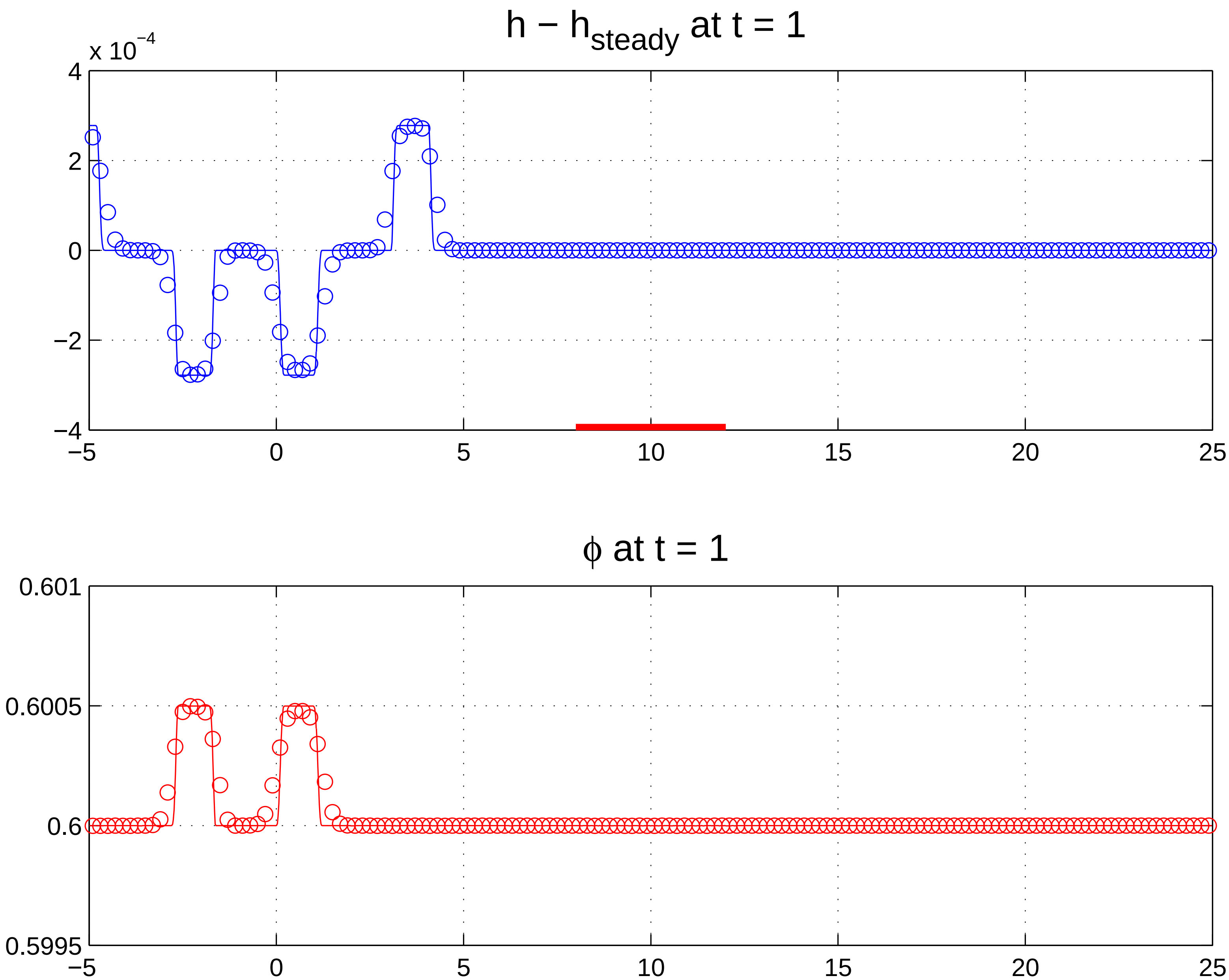

Perturbation of a steady flow in motion

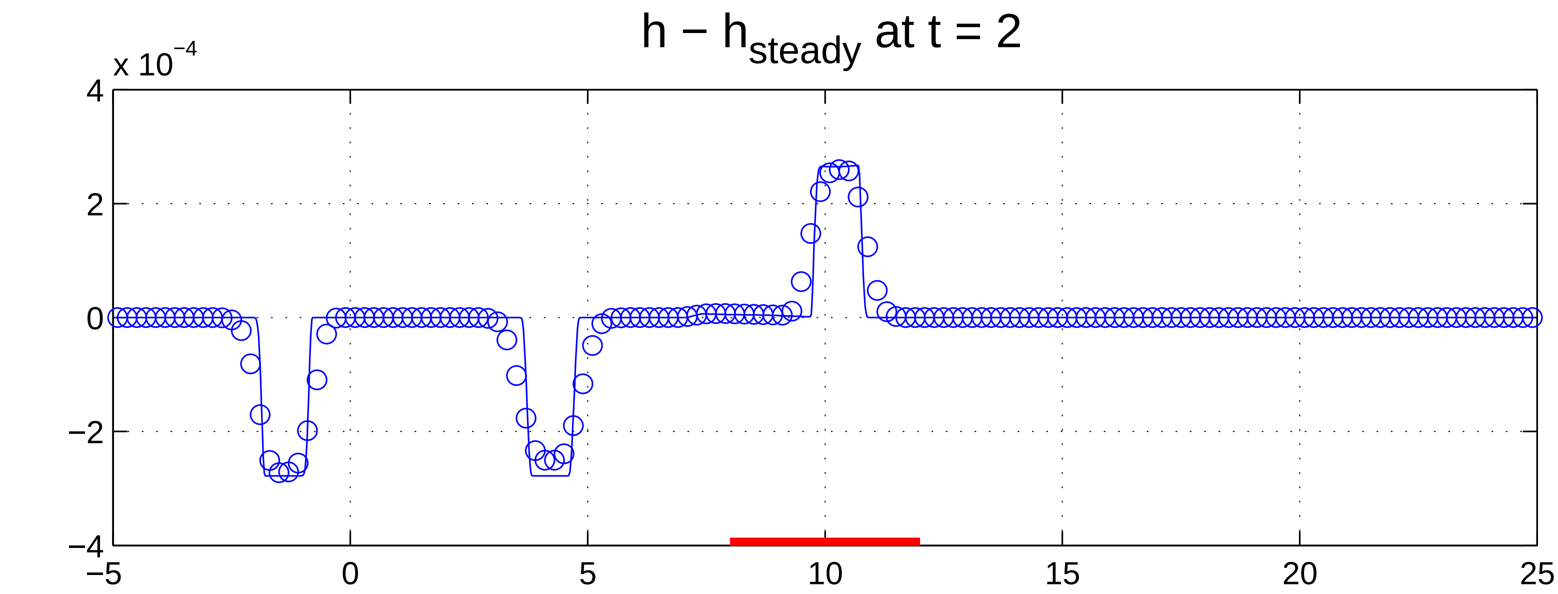

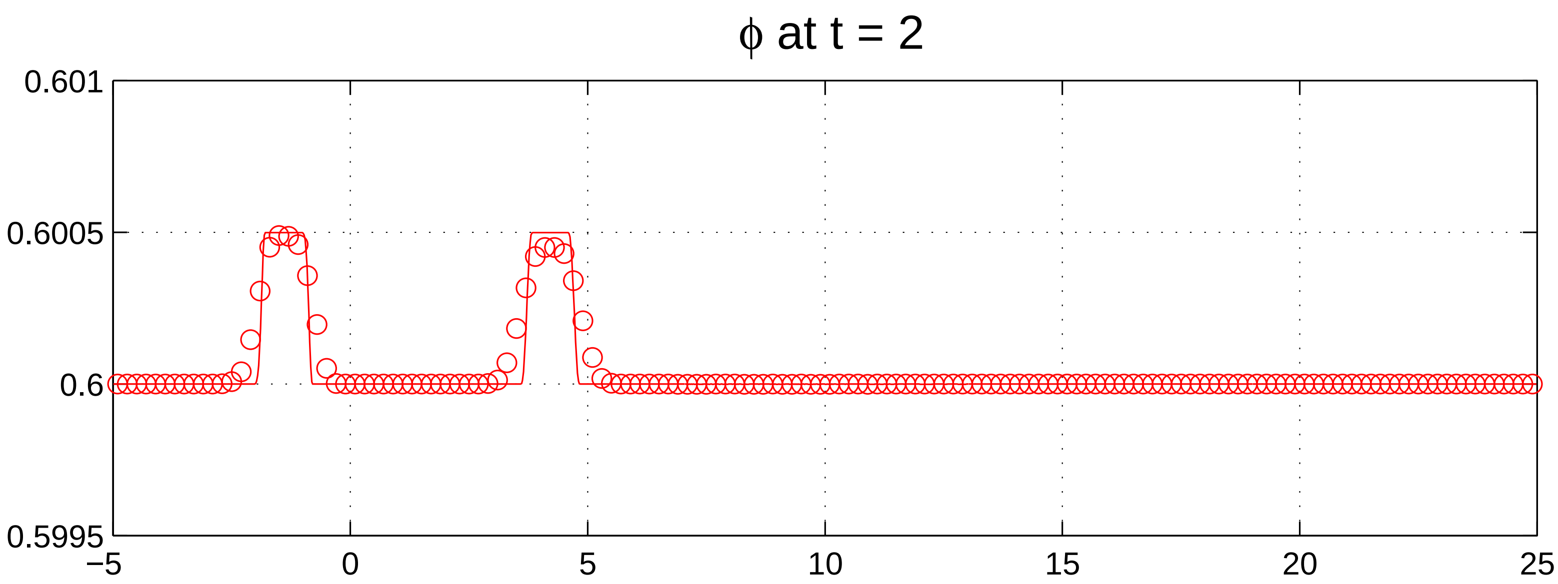

Perturbation of a steady flow in motion

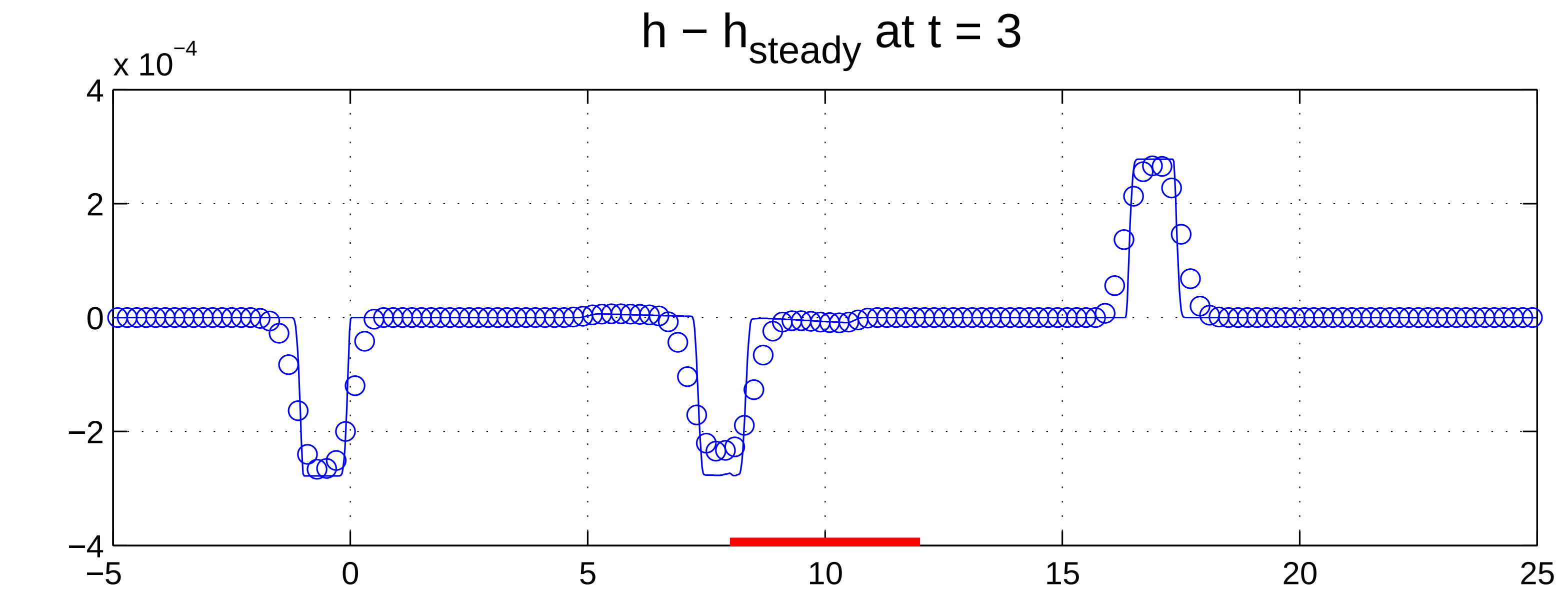

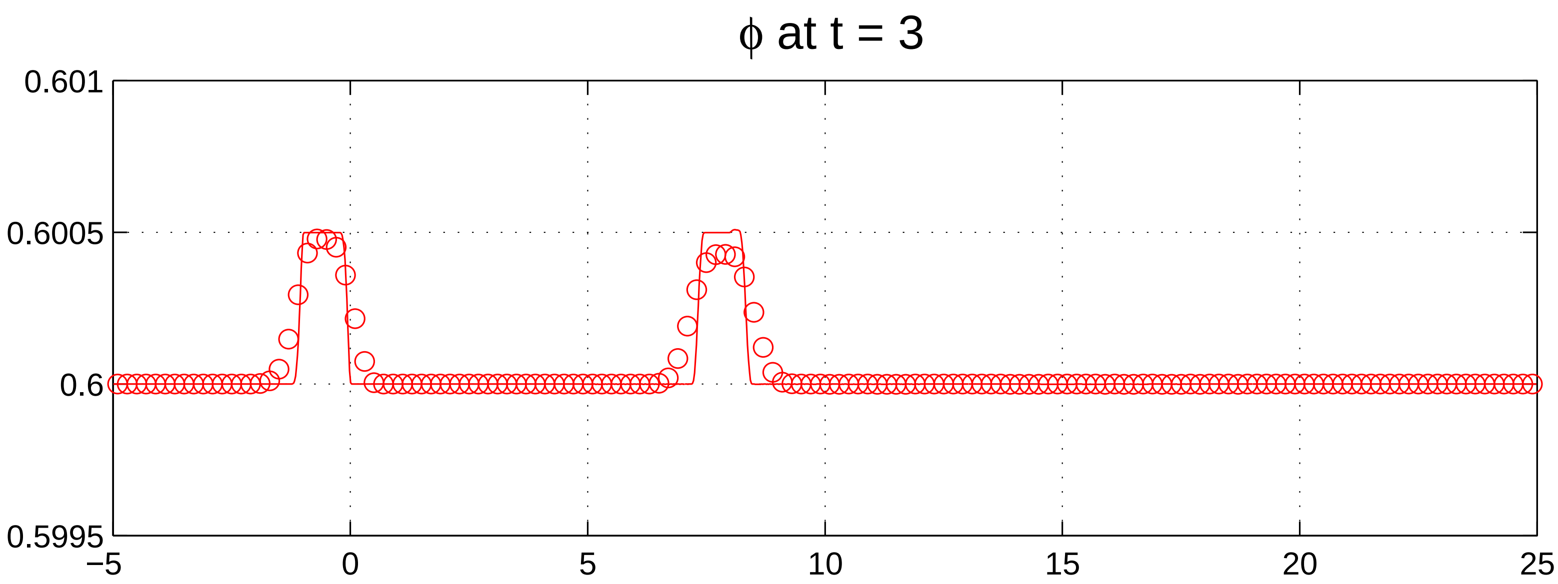

Perturbation of a steady flow in motion

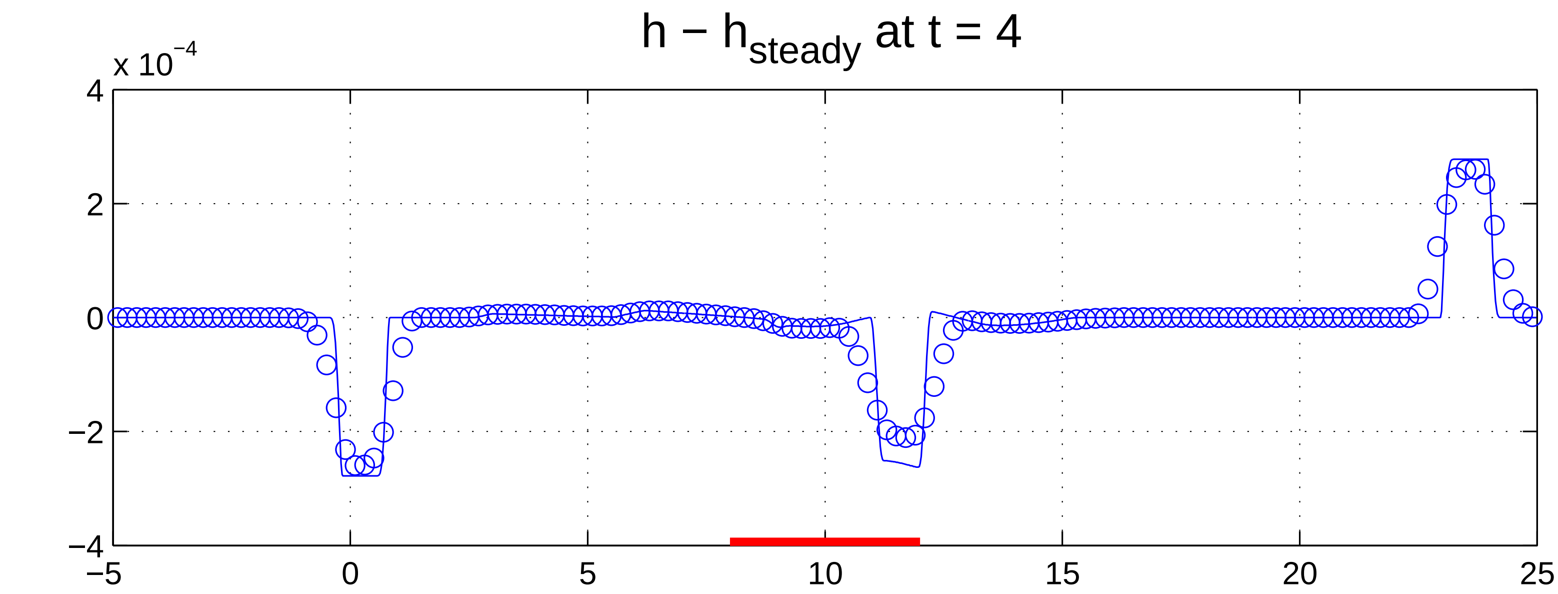

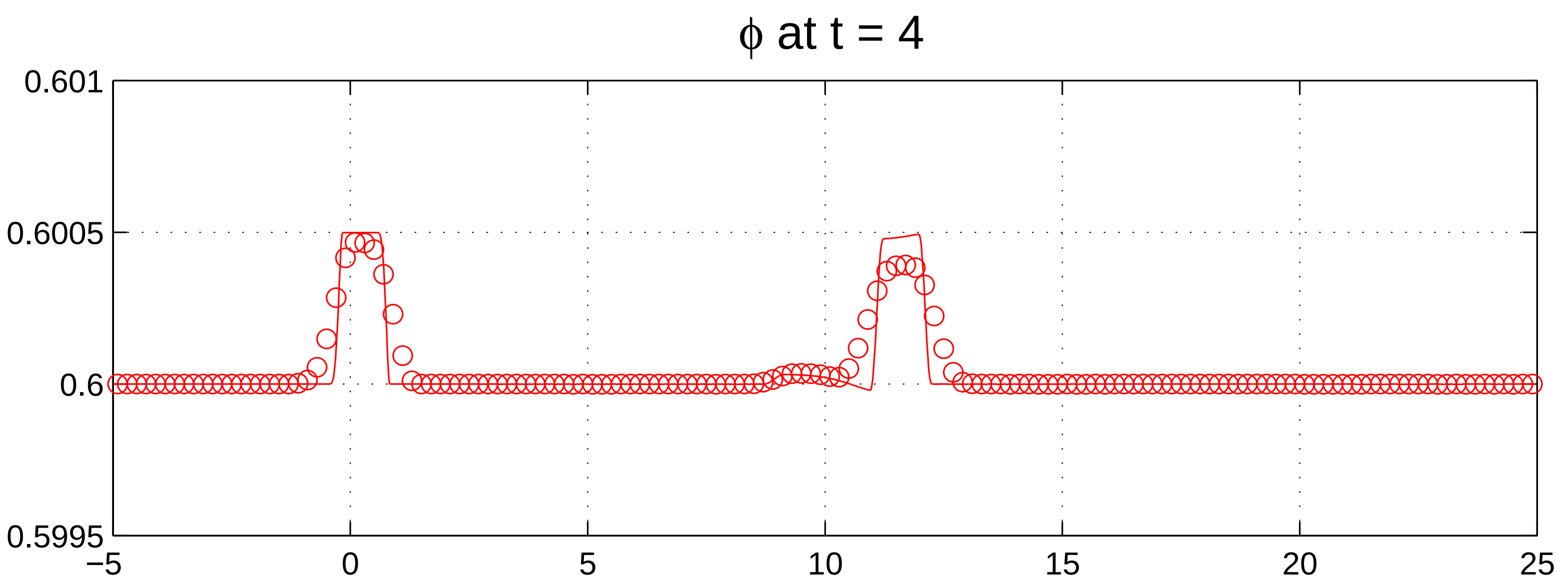

Perturbation of a steady flow in motion

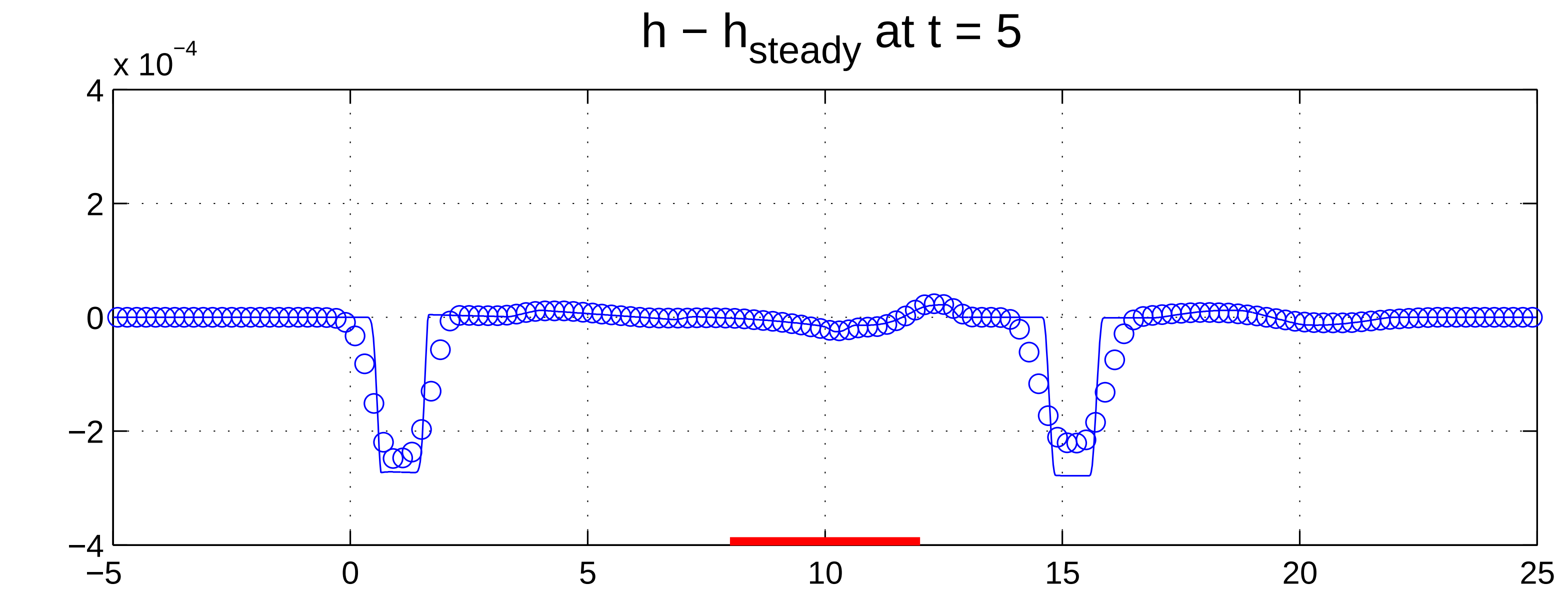

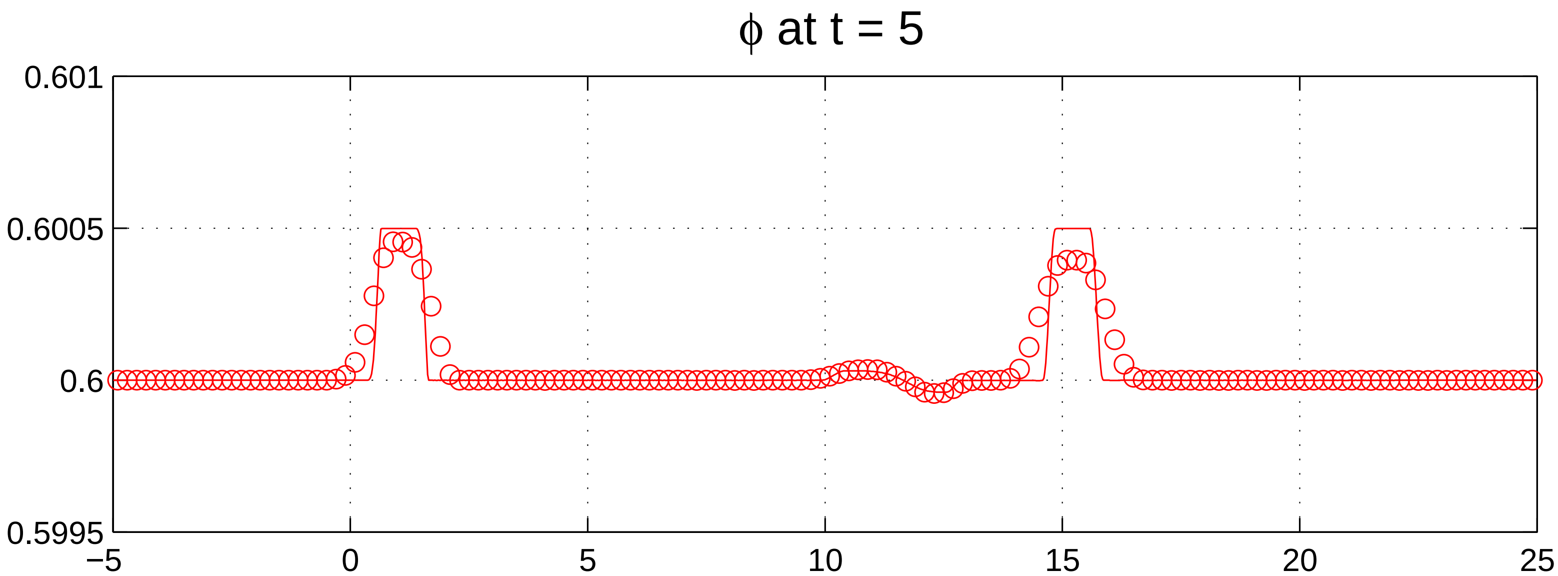

Perturbation of a steady flow in motion

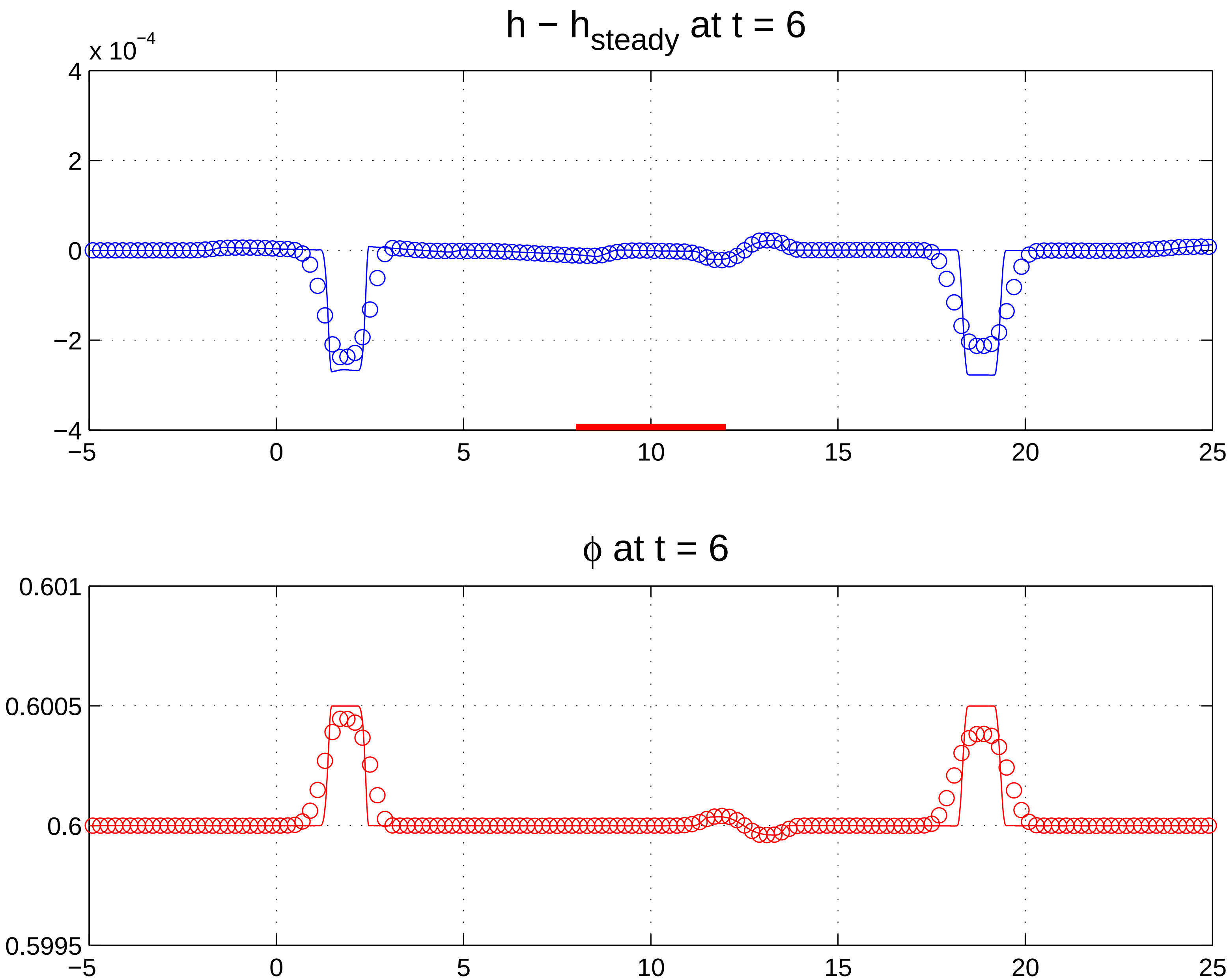

Perturbation of a steady flow in motion

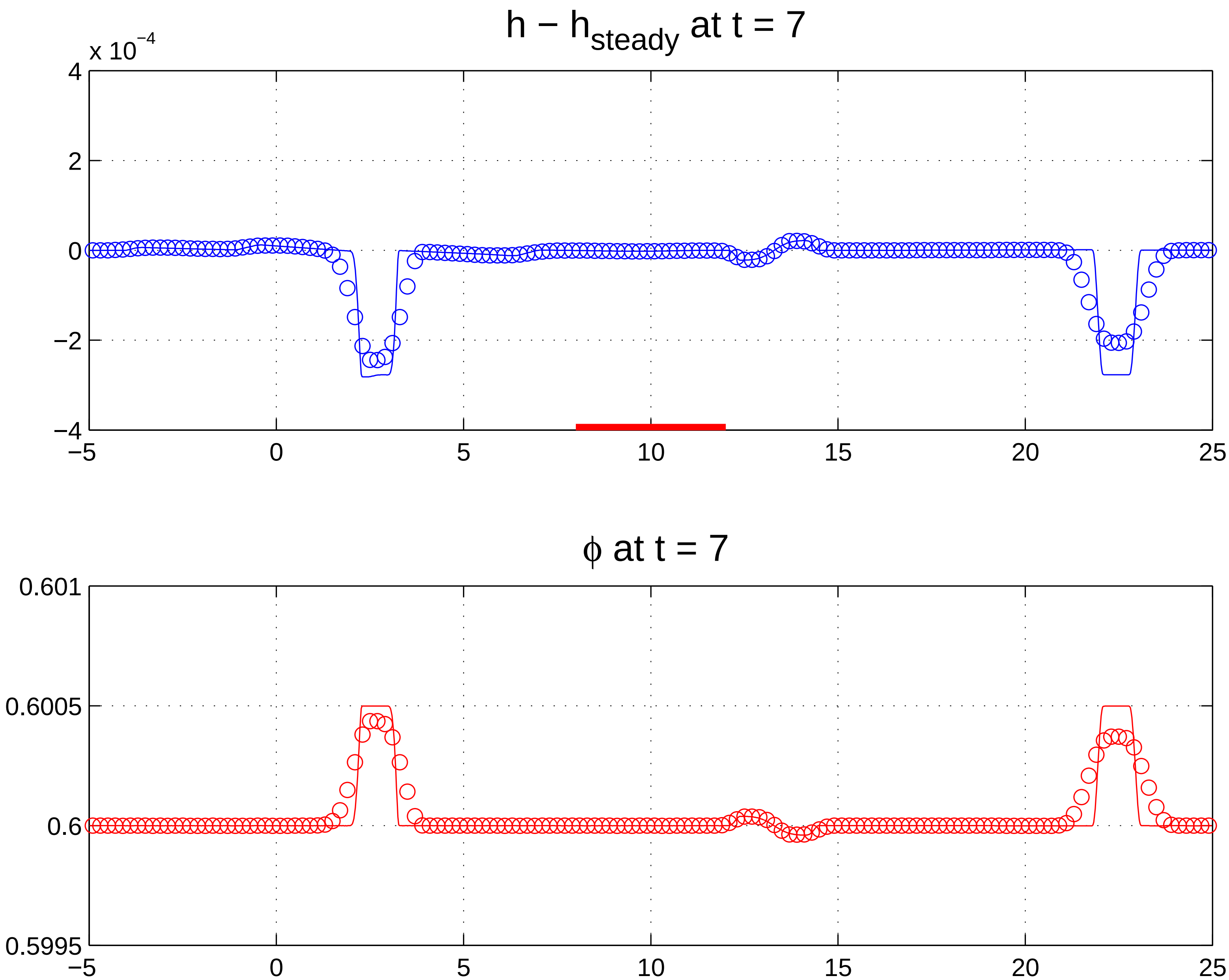

Perturbation of a steady flow in motion

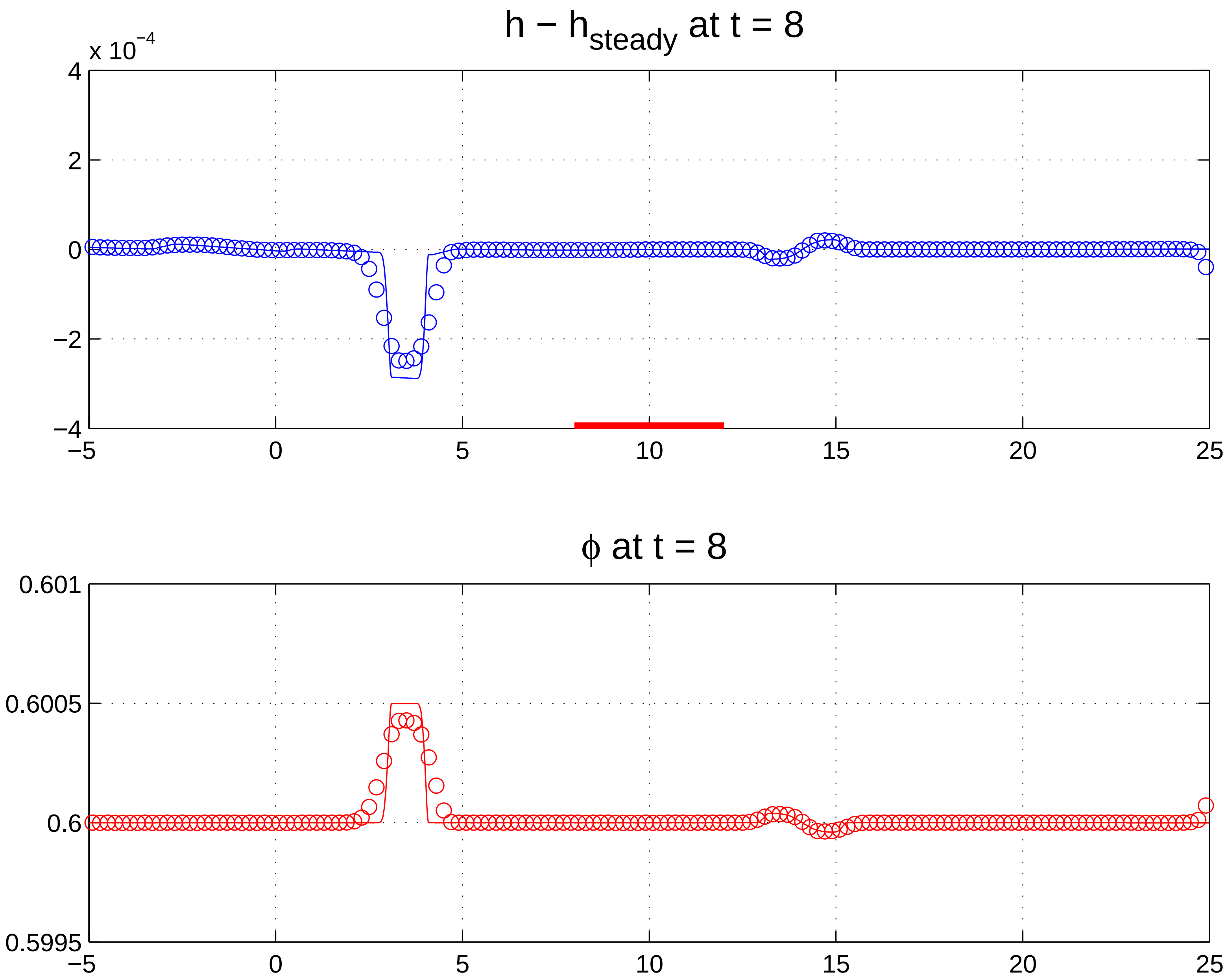

Perturbation of a steady flow in motion

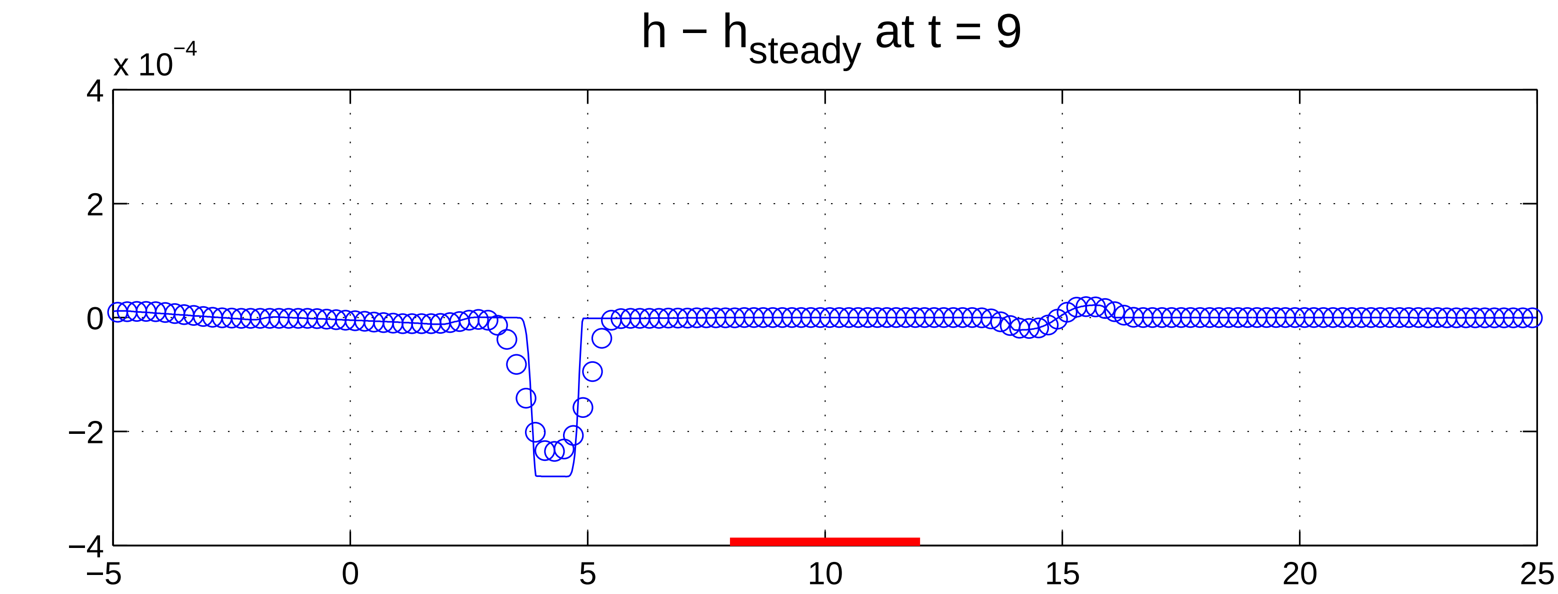

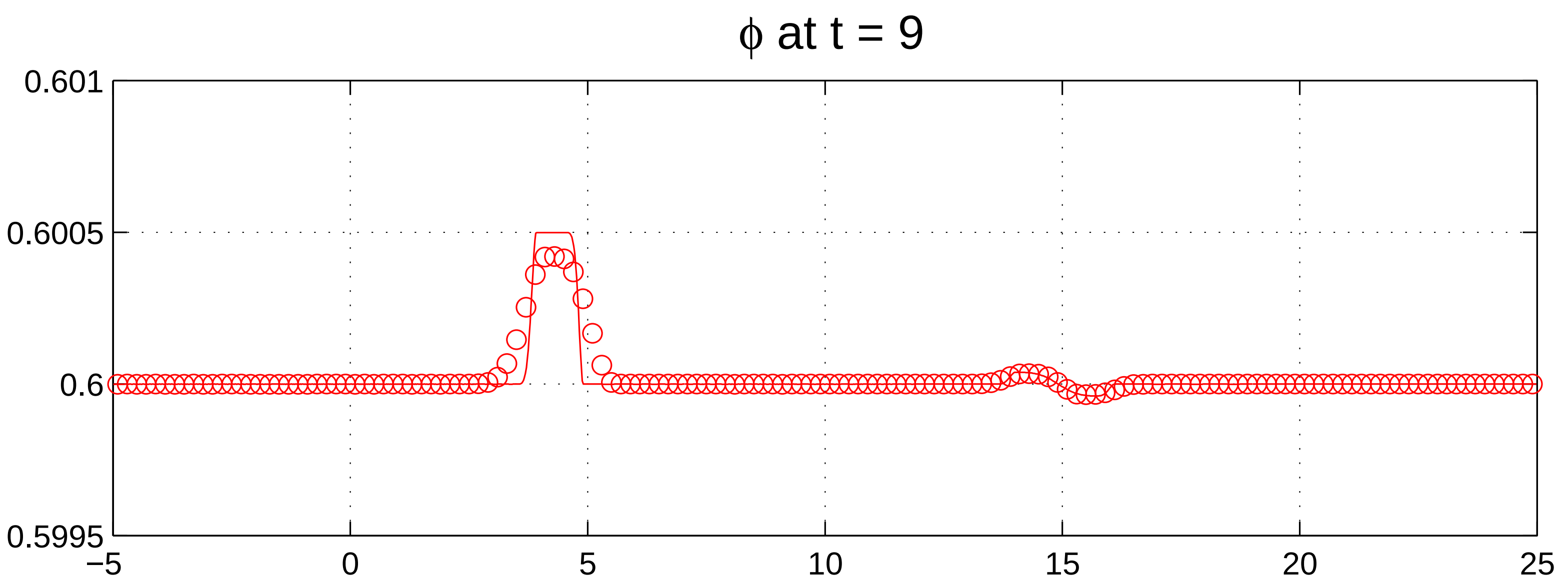

Perturbation of a steady flow in motion

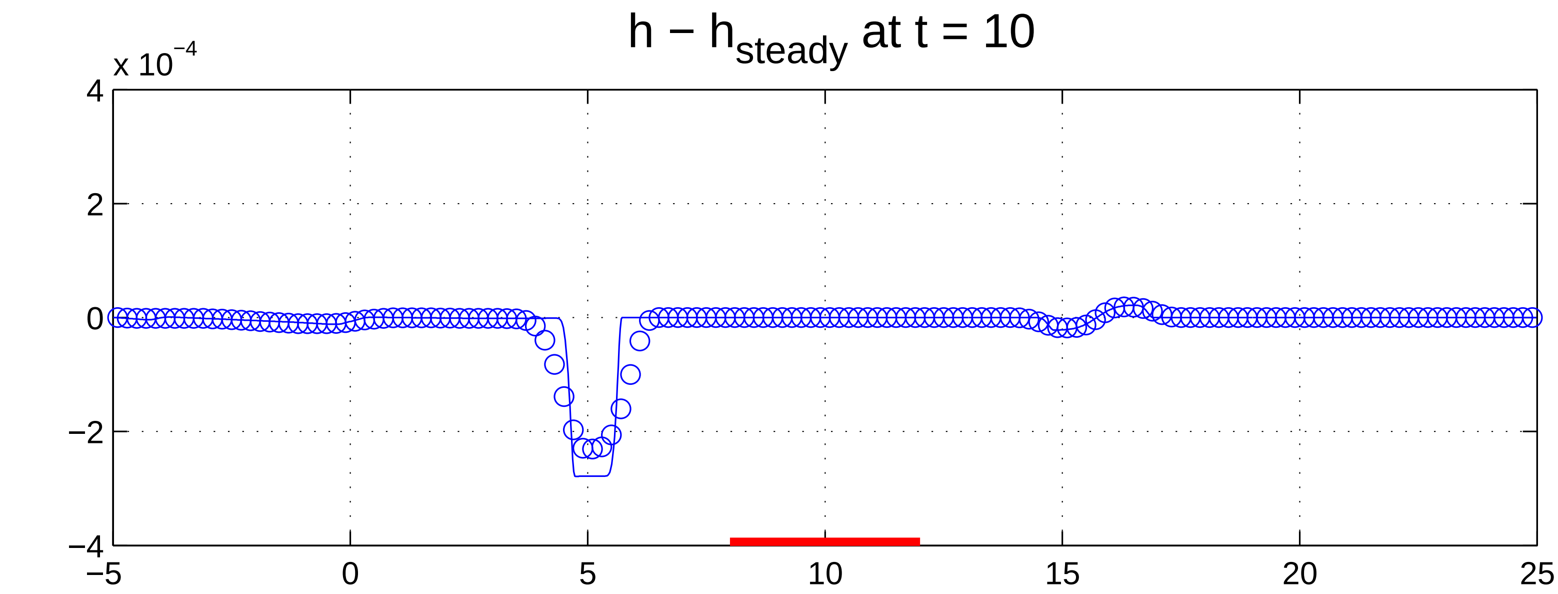

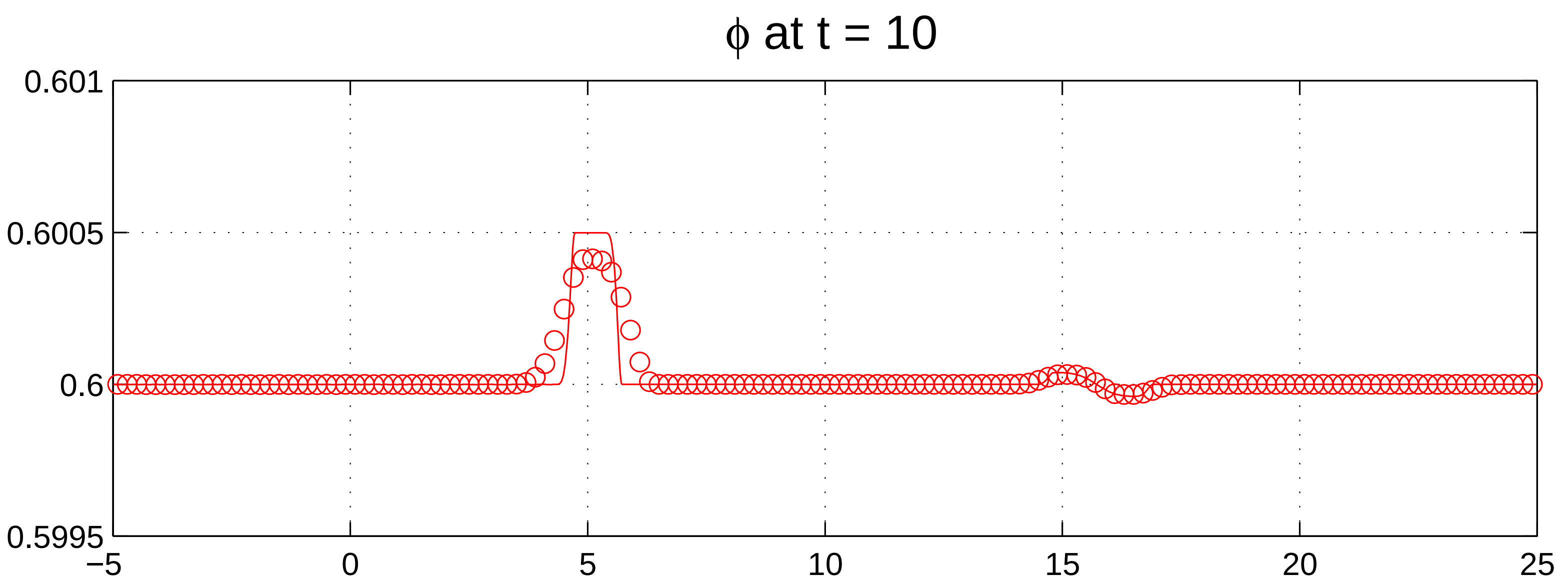

Perturbation of a steady flow in motion

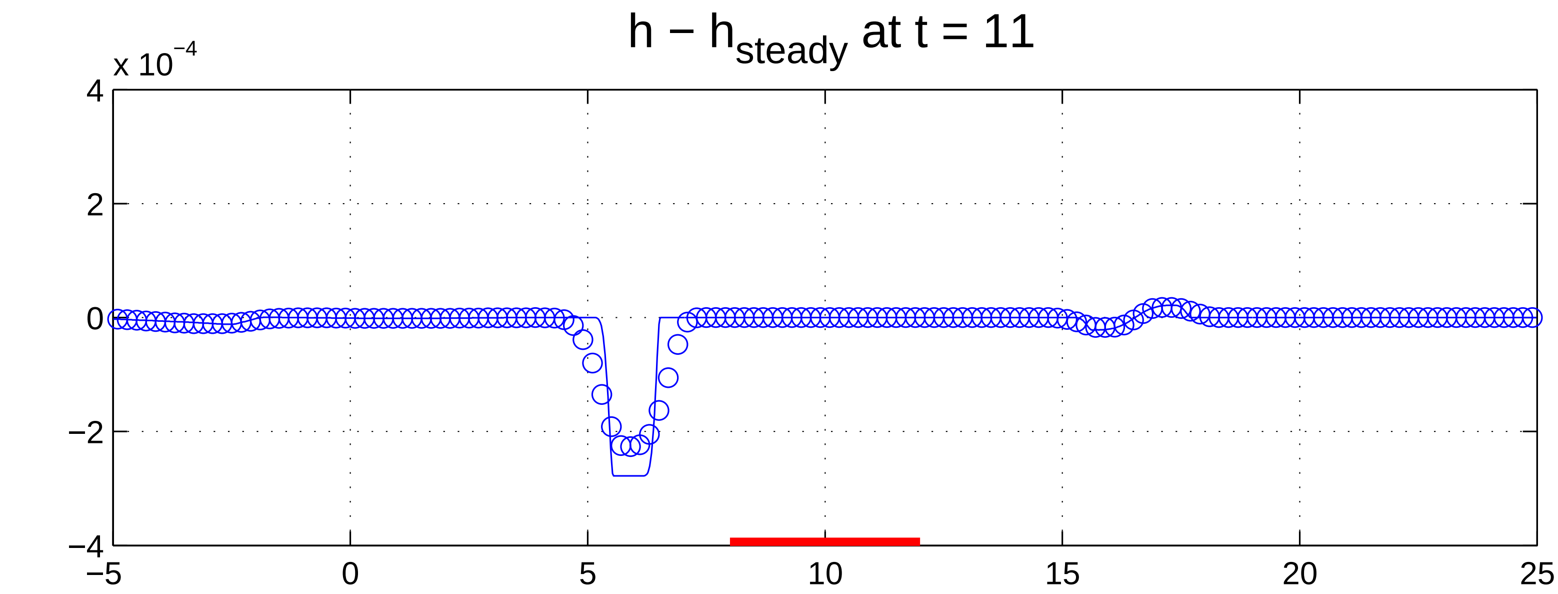

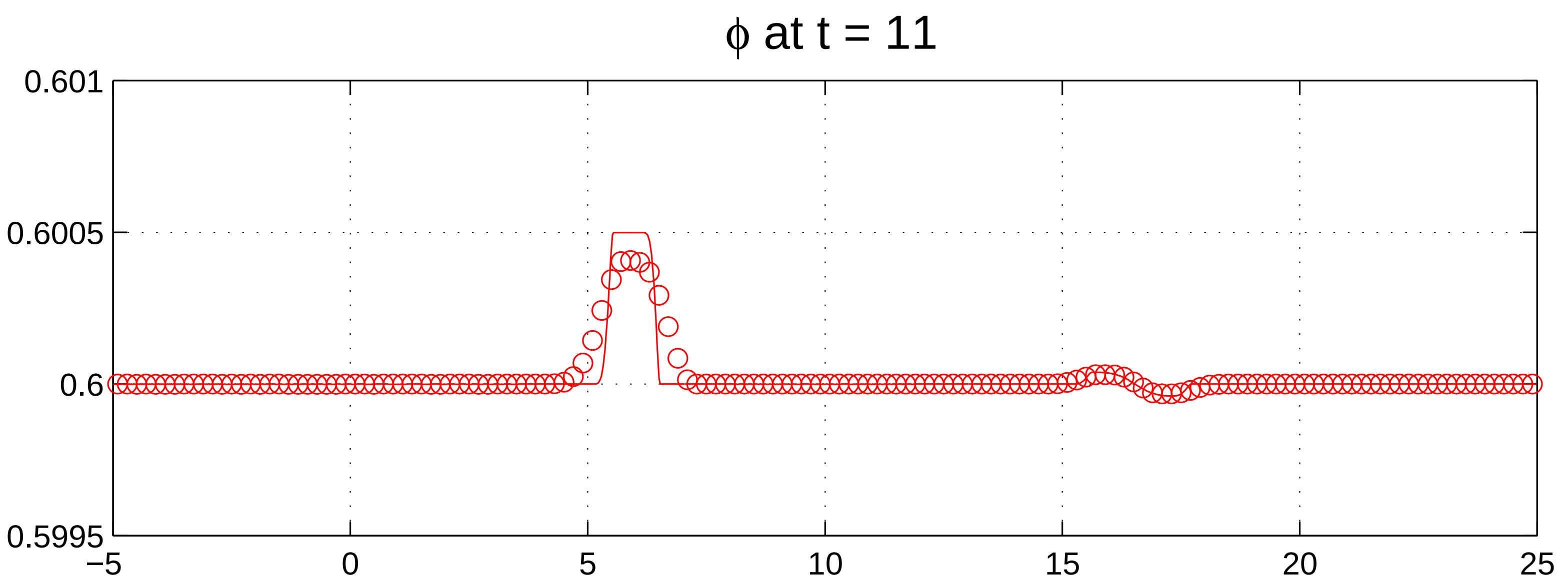

Perturbation of a steady flow in motion

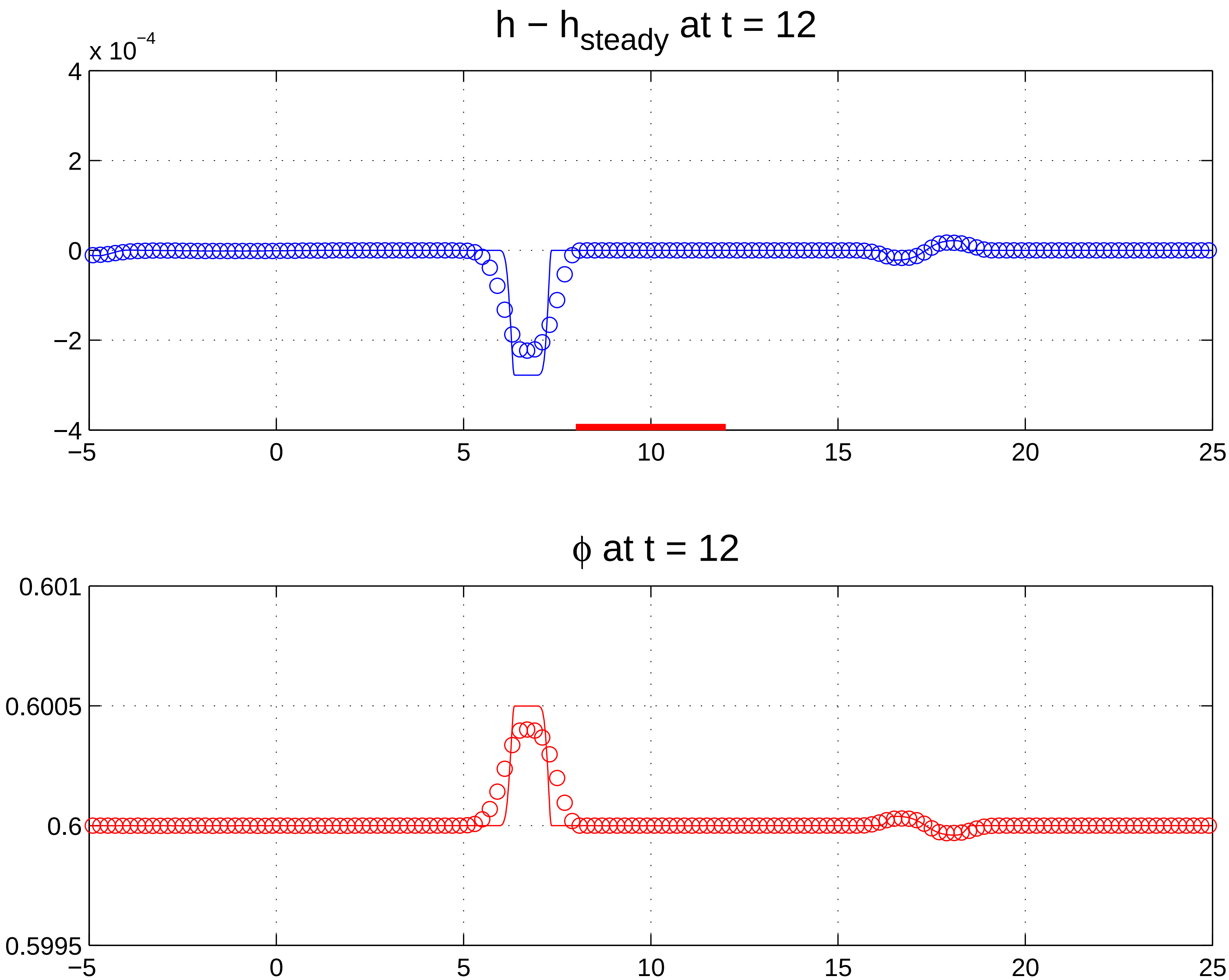

Perturbation of a steady flow in motion

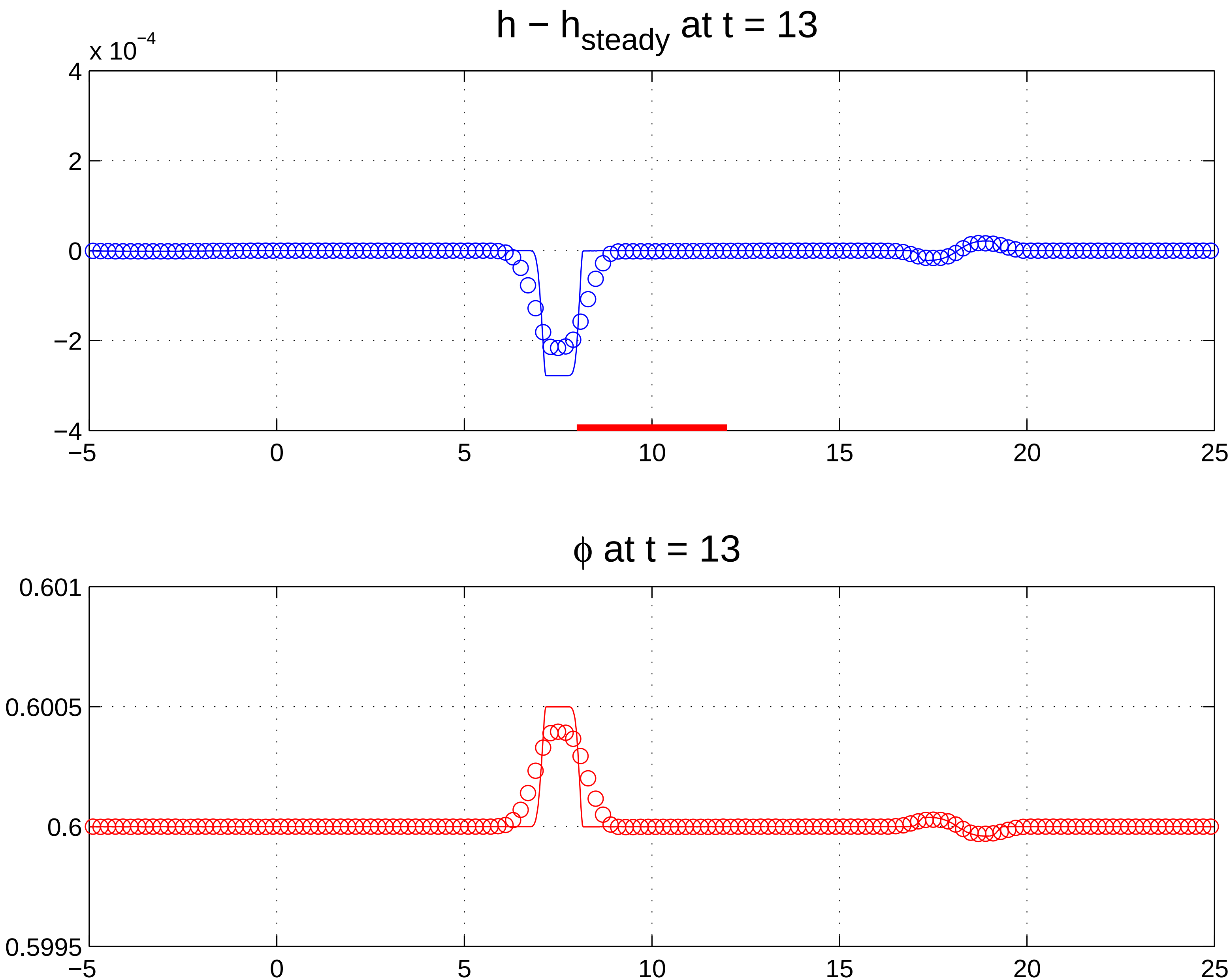

Perturbation of a steady flow in motion

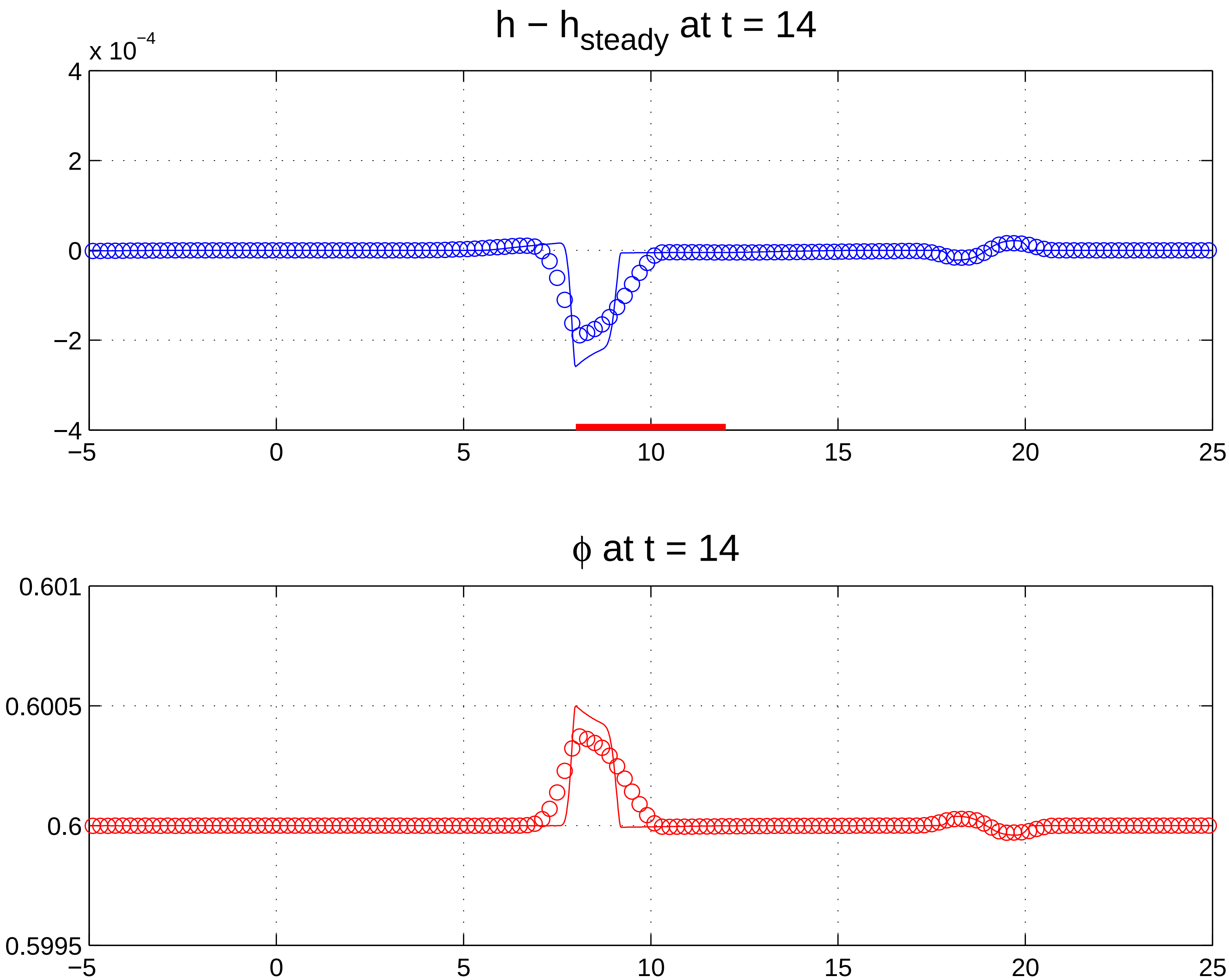

Perturbation of a steady flow in motion

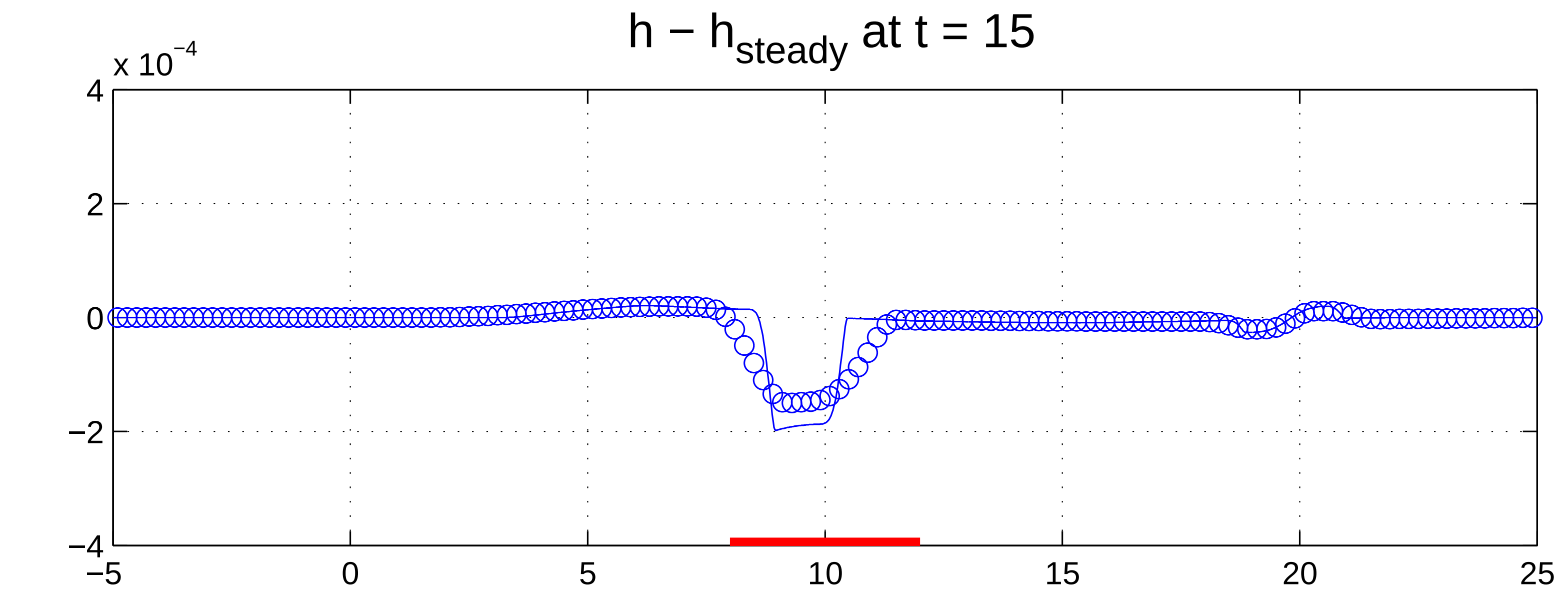

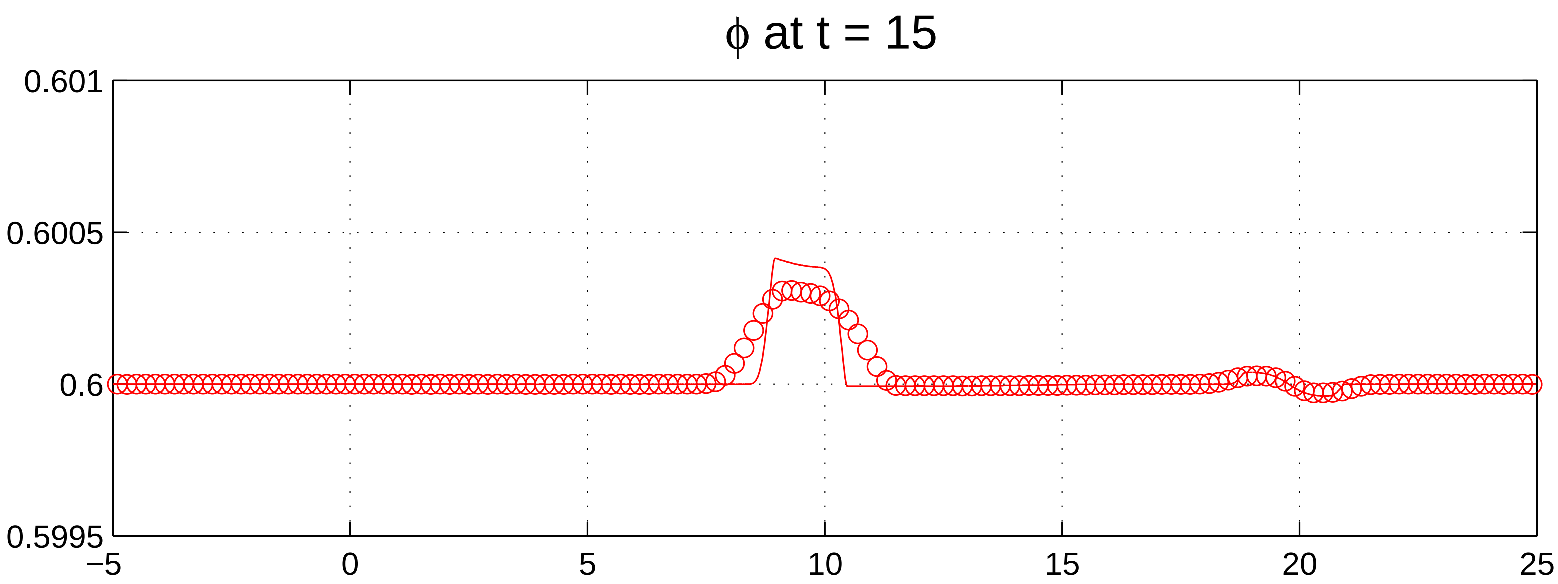

Perturbation of a steady flow in motion

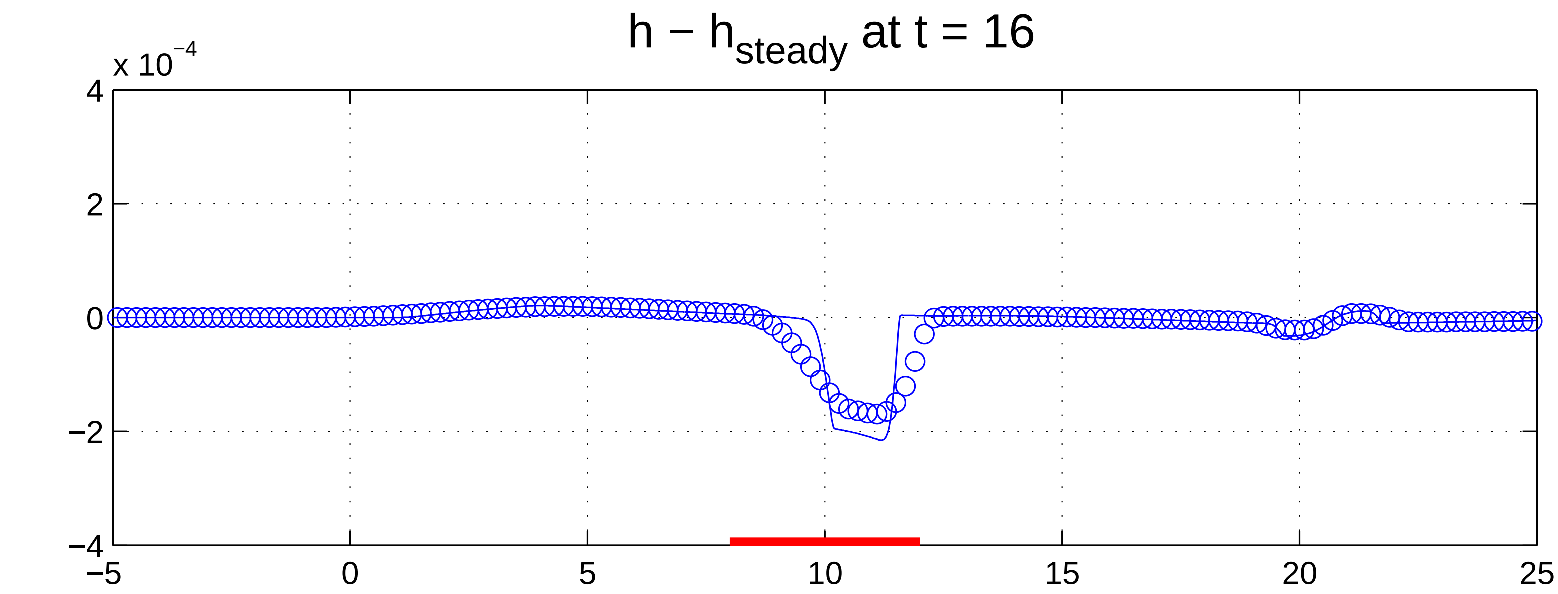

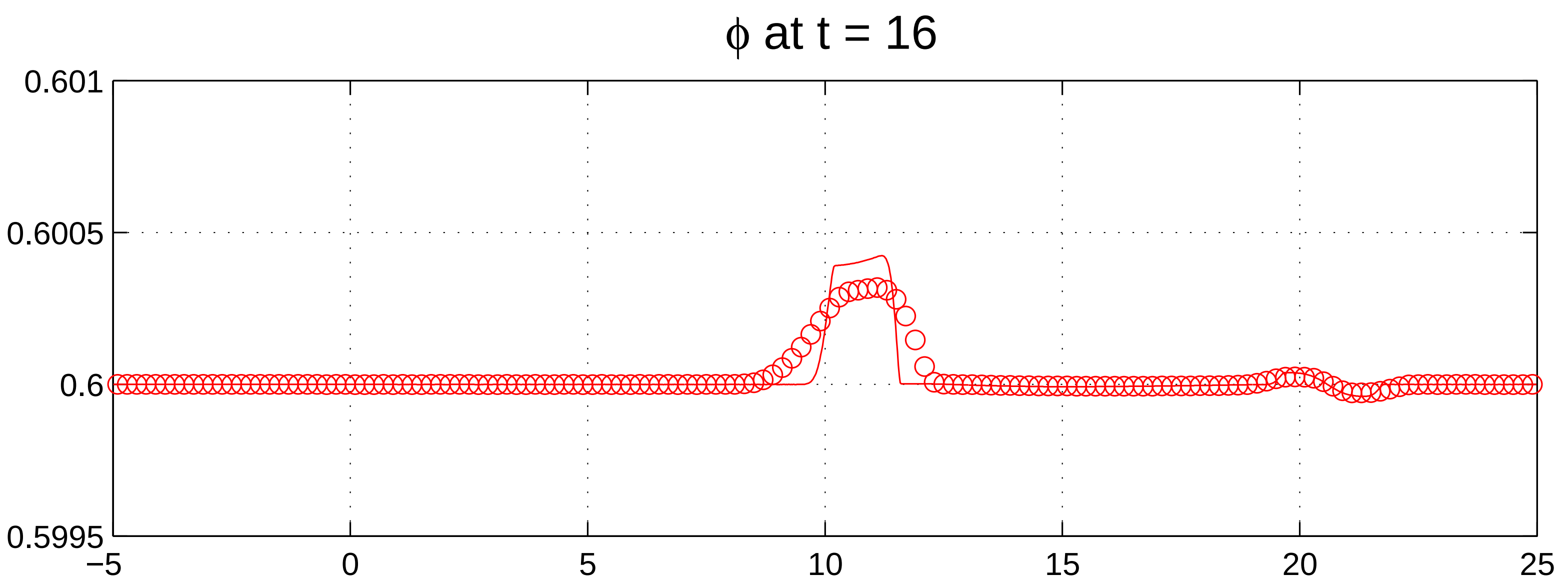

Perturbation of a steady flow in motion

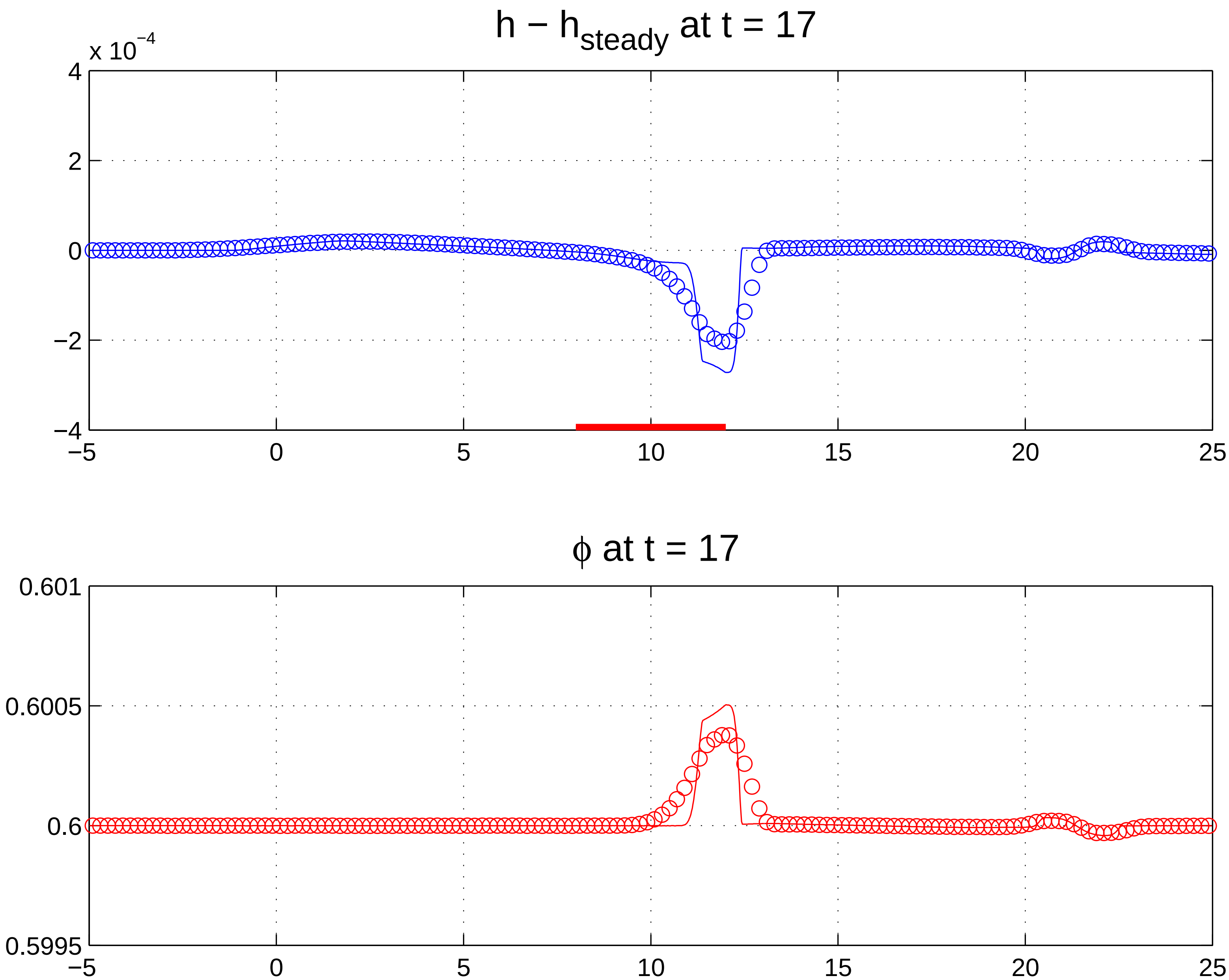

Perturbation of a steady flow in motion

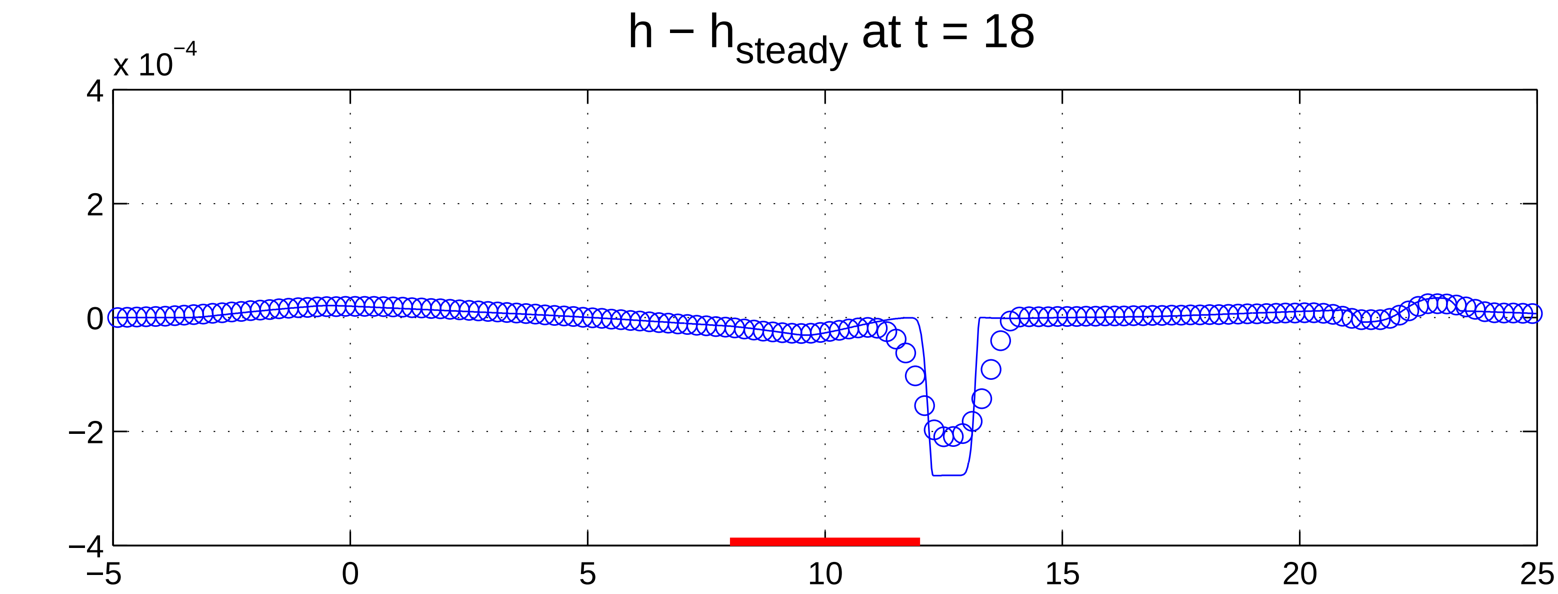

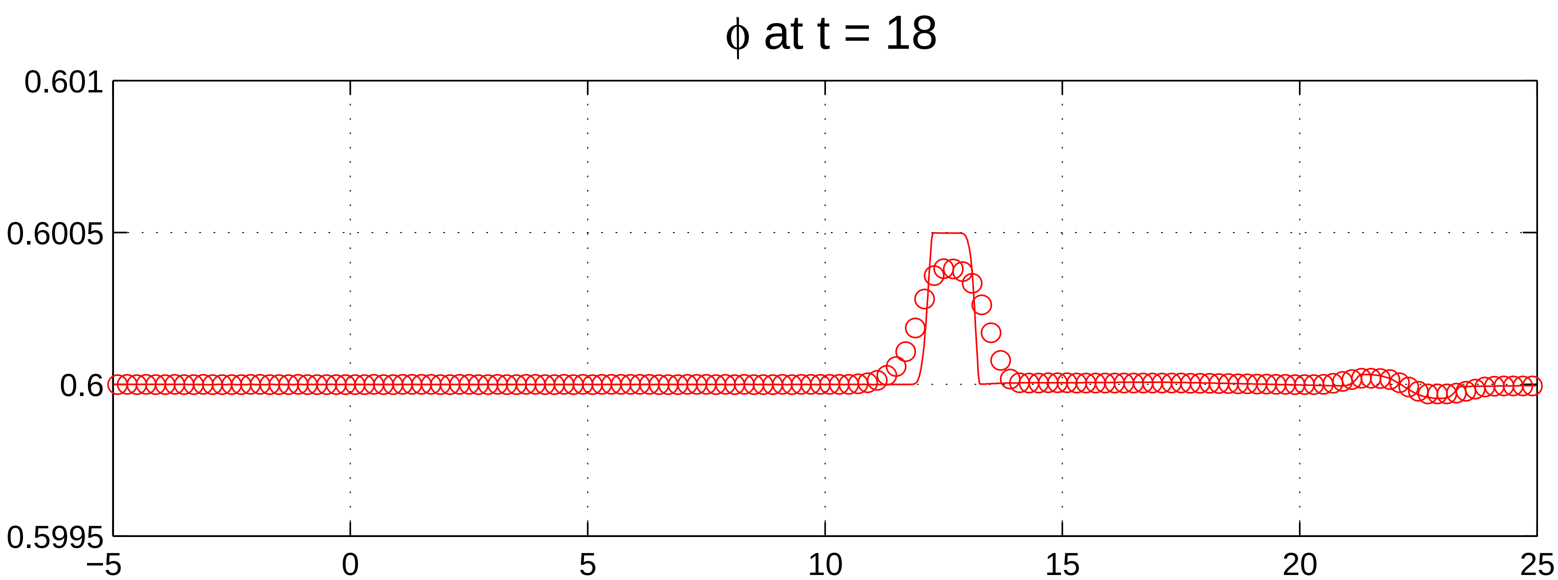

Perturbation of a steady flow in motion

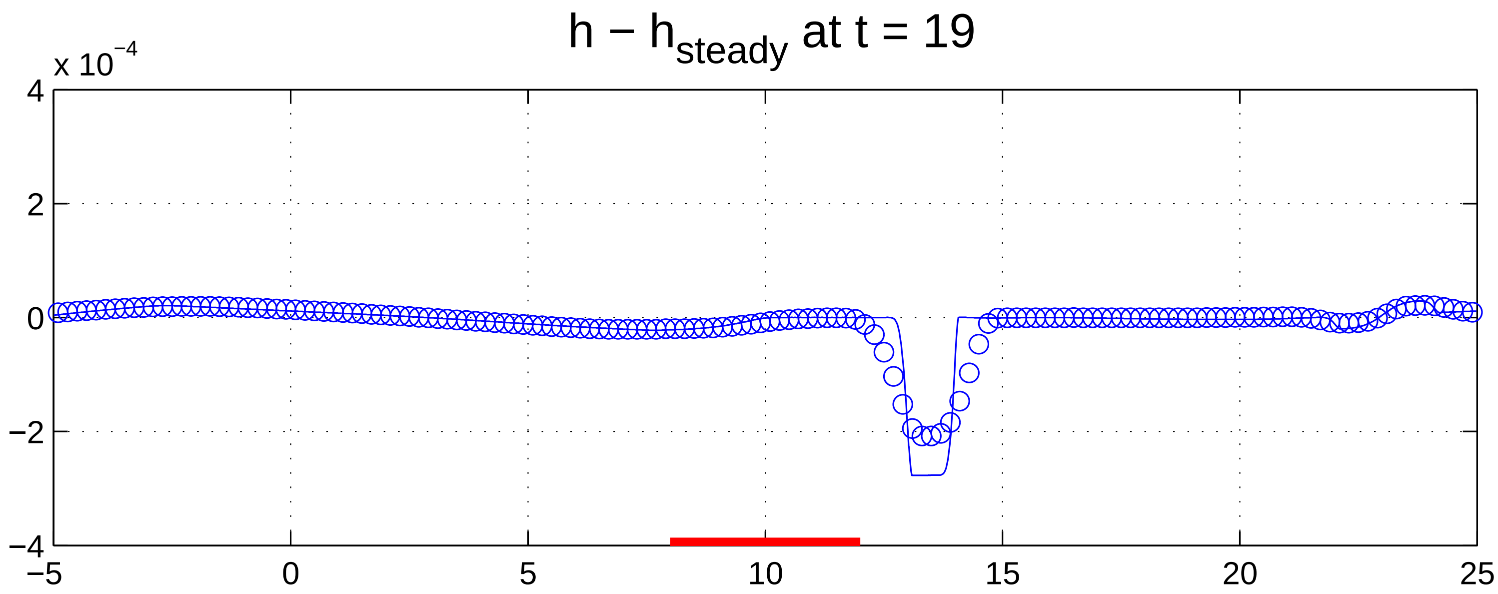

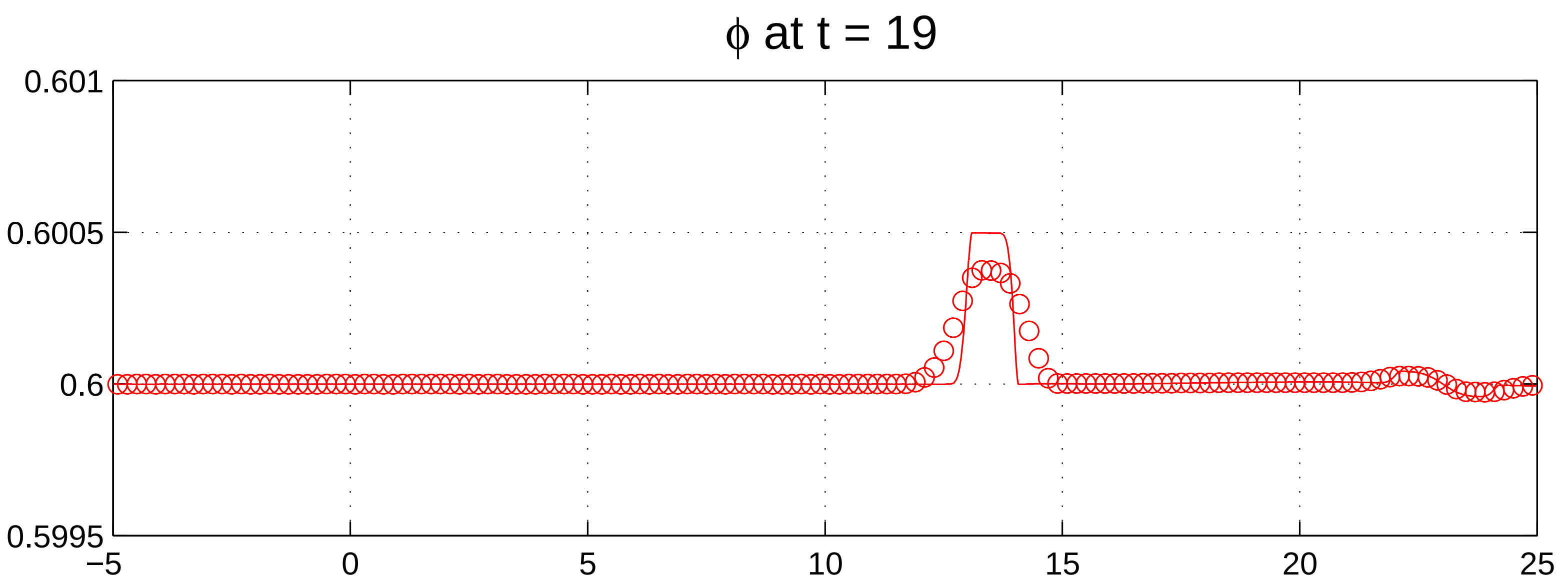

Perturbation of a steady flow in motion

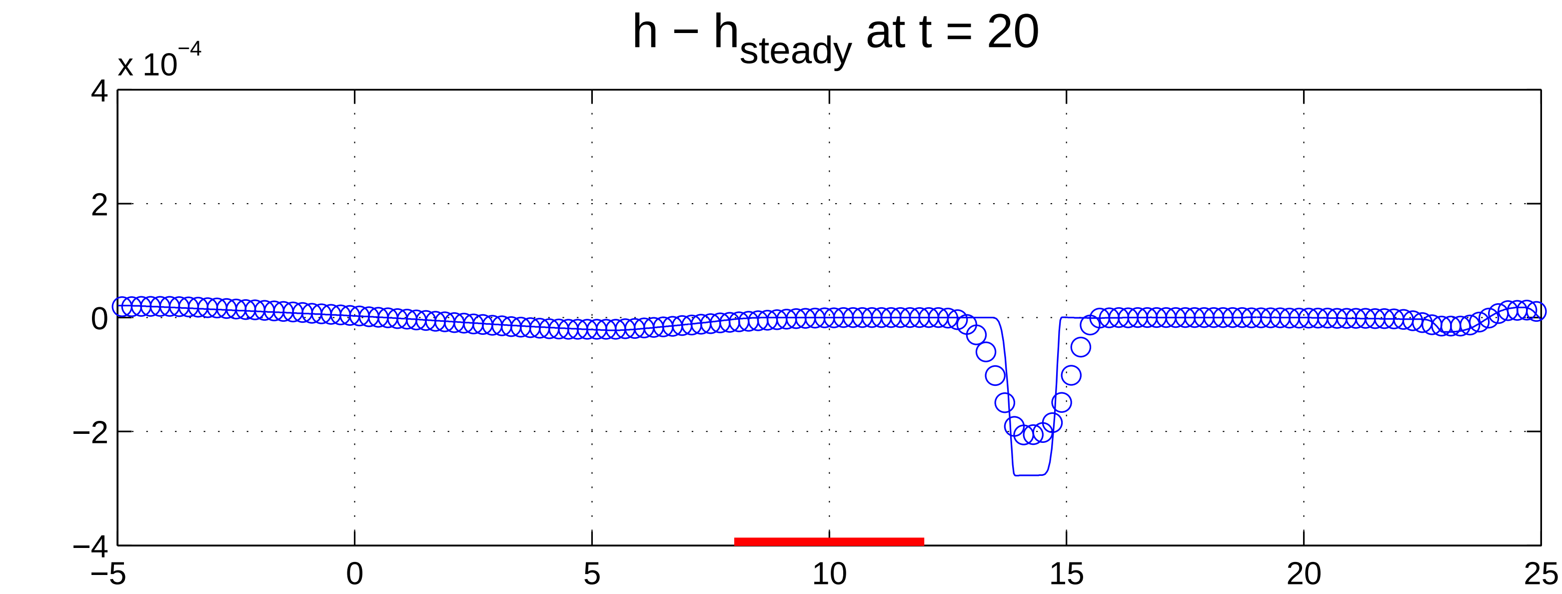

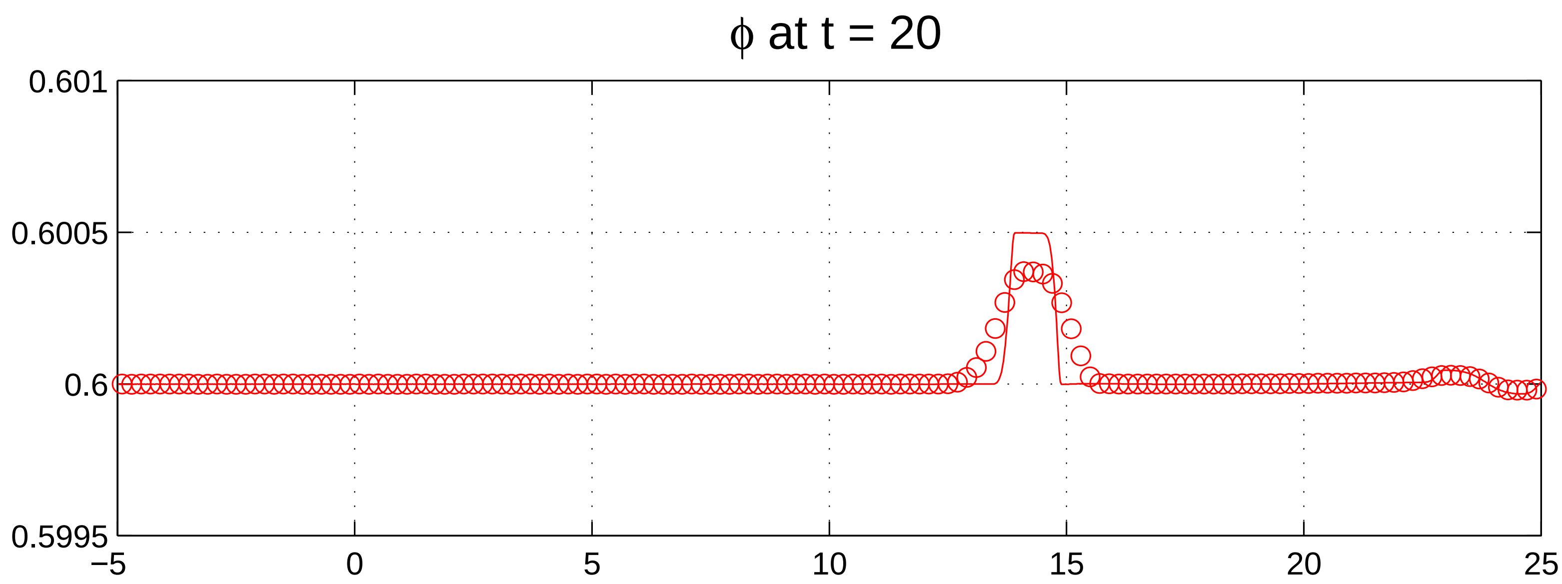

Perturbation of a steady flow in motion

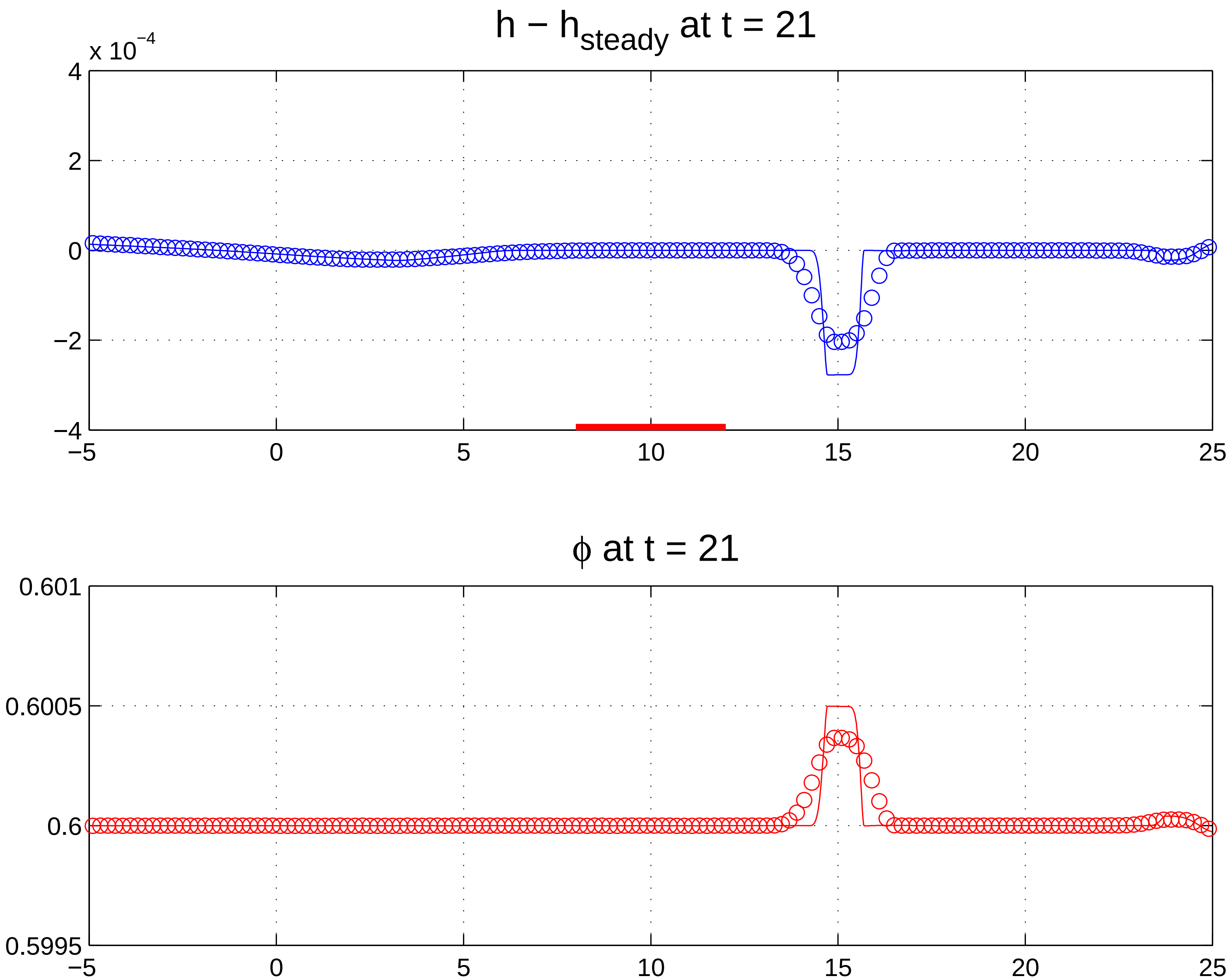

Perturbation of a steady flow in motion

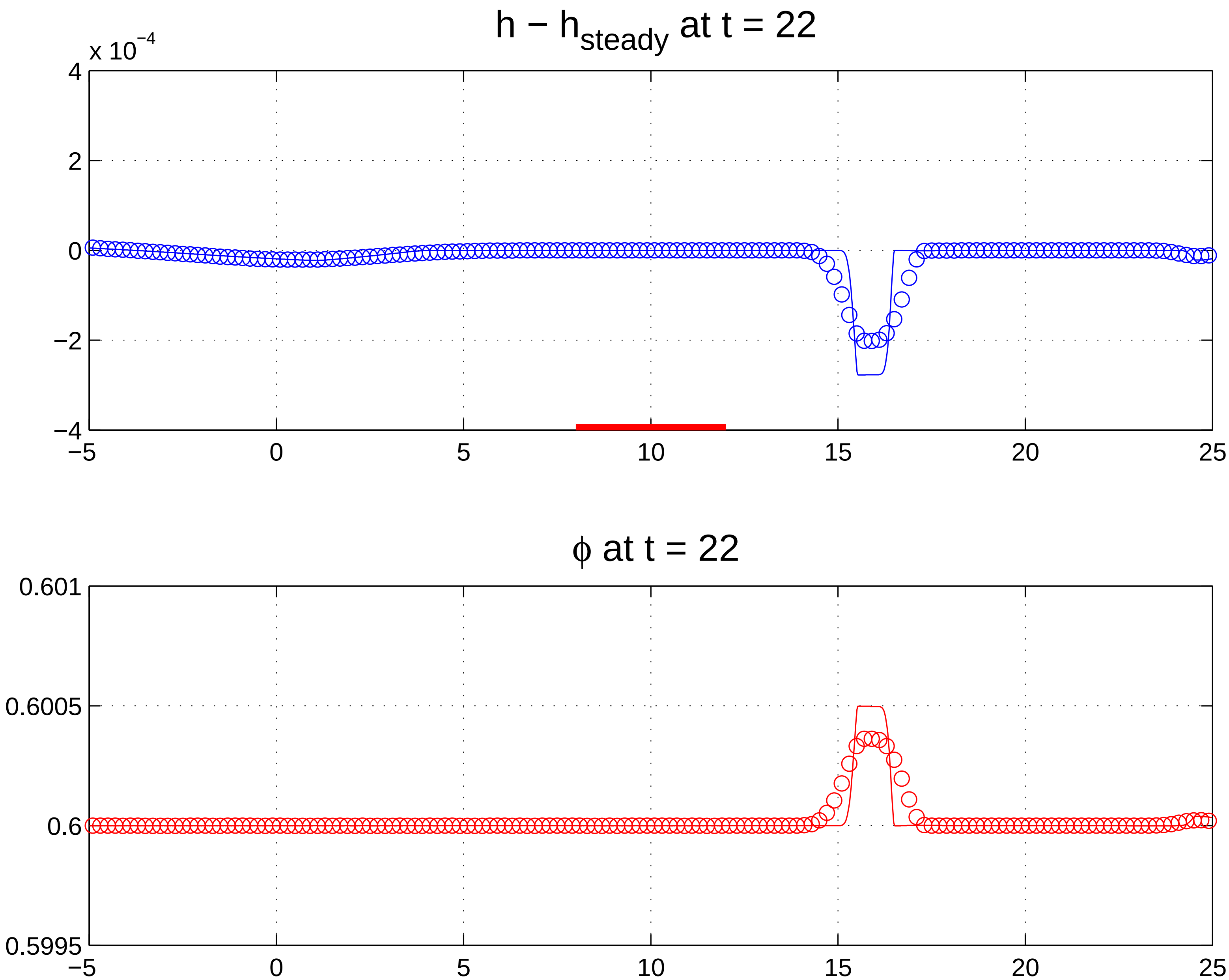

Perturbation of a steady flow in motion

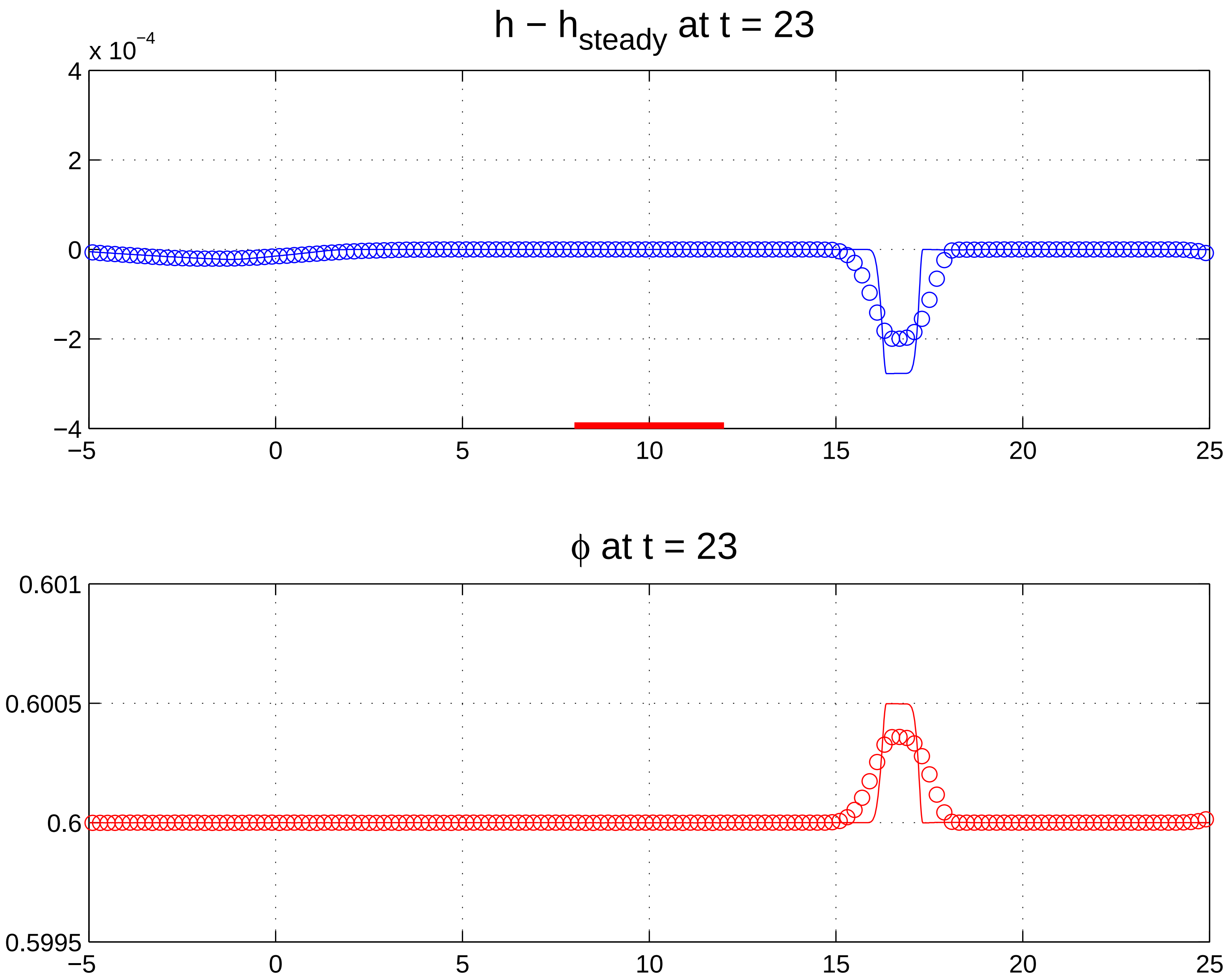

Perturbation of a steady flow in motion

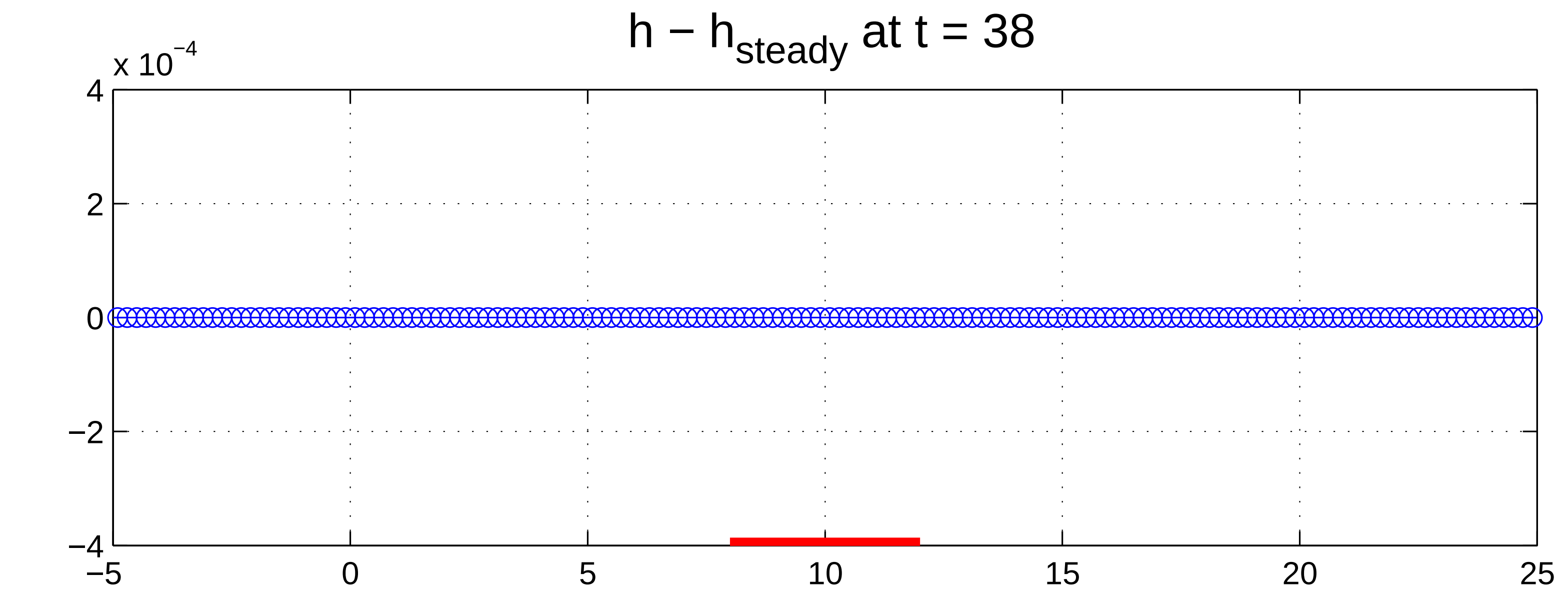

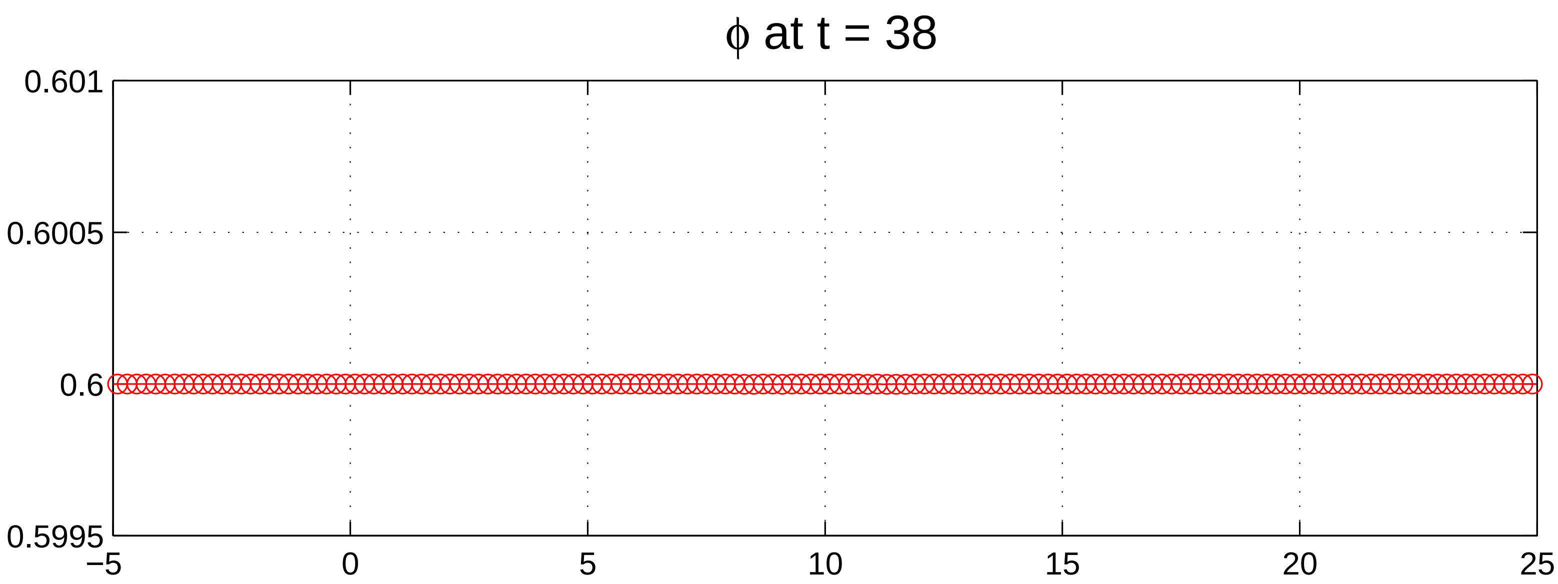

Numerical experiments with drag

Flow hump with higher fluid content

No drag

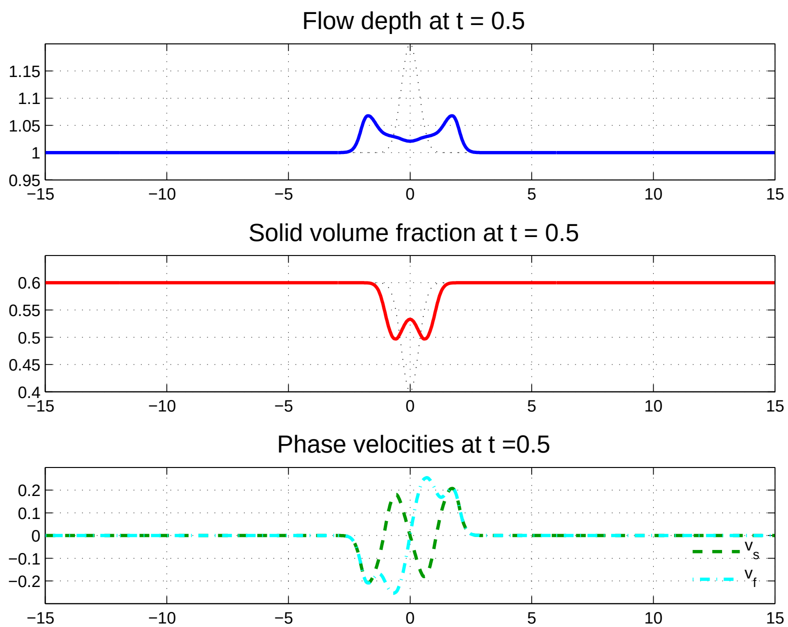

Drag included

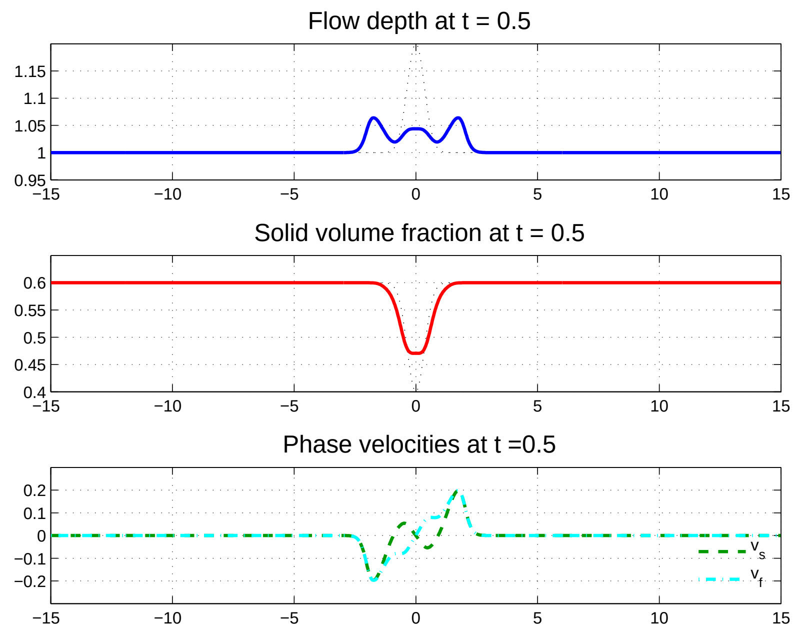

Numerical experiments with drag

Flow hump with higher fluid content

No drag

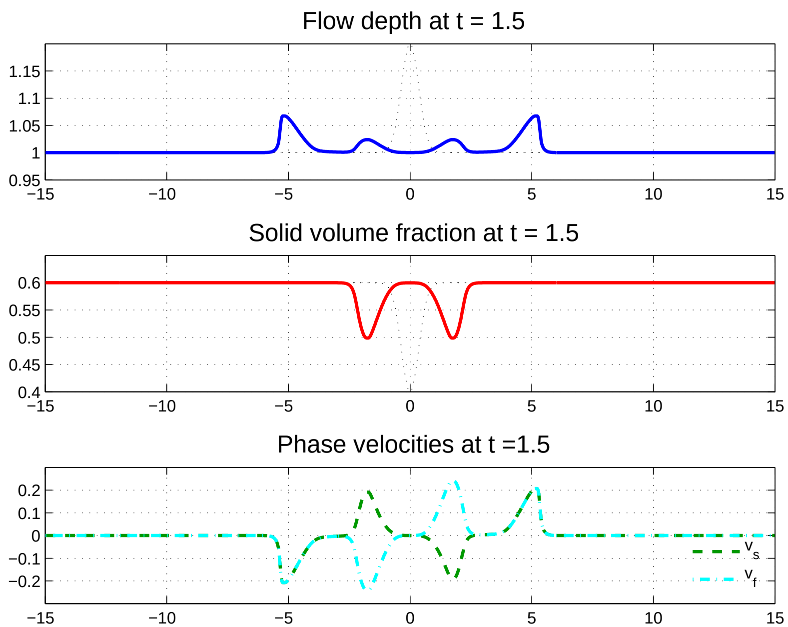

Drag included

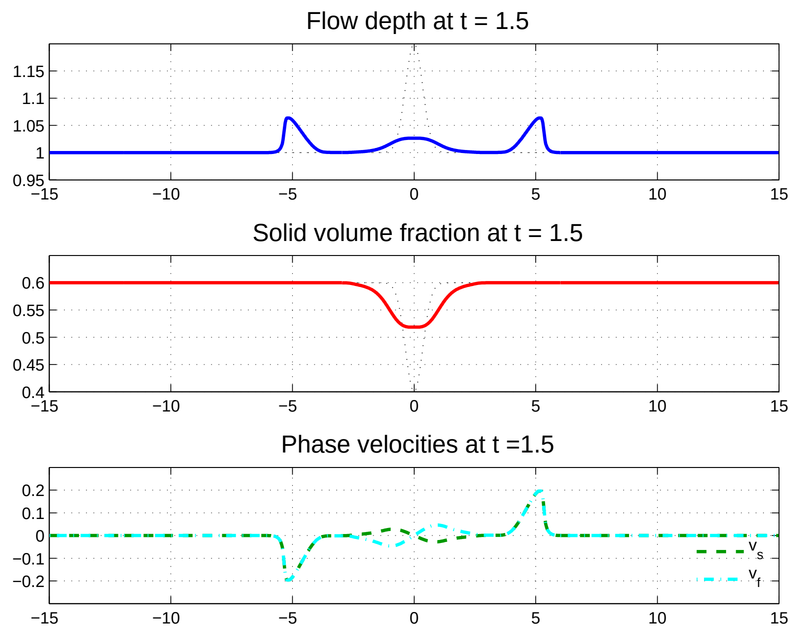

Numerical experiments with drag

Flow hump with higher fluid content

No drag

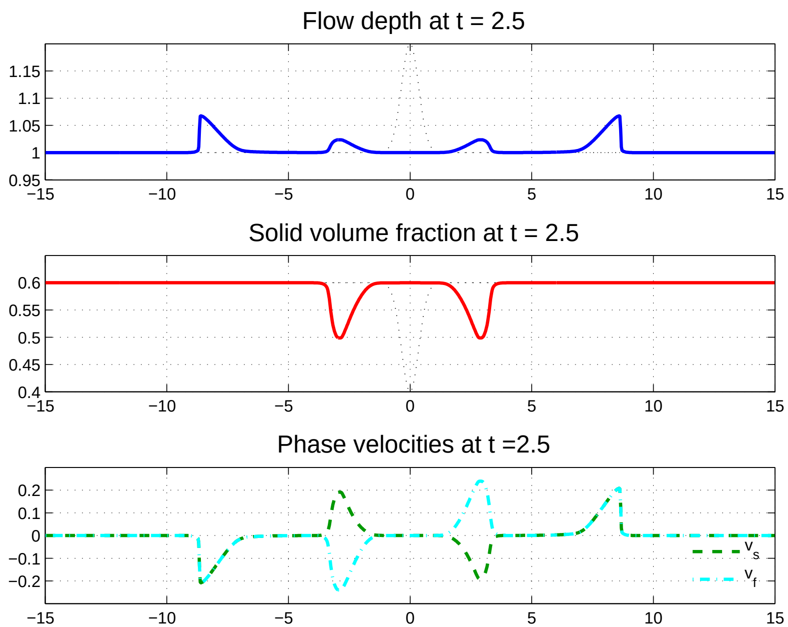

Drag included

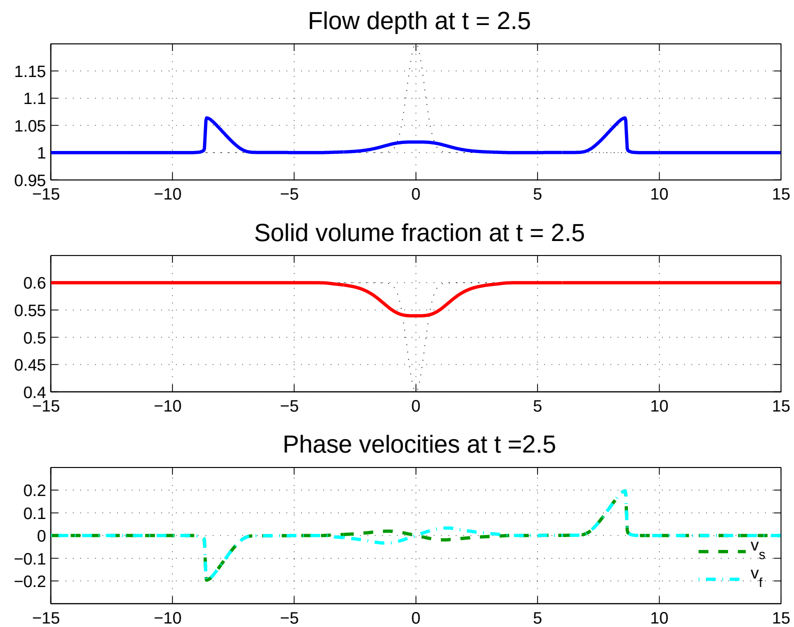

Numerical experiments with drag

Flow hump with higher fluid content

No drag

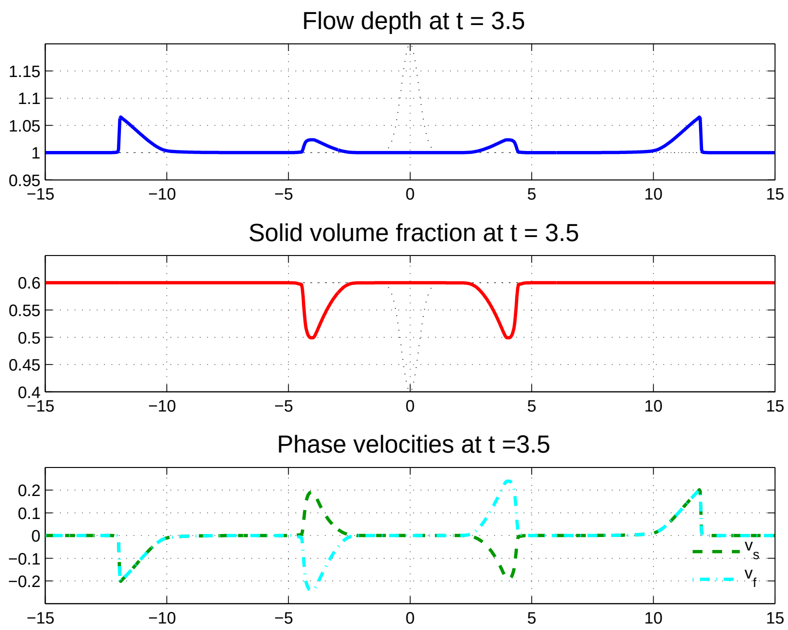

Drag included

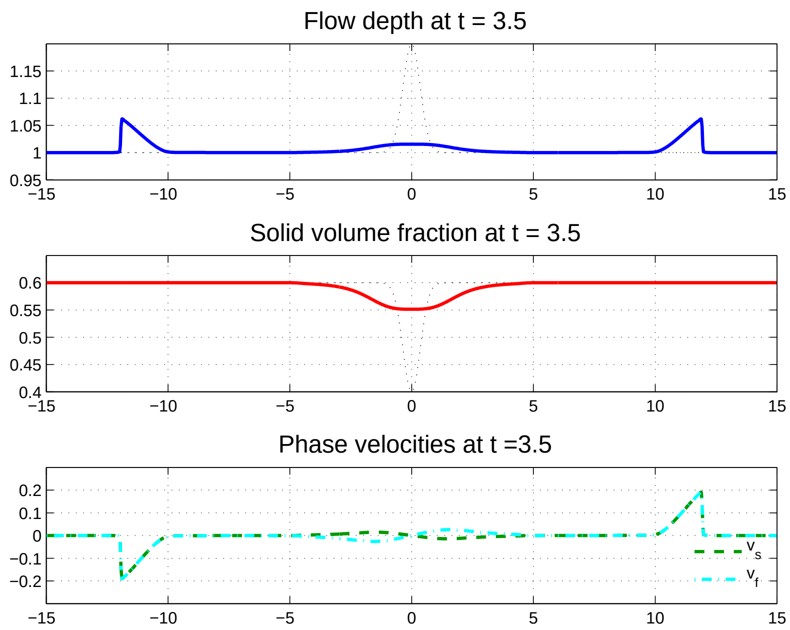

Numerical Experiment: Dam-Break Problem

Initially: discontinuity between two constant states with flow at rest ($v_s = v_f = 0$).

Left: $h_\ell = 3$, $\varphi_\ell = 0.7$; Right: $h_r = 2$, $\varphi_r = 0.4$.

Numerical Experiment: Dam-Break Problem

Initially: discontinuity between two constant states with flow at rest ($v_s = v_f = 0$).

Left: $h_\ell = 3$, $\varphi_\ell = 0.7$; Right: $h_r = 2$, $\varphi_r = 0.4$.

Compare:

1. Solution of two-phase model with no drag.

Numerical Experiment: Dam-Break Problem

Initially: discontinuity between two constant states with flow at rest ($v_s = v_f = 0$).

Left: $h_\ell = 3$, $\varphi_\ell = 0.7$; Right: $h_r = 2$, $\varphi_r = 0.4$.

Compare:

1. Solution of two-phase model with no drag.
2. Solution of two-phase model with drag effects.

Numerical Experiment: Dam-Break Problem

Initially: discontinuity between two constant states with flow at rest ($v_s = v_f = 0$).

Left: $h_\ell = 3$, $\varphi_\ell = 0.7$; Right: $h_r = 2$, $\varphi_r = 0.4$.

Compare:

1. Solution of two-phase model with no drag.
2. Solution of two-phase model with drag effects.
3. Solution of reduced model derived theoretically from two-phase model by assuming drag strong enough to drive instantaneously phase velocities to equilibrium. $\Rightarrow$ Hyperbolic system of three equations:

   $\star$ Mass and momentum conservation for the mixture + advection for φ.

   Riemann problems can be solved exactly.

Numerical Experiment: Dam-Break Problem

Initially: discontinuity between two constant states with flow at rest ($v_s = v_f = 0$).

Left: $h_\ell = 3$, $\varphi_\ell = 0.7$; Right: $h_r = 2$, $\varphi_r = 0.4$.

Compare:

1. Solution of two-phase model with no drag.
2. Solution of two-phase model with drag effects.
3. Solution of reduced model derived theoretically from two-phase model by assuming drag strong enough to drive instantaneously phase velocities to equilibrium. $\Rightarrow$ Hyperbolic system of three equations:

   $\star$ Mass and momentum conservation for the mixture + advection for φ.

   Riemann problems can be solved exactly.
4. Solution of two-phase model in the limit of infinitely large drag: Impose numerically instantaneous velocity equilibrium by setting $v_s = v_f = v_{\text{eq}}$ in fractional step.

   $v_{\text{eq}} = \left.\frac{h_s v_s + \gamma h_f v_f}{h_s + \gamma h_f}\right|_{t^0}$ = limit for $t \to \infty$ of solution of $\partial_t q = \psi^{\mathsf{D}}(q)$.

Dam-Break Problem

$$h_\ell = 3, \varphi_\ell = 0.7\,; \quad h_r = 2, \varphi_r = 0.4\,.$$

1. No drag contribution

Grid cells = 1000

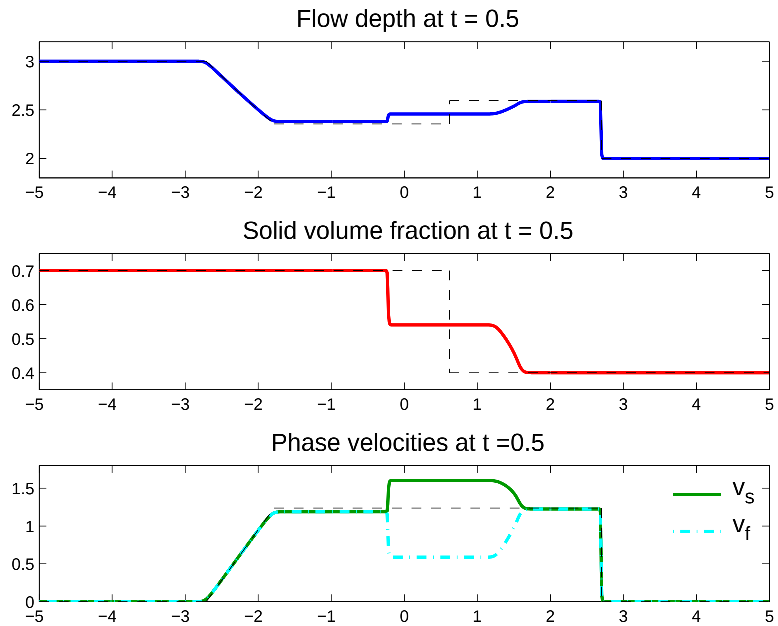

— — — Exact solution reduced model (instantaneous velocity equilibrium)

Dam-Break Problem

$$h_\ell = 3, \varphi_\ell = 0.7\,; \quad h_r = 2, \varphi_r = 0.4\,.$$

2. Drag effects included

Grid cells = 1000

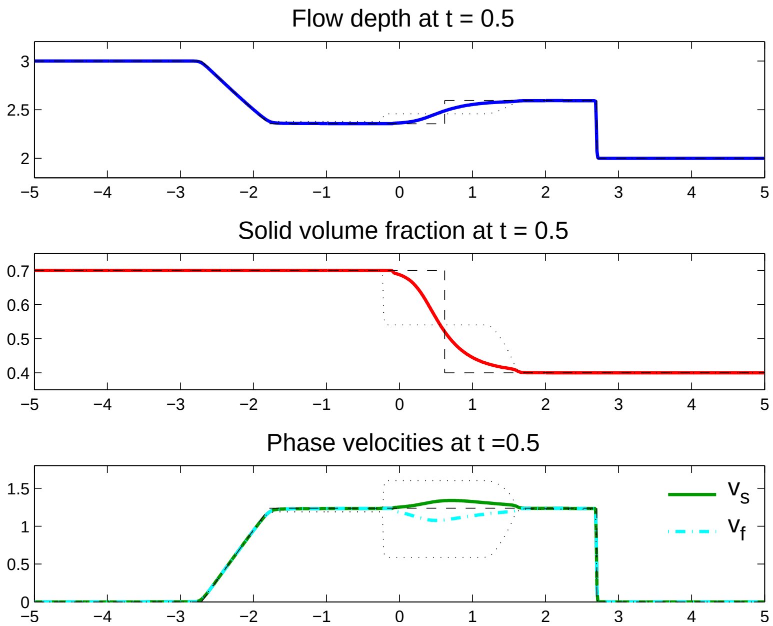

— — — Exact solution reduced model (instantaneous velocity equilibrium)

· · · No drag

Dam-Break Problem

$$h_\ell = 3,\ \varphi_\ell = 0.7\,; \qquad h_r = 2,\ \varphi_r = 0.4\,.$$

2. Drag effects included

Grid cells = 1000

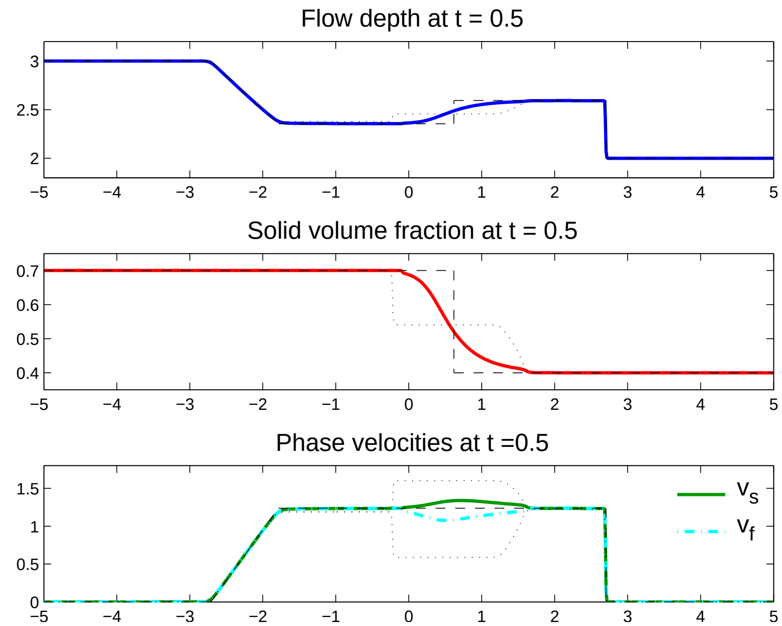

Infinitely large drag

$v_s = v_f = v_{\text{eq}}$ in fractional step

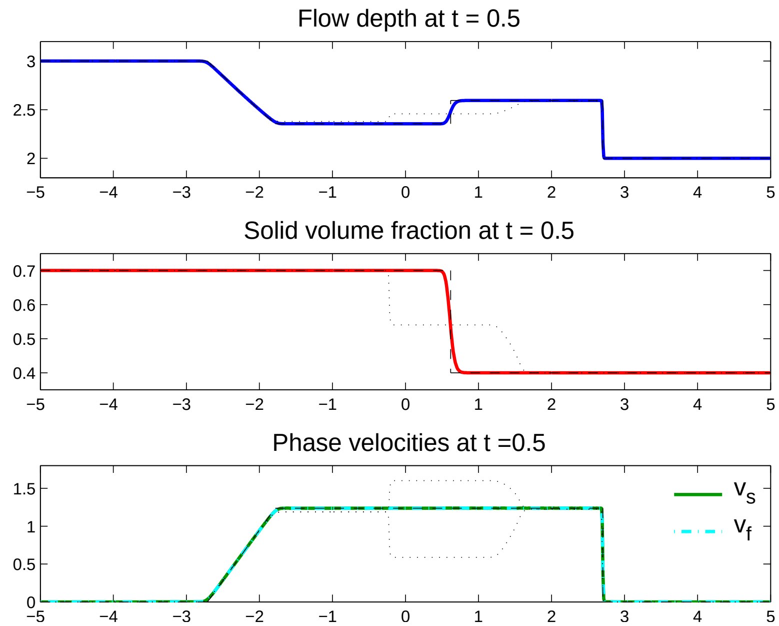

— — — Exact solution reduced model (instantaneous velocity equilibrium)

$\cdots$ No drag

$$v_{\text{eq}} = \frac{h_s v_s + \gamma h_f v_f}{h_s + \gamma h_f} = \text{equilibrium velocity.}$$

Summary

A mathematical and numerical two-phase shallow flow model has been presented for grain/fluid mixtures over variable topography.

Numerical solution technique: Finite Volume Method based on a Roe-type Riemann Solver, which includes treatment of topography and inter-phase drag terms.

This is only a very first step towards the modeling of realistic geophysical flows.

Summary

A mathematical and numerical two-phase shallow flow model has been presented for grain/fluid mixtures over variable topography.

Numerical solution technique: Finite Volume Method based on a Roe-type Riemann Solver, which includes treatment of topography and inter-phase drag terms.

This is only a very first step towards the modeling of realistic geophysical flows.

Current Work

Major issue: positivity preservation of flow depth and phase volume fractions, to handle dry bed states ($h = 0$) and/or vanishing of one phase ($\varphi = 0$, $\varphi = 1$).

Need to guarantee $h_s, h_f \geq 0 \Leftrightarrow h \geq 0,\ \varphi \in [0, 1]$.

Further work: friction terms, 2D model, complex topography...

Summary

A mathematical and numerical two-phase shallow flow model has been presented for grain/fluid mixtures over variable topography.

Numerical solution technique: Finite Volume Method based on a Roe-type Riemann Solver, which includes treatment of topography and inter-phase drag terms.

This is only a very first step towards the modeling of realistic geophysical flows.

Current Work

Major issue: positivity preservation of flow depth and phase volume fractions, to handle dry bed states ($h = 0$) and/or vanishing of one phase ($\varphi = 0$, $\varphi = 1$).

Need to guarantee $h_s, h_f \geq 0 \Leftrightarrow h \geq 0,\ \varphi \in [0, 1]$.

Further work: friction terms, 2D model, complex topography...

...Thank you for your attention!